CUMULATIVE SUM CONTROL CHARTS FOR MONITORING PROCESS MEAN AND/OR VARIANCE YANG MEI 2012

NANYANG TECHNOLOGICAL UNIVERSITY

CUMULATIVE SUM CONTROL CHARTS FOR MONITORING PROCESS MEAN AND/OR VARIANCE

YANG MEI

SCHOOL OF MECHANICAL AND AEROSPACE ENGINEERING

2012

CUMULATIVE SUM CONTROL CHARTS FOR MONITORING PROCESS MEAN AND / OR VARIANCE

YANG MEI

School of Mechanical and Aerospace Engineering

A thesis submitted to the Nanyang Technological University

in partial fulfillment of the requirement for the degree of

Doctor of Philosophy

2012

Acknowledgements

I would like to express the sincerest gratitude and appreciation to my supervisor, Dr. Wu Zhang, for his guidance in my Ph. D program study. His kindness warms me when I make mistakes; his patience clears my mind when I am messed; his strictness stimulates me to make progress step by step and do not act rush; his diligence encourages me to continuously devote on the right directions.

I would like to thank the school and the laboratory to provide me a convenient environment to study and an international circumstance to learn from others. My friends acquainted here not only help me in the study, but also enrich my learning about the world.

I sincerely thank my dearest parents and relatives. Their love and tolerance provide me a warm and safe haven. My countless thanks would be given to the good friends. Their understanding, encouragement and timely help accompany me on the way to growth.

Table of Contents

Chapter 4

Abstract

Nowadays quality is an extremely important tool in satisfying customers and winning market shares. When a quality problem occurs, it is crucial to detect it quickly in order to avoid serious economic loss. Control chart is a powerful Statistical Process Control (SPC) method to monitor and diagnose the processes.

The cumulative sum (CUSUM) control chart which accumulates historical information in the process is effective to detect process changes including mean and variance shifts. This thesis proposes several new CUSUM charts in detecting process shifts in mean and/or variance. An optimization model which uses an overall performance measure, Average Extra Quality Loss (*AEQL*), as the objective function is adopted to design these charts. The performance of these charts is compared with that of the most effective CUSUM charts that can be found in current literature. Furthermore, the effect of sampling cost and the probability distribution of process shifts on charts design and performance has also been investigated.

The researches fall mainly into two categories. One is to study the CUSUM charts which only detect process mean shift. The other is for the CUSUM charts detecting process shifts in both mean and variance.

(1) CUSUM charts for detecting mean shifts

For the first category, an optimal *X*&CUSUM control chart (a combination of Shewhart *X* chart and CUSUM chart with sample size $n = 1$) is first designed. Then a new adaptive CUSUM (ACUSUM II) chart is developed which adapts the reference parameter *k* and exponential *w* of the sample mean shift for best performance. The flexible sampling strategy of this chart improves the overall performance in detecting mean shifts.

A comparative study compares the performance of these two new charts with that of four other CUSUM charts. These two new charts perform similarly to a very effective

3-CUSUM(μ) chart (consisting of three individual CUSUM charts (Sparks 2000)) in terms of detection speed. However, they are simpler than the 3-CUSUM(μ) chart in understanding, design and implementation and, therefore, may be more attractive for practical applications.

The optimal sample size of three typical control charts, the Shewhart $\overline{X}$ chart, the CUSUM chart and the $\overline{X}$ &CUSUM chart is also studied. These charts are designed by an optimization algorithm which considers sampling cost. This study leads to some important findings regarding the chart effectiveness and optimal sample sizes. Many findings are different from current common wisdom.

(2) CUSUM charts for detecting shifts in both mean and variance

In the second category, two simple charts, the X chart and ABS CUSUM chart (a CUSUM chart monitoring the absolute value of process shift), and a combined 3-CUSUM($\mu+\sigma$) scheme (consisting of three CUSUM charts (Reynolds and Stoumbos 2004*a*)) for detecting process shifts in mean and variance are optimally designed. It is surprising to find that the detection effectiveness of the X chart and ABS CUSUM chart is inferior to the most effective 3-CUSUM($\mu+\sigma$) scheme only to a minor degree.

Then the effect of sampling cost on chart design and performance is also studied for the $\overline{X}$ chart, the ABS CUSUM chart and 3-CUSUM($\mu+\sigma$) scheme. Many new findings are obtained regarding the detection effectiveness and sample sizes of the control charts.

Finally, the effect of process shift distribution on chart design and performance is investigated. It reveals that the overall performances of the ABS CUSUM and 3-CUSUM($\mu+\sigma$) charts are almost identical no matter the charts are designed with the uniform assumption or based on the real probability distributions of process shifts, and no matter what the real distributions are. The detective effectiveness of the X chart is also nearly equal to what the ABS CUSUM and 3-CUSUM($\mu+\sigma$) charts do when process shift domain is large.

List of Tables

List of Figures

List of Abbreviations

(Approximately in order of appearance)

x	=	quality characteristic
z	=	standard normal value of x
μ_0	=	in-control process mean
σ_0^2	=	in-control process variance
μ_1	=	out-of-control process mean
σ_1^2	=	out-of-control process variance
μ	=	current process mean
$\bar{x}_t$	=	sample mean for the tth sample
n	=	sample size
R	=	rang of value for one sample
$\boldsymbol{R_0}$	=	in-control transition probability matrix
$\boldsymbol{R}$	=	out-of-control transition probability matrix
α	=	Probability of type I error
β	=	Probability type II error
p	=	the probability that a sample point exceeds the control limits
UCL	=	upper control limit
LCL	=	lower control limit
C_t	=	quality statistic for CUSUM chart
E_t	=	quality statistic for EWMA chart
λ	=	smoothing or weighting parameter of EWMA chart
ATS	=	average time to signal
ARL	=	average run length
VSI	=	variable sampling interval
VSS	=	variable sample size
$VSSI$	=	variable sample size and sampling interval

δ_μ	=	mean shift in terms of the in-control standard deviation σ_0
δ_σ	=	standard deviation shift in terms of σ_0
ζ_μ	=	specified value of δ_μ
ζ_σ	=	specified value of δ_σ
$\delta_{\mu,\max}$	=	upper bound of process mean shift
$\delta_{\sigma,\max}$	=	lower bound of process mean shift
L	=	distance from the center line of the control chart
A_2	=	constant to calculate control limits of xbar chart
D_3, D_4	=	constant to calculate control limits of R chart
k	=	reference parameter of CUSUM chart
H	=	control limit of CUSUM chart
H_{CX}, $H_{CX}{}^2$	=	control limits of 3-CUSUM($\mu+\sigma$) scheme
k^X, k^{X^2}	=	reference parameter of 3-CUSUM($\mu+\sigma$) scheme

Publication List

Based on the results of this Ph.D project, the following papers have been submitted and published.

Published or Accepted Journal papers

(1) Wu, Z.; **Yang, M.**; Jiang, W. and Michael, B.C. Khoo. (2008). "Optimization Designs of the Combined Shewhart-CUSUM Control Charts." Computational Statistics and Data Analysis, v53, pp. 495-506.

(2) Wu, Z.; Jiao, J. X.; **Yang, M.**; Liu, Y. and Wang, Z. J. (2009). "An Enhanced Adaptive CUSUM Control Chart." IIE Transactions, v41, pp. 642-653.

(3) Wu, Z.; **Yang, M.**; Khoo, M. B. C. and Yu, F. J. (2010). "Optimization Designs and Performance Comparison of Two CUSUM Schemes for Monitoring Process Shifts in Mean and Variance." European Journal of Operational Research, v205, pp. 136-150.

(4) Wu, Z.; **Yang, M.**; Khoo, M. B. C. and Castagliola, P. (2011) "What Are the Best Sample Sizes for the Xbar and CUSUM Charts?" International Journal of Production Economics, v131, pp.650-662.

(5) **Yang, M.**; Wu, Z.; Lee, C. K. M. and Khoo, B.C. (2011) "The *X* Control Chart for Monitoring Process Shifts in Mean and Variance." Accepted by International Journal of Production Research.

(6) **Yang, M.**; Wu, Z. and Li, T. I. (2011) "The effect of shift distribution on the design and performance of the X and CUSUM charts in monitoring mean and variability" Accepted by European Journal of Industrial Engineering.

Submitted Journal Papers

(1) **Yang, M.** and Wu, Z. "Effect of sampling cost on the design of control charts for monitoring process mean and variance." Submitted to Computers & Industrial Engineering.

Conference papers

(1) **Yang, M.** and Wu, Z. (2008) "New Design Algorithm of the Shewhart & CUSUM Chart for Monitoring Process Mean Shifts." Proceedings of the 2008

IEEE International Conference of Management of Innovation and Technology, Bangkok.

(2) Wu, Z. and **Yang, M.** (2008) "An Adaptive CUSUM Chart with Exponential of Mean Shift." Proceedings of the 2008 IEEE International Conference on. Industrial Engineering and Engineering Management, Singapore.

(3) **Yang, M.** (2009) "The Optimal Sample Sizes of the Xbar and CUSUM Charts." Proceedings of the 2009 IEEE International Conference on. Industrial Engineering and Engineering Management, Hongkong.

(4) Wu, Z. and **Yang, M.** (2009) "A CUSUM Chart Using Absolute Sample Values to Monitor Process Mean and Variance." Proceedings of the 2009 IEEE International Conference on. Industrial Engineering and Engineering Management, Hongkong.

Chapter 1
Introduction

1.1 Background

Evolving through more than one hundred years, the importance of quality in industry and other activities has been widely accepted in modern economic life. When the hot competitive market is full of similar products, it is not easy for one product or service to excel its competitors. Great effort is made by organizations to achieve continuous quality improvement and to make themselves differentiated from their compeers.

The concept of quality is implicitly or explicitly expatiated in different manners. A traditional thought is that quality means fitness for use. According to the two aspects of fitness for use, quality can be divided into quality of design and quality of conformance. Montgomery (2009) mentioned that, in shop floors, quality is more associated with the conformance aspect than with design, since most designers and engineers do not receive formal education in quality engineering methodology.

Quality can be decomposed into the following several dimensions (Garvin 1987):

1. Performance (will the product do the intended job?)
2. Reliability (how often does the product fail?)
3. Durability (how long does the product last?)
4. Serviceability (how easy is it to repair the product?)
5. Aesthetics (what does the product look like?)
6. Features (what does the product do?)
7. Perceived Quality (what is the reputation of the company or its products?)
8. Conformance to Standards (is the product made exactly as the designer intended?)

These dimensions provide a comprehensive understanding about quality. However,

the practitioners or professionals may have trouble in selecting certain aspects that qualitatively or quantitatively describe the quality problems in their particular scenarios, let alone taking appropriate measures to rectify them.

In his textbook of Introduction to Statistical Quality Control, Montgomery (2009) defined that "Quality is inversely proportional to variability". As it is shown below, this definition is consistent with many practical applications in industries. After World War II, the products manufactured in Japan have been thought with high quality. In an investigation (Montgomery 2009), an American plant and a Japanese plant were chosen for a comparison regarding warranty claims and repair costs of transmission. It was found that the Japanese plant provided products with high performance and low repair cost. For the Japanese products, the proportion that the critical characteristics took up in the specification band was only one-third of that found in the American products, under the condition that products from both plants were conforming to the specification. It was then concluded that the considerably less variability in the critical characteristics of the Japanese product led to a smoother operation, a quieter run, a lower repair cost and a superior felt quality.

Along the same line, quality improvement is the reduction of variability in process and production. Since variability can only be described in statistical terms, statistical methods play a central role in quality improvement efforts (Montgomery 2009). It is claimed that the impressive Japanese automobile success in 1980s is due to the application of statistical process control (*SPC*) tools, which function vitally and outperform the traditional techniques in quality management. Dramatically, the SPC technique originating in the United States during World War II did not acquire sufficient attention locally and thus led to the competition failure of American automobiles in the global automobile market.

Among the seven well-known tools of SPC technology, such as histogram or stem-and-leaf plot, check sheet, pareto chart, cause-and-effect diagram, defect

concentration diagram, scatter diagram and control chart, the control chart is undeniably the most popular and effective one (Montgomery 2009).

1.2 Motivation

The cumulative sum (*CUSUM*) control chart is one of the basic control charts, and is the chart to be studied in this thesis. It has a recursive form. If an increasing mean shift is to be detected, the quality statistic C_t^+ corresponding to the tth observation x_t is updated by:

$$\begin{aligned} C_0^+ &= 0 \\ C_t^+ &= \max(0,\ C_{t-1}^+ + x_t - u_0 - k) \end{aligned} \tag{1-1}$$

where μ_0 is the in-control mean or target of the quality characteristic x, and k is called the reference parameter which can monitor the chart's sensitivity to shifts of different sizes. If a decreasing mean shift is of interest, the quality statistic C_t^- is updated similarly:

$$\begin{aligned} C_0^- &= 0 \\ C_t^- &= \min(0,\ C_{t-1}^- + x_t - u_0 + k) \end{aligned} \tag{1-2}$$

Unlike the Shewhart control chart which only records the latest process information the CUSUM chart takes advantage of historical information on the process. As a result, the CUSUM chart is very sensitive to small and moderate shifts and thus has a high overall effectiveness. However, the CUSUM chart has not received enough attention as the Shewhart chart has and its application is not recognized widely in workshop floor. By applying optimization algorithms and including new control features, the capability of CUSUM chart can be further enhanced in detecting process shifts in mean and/or variance in a broader shift range. Meanwhile, progress can be made to simplify the design and implementation of the CUSUM chart.

1.3 Research Objectives

The primary objective of this Ph.D thesis is to develop new CUSUM charts which are more effective for detecting process shifts and easier in design and implementation than the existing CUSUM charts. The detection effectiveness of the CUSUM charts

will be improved from several aspects:

1. Using adaptive features to conduct the on-line adjustment of charting parameters.
2. Developing the CUSUM schemes which are composed of (i) two or three CUSUM charts or (ii) a CUSUM chart and another chart of different type, such as the Shewhart X chart.
3. Developing new design algorithms that determine the optimal charting parameters to achieve the optimal performance of the CUSUM charts. For this purpose, the formulae for calculating the Average Time to Single (*ATS*) of different charts must be derived and a suitable performance measure, such as Average Extra Quadratic Loss (*AEQL*), has to be identified.

The second objective is to investigate the effect of some critical factors (such as the sampling cost and the distribution of process shift) on the design and performance of the control charts. These studies bring about many new findings that are quite different from some well accepted results in SPC circle. These findings should be quite useful and interesting to many SPC practitioners and researchers.

In order to test the performance of the new charts and algorithms proposed in this PhD thesis, it is essential to carry out systematic comparative studies among the new charts and many other existing charts. A comprehensive discussion on the effectiveness and simplicity of different charts is also given. These comparative studies will greatly facilitate SPC users to select appropriate CUSUM chart for their particular applications.

1.4 Organization of the Thesis

This thesis consists of five chapters, including this introductory chapter. The literature review is presented in chapter 2, which starts from the statistical process control, and then focuses on the CUSUM chart. Chapter 3 mainly presents the new CUSUM charts detecting process mean shift; one is a combined chart and the other is an adaptive chart. A comparison study including seven CUSUM charts is also conducted. In

addition, the effect of sampling cost on chart design and performance is investigated.

Chapter 4 is centered on the CUSUM charts detecting process shifts in mean and variance. Two simple control charts are first proposed. These two new charts and a multi-chart will be then designed by optimal design. Their performance is compared with two highly effective charts, the 3-CUSUM($\mu+\sigma$) scheme (Reynolds and Stoumbos 2004*a*) and scale CUSUM chart (Hawkins 1981). Furthermore, the effect of sampling cost and the probability distribution of process shift on chart design and performance are also studied. Finally, chapter 5 presents the conclusions that summarize all the research projects conducted in this thesis. At the end, suggestion for future research and outlook is provided.

Chapter 2

Literature Review

2.1 History of Quality

Quality originated along with the emergence of manufacturing and production. In the late 13th century, the European craftsmen were organized into unions called guilds. They were responsible to make and check the product. Until the early 19th century, manufacturing in the industrialized world tended to follow this craftsmanship model.

According to Klyatis and Klyatis (2006), in early 20th century, most production departments were supervised by a foreman who was also in charge of inspecting the product. During World War II, many non-conforming products were delivered to the military units because of high demand. To improve product quality, the manufacturing companies moved inspectors out of production department and organized them in a special inspection department. Such arrangement inspired the emergence of the new technical specialists who employed sampling and SPC technology and were later called quality control engineers.

Based on the fundamental work of Deming, Juran and the early Japanese practitioners in quality, quality and its management tools, such as SPC, have extended their applications into a broader scope, involving service, healthcare, education and government sectors, *etc*.

2.2 Quality Control and Quality Assurance

Statistical techniques including SPC and designed experiment are often used to reduce the process variability (Montgomery 2009). Quality control (*QC*) engineer and quality assurance (*QA*) engineer are two common positions in industry. QA consists of the planned and systematic activities which ensure that the quality levels of products and services are properly maintained and that supplier and customer quality issues are properly resolved. It i**s** mainly executed through quality system documentation which involves the policies, procedures, work instructions, specifications, and records created in the organizational activities. QC indicates the inspection techniques and activities to fulfill requirements for quality.

Montgomery (2009) did not specially indicate the hierarchy relationship between QA and QC; he suggested that they are both effective management of quality. However, some people believe that there is a hierarchy relationship, as showed in Figure 2-1 (McCormick 2002). This illustration shows that, in a pharmaceutical industry, QC and QA are both responsible for quality management (*QM*). QM includes the overall policy of the organization towards quality. QA deals with all the risks from manufacturing or managerial aspects which may cause poor quality, and prevents quality problems by giving warnings of difficulties ahead. In the pharmaceutical industry, QC focuses on the processes in the manufacturing floor, testing of the environment, facilities, materials, components and product in accordance with the standard.

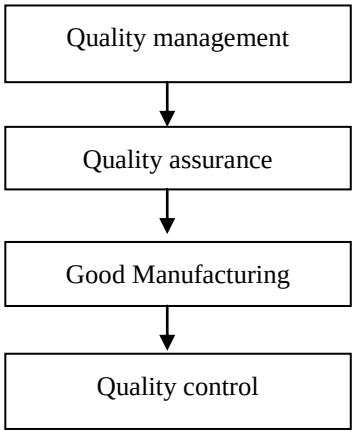

Figure 2-1. Relationship among QM, QA, GM and QC

No matter what the relationship is, it is agreed that QC is using techniques, especially the statistical techniques, to ensure quality.

2.3 Introduction to Control Chart

As the name indicates, Statistical Process Control (SPC) is to monitor the process using statistical tools. Statistical tools have become popular since 1940s. During the mid-1980s, statistical methodology was the most important study under the title of SPC (Klyatis and Klyatis 2006). Among the seven major SPC problem-solving tools, control chart is the primary technique of SPC to monitor the process (Montgomery 2009, Stoumbos *et al.* 2000).

Statistically, a process is often described by a group of data pertaining to its location and dispersion. When a process deviates from its target value, the mean and/or variance of the quality characteristic will change. To detect a process shift, a control chart records and analyzes the data of quality characteristics of interest which are sampled randomly while the process operates.

Quality characteristics are elements that jointly describe what the user or consumer thinks of quality (Montgomery 2009). It can be divided into several categories, such as the physical category and the sensory category. If the quality characteristics can be expressed in terms of a continuous numerical measurement, they are called variables. On the other hand, those that cannot be conveniently represented as the numerical, but as discrete data, are called attributes. They are classified as either conforming or nonconforming to the specifications. The variables usually contain more information of the process. Accordingly, control charts can be generally divided into two categories, the control charts for variables and the control charts for attributes.

Through proper transformation and organization, a quality statistic is formed from the quality characteristics and used to plot the control chart. The plotting of control chart started from the Shewhart 3-sigma control chart. Its fundamental theory is built based on hypothesis testing. From a statistical viewpoint, when a sample point falls outside of the control limits, it is regarded as an abnormal event. Since this event hardly occurs when the process is in control, thus there is sufficient reason to speculate that the process is out of control. Under such condition, the process will be stopped immediately and diagnosis is conducted to identify and remove the assignable cause.

2.3.1 Basic Control Chart

The first control chart is the Shewhart $\overline{X}$ control chart invented by Walter A. Shewhart while he worked for Bell Labs in the 1920s. This chart is effective in detecting large shifts. The cumulative sum (*CUSUM*) control chart and exponentially weighted moving average (*EWMA*) control chart are specially developed to detect small and moderate process shifts. Based on these basic charts, many other control charts and their combinations have been developed to achieve superior performance. Control chart has been proved in industries to be effective for detecting the variability of a process, preventing defects, reducing unnecessary process adjustment, providing information about process capabilities, and thus winning higher productivity at lower cost (Montgomery 2009).

Shewhart $\overline{X}$ Chart and *R* Chart

The construction of Shewhart $\overline{X}$ chart is based on hypothesis testing. When quality characteristic follows a probability distribution with in-control mean μ_0 and variance σ_0^2, the hypothesis could be set as follows if only the process mean is to be monitored:

$$\begin{aligned} &H_0 : \mu = \mu_0, \\ &H_1 : \mu \neq \mu_0, \end{aligned} \tag{2-1}$$

where μ is the current process mean. The control chart tests this hypothesis repeatedly at different points in time (Montgomery 2009). The general model to plot the control chart is proposed as follows:

$$\begin{aligned} &UCL = \mu_0 + L\sigma_0 / \sqrt{n}, \\ &\text{Center line} = \mu_0, \\ &LCL = \mu_0 - L\sigma_0 / \sqrt{n}, \end{aligned} \tag{2-2}$$

where *UCL* is the upper control limit, *LCL* is the lower control limit, *L* is the control limit coefficient (the distance from the center line expressed in the multiple of the in-control standard deviation), and *n* is the sample size (the number of units inspected in a sample). Equation (2-2) represents a standard practice and the chart with such form is referred to Shewhart control chart. The graph of a Shewhart $\overline{X}$ control chart is illustrated in Figure 2-2, in which process mean is to be tracked.

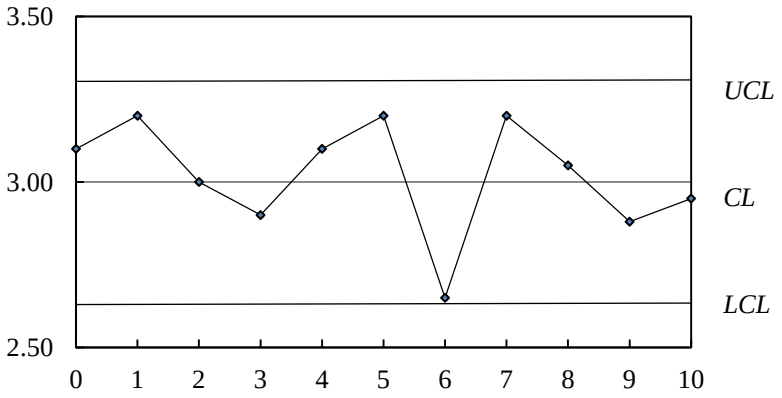

Figure 2-2. A Shewhart $\overline{X}$ Control Chart

Suppose a sample is collected at time *t* and the quality characteristic *x* of *n* units are measured, the horizontal axis records the time series and the vertical axis shows the corresponding sample mean value $\overline{x}_t$ of *n* observations in the *t*th sample. The process status is judged by observing the sample points. The simplest rule is to signal an out-of-control case when one single point falls out of the control limits. Two types of errors may be produced in the decision-making. The probability of type I error α means that the chance of the process is signaled as out of control because a point is plotted outside of the control limits while the process is actually in control; contrarily, the probability of type II error β means that the chance of the control chart does not signal when the process is already out of control, as the points are still plotted within the control limits. There are also many other run rules that can be used to make a decision about the process status. These run rules observe the nonrandom patterns of the points which can tell whether a process is in control or not. In 1956, the Western Electric Handbook suggested a set of run rules for detecting nonrandom patterns on control chart. These supplementary rules help to increase the sensitivity of control chart to detect small shifts and may aid diagnosing the cause of process shift. However, it is not recommended to simultaneously apply them, because it may increase the probabilities of type I error (Montgomery 2009).

Probability of Type I error α and type II error β are the bases to evaluate the performance of control chart. Suppose the quality characteristic has a normal distribution with mean μ_0 and standard deviation σ_0. During operation, a process shift

changes the mean to a new value μ_1. In Figure 2-3, the in-control probability curve is depicted in solid line while the curve of the shifted or out-of-control process is plotted using dashed line.

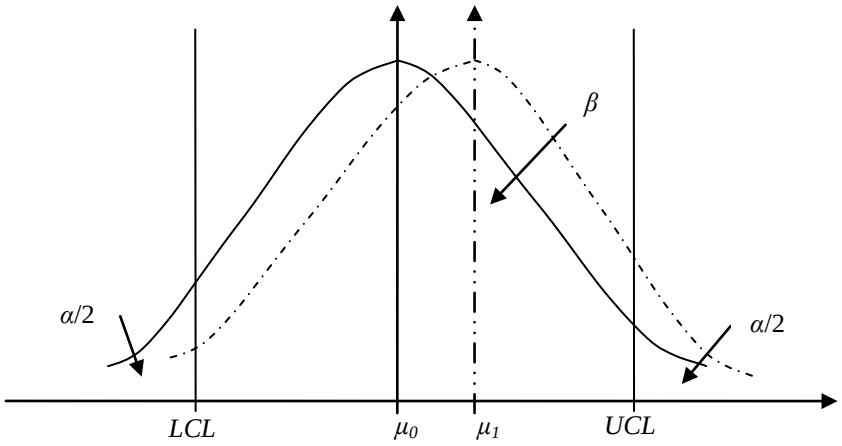

Figure 2-3. Normal Distribution of Sample Mean

Then probability of type I error α is the areas beyond the control limits *LCL* and *UCL* covered by the in-control curve. The probability of type II error β is the area within the control limits covered by the out-of-control curve. The two probabilities of type of errors are calculated as follows:

$$\alpha = \Phi\left(\frac{LCL-\mu_0}{\sigma_0/\sqrt{n}}\right)+1-\Phi\left(\frac{UCL-\mu_0}{\sigma_0/\sqrt{n}}\right), \tag{2-3}$$

$$\beta = \Phi\left(\frac{UCL-\mu_1}{\sigma_1/\sqrt{n}}\right)-\Phi\left(\frac{LCL-\mu_1}{\sigma_1/\sqrt{n}}\right). \tag{2-4}$$

It is customary to set *L* in Equation (2-2) as three, which creates the "three-sigma" control limit with probability of type I error approximately equal to 0.00135 in both ends. In fact, "three-sigma" limits are usually employed, regardless of the type of chart employed (Montgomery 2009). The design using "three-sigma" limits are called the heuristic design of control chart.

In practice, the process mean and variance are unknown, and have to be estimated from preliminary samples taken when the process is in-control. Let $\bar{x}_1, \bar{x}_2, ..., \bar{x}_m$ be the sample mean of *m* preliminary samples. The process mean (center line) is estimated as:

$$\bar{\bar{x}} = \frac{\bar{x}_1 + \bar{x}_2 + ... + \bar{x}_m}{m}. \quad (2\text{-}5)$$

Similarly, the standard deviation σ is estimated from either the sample standard deviations or the sample ranges of the m preliminary samples. Let R_1, R_2,…, R_m be the sample ranges of the m samples.

$$R_i = x_{i\max} - x_{i\min} \qquad i = 1, 2, \ldots, m, \quad (2\text{-}6)$$

where $x_{i\max}$ and $x_{i\min}$ are the maximum and minimum values of observations for the ith sample, respectively.

The average range is

$$\bar{R} = \frac{R_1 + R_2 + \cdots + R_m}{m}. \quad (2\text{-}7)$$

Then the control limits for the $\bar{x}$ chart is:

$$\begin{aligned} UCL &= \bar{\bar{x}} + A_2\bar{R}, \\ \text{Center line} &= \bar{\bar{x}}, \\ LCL &= \bar{\bar{x}} - A_2\bar{R}. \end{aligned} \quad (2\text{-}8)$$

And the R control chart for monitoring process variability through sample range can be constructed as:

$$\begin{aligned} UCL &= D_4\bar{R}, \\ \text{Center line} &= \bar{R}, \\ LCL &= D_3\bar{R}. \end{aligned} \quad (2\text{-}9)$$

The parameters A_2 in Equations (2-8), D_3 and D_4 in Equation (2-9) are constants used to calculate the control limits of the conventional 3-sigma $\bar{X}$ and R charts. Their values depend on sample size n. To simplify the design procedure, researchers have calculated their value and tabulated them for various values of sample size n. The table is available in any textbook for quality control.

CUSUM Control Chart

The CUSUM chart was first proposed by Page (Page 1954) as a supplement to the Shewhart chart. As the name indicates, the CUSUM chart is based on cumulative sum

of sample observations, using both previous and current information in process to check process status. Owing to the fact that on-line measurement and distributed computing systems become a norm in today's SPC applications (Woodall and Montgomery 1999), the application of CUSUM chart is becoming popular. For example, the CUSUM chart is widely used in the chemical and process industries. In these applications, the CUSUM charts are able to detect process shifts in both mean and variance, and to identify the point in time when the process shift occurs (Khoo 2005, Wu and Wang 2007).

The quality statistic C_t for the tth sample in the original CUSUM chart (Hawkins and Olwell 1998) is updated as follows:

$$C_t = \sum_{i=1}^{t} (x_i - \mu_0). \tag{2-10}$$

Equation (2-10) can be written in a recursive form:

$$\begin{aligned} C_0 &= 0, \\ C_t &= C_{t-1} + (x_t - \mu_0). \end{aligned} \tag{2-11}$$

If the standard value z_t $(=(x_t - u_0)/\sigma_0)$ of the quality characteristic x_t is used instead, Equation (2-10) is transformed into:

$$C_t = \sum_{j=1}^{t} z_t. \tag{2-12}$$

Or in a corresponding recursion form

$$\begin{aligned} C_0 &= 0, \\ C_t &= C_{t-1} + z_t. \end{aligned} \tag{2-13}$$

The plotting of the CUSUM control chart is similar to that of the Shewhart chart in Figure 2-2, except that the plotted statistic is C_t for the tth sample. When a plotted point C_t exceeds the control limit, the process is thought to be out-of-control. The design of the CUSUM charts has attracted a lot of research effort in recent years. More details will be expatiated in section 2.4.

EWMA Control Chart

The exponentially weighted moving average (EWMA) chart was introduced by Roberts in 1959 (Montgomery 2009). It accumulates historical and current information in a

different way. The statistic in an EWMA chart is defined as:

$$E_0 = \mu_0,$$
$$E_t = \lambda x_t + (1-\lambda)E_{t-1}, \quad \text{(2-14)}$$

where λ is the smoothing parameter which is chosen between zero and one.

The control limits can be constructed using the standard practice as showed in Equation (2-2). This chart is inferior to the CUSUM chart in determining the changing point (the time when a shift occurs). Same as the CUSUM chart, it is an ideal chart to use individual observation. Moreover, both CUSUM chart and EWMA chart have similar average speed of response to process shifts (Montgomery 2009).

2.3.2 Performance Measures

In any SPC application, it is not easy to select an appropriate control chart from the numerous ones if there is not a valid and unique standard to judge the charts. Generally, the performance of a control chart can be measured from two aspects: the response speed to a shift and the simplicity to design and implement. Detection effectiveness (or detection capability) of control charts is widely used as one of the performance measures. Statistically, it indicates the power of a control chart to signal the out-of-control cases. Then the response speed can be expressed as a function of the power. Detection effectiveness is often used as the objective function in the chart design. Since there is usually no numerical method to evaluate the simplicity in design and implementation of control chart, this performance measure is usually used in a descriptive manner.

ARL and *ATS*

The average run length (*ARL*) or the average time to signal (*ATS*) to detect a particular type of process change can be used as the performance measure for detection effectiveness. The expected number of samples for a control chart to signal the process shift after the change occurs is designated as *ARL*. If the process starts from out-of-control status, the expected number of samples before the chart signals is called the out-of-control *ARL* (ARL_1). Since ARL_1 shows the speed of a control chart responding to a process shift, it is commonly used as an indicator of the power (or effectiveness) of the control chart. Sometimes, there is no process shift, whereas the

chart will also issue a signal. In such condition, the expected number of samples from the process starts until the chart signals is called the in-control *ARL* (ARL_0), which indicates a false alarm rate. The ARL_1 values at one or a few specified process shift levels are often used as the objective function to be minimized in the optimal design of a control chart.

ATS indicates the expected value of time from the start of the process to the time when the chart signals. If the period of time is of interest, *ATS* is used instead and it equals the product of *ARL* and the sampling interval.

For a Shewhart chart where the sample data is uncorrelated, the *ARL* is calculated as：

$$ARL = \frac{1}{p}, \tag{2-15}$$

where p is the power of the chart or the probability that a sample point exceeds the control limits. The power p is equivalent to the probability of type I error α when process is in control, and it is complementary to the probability of type II error β (*i.e.* $p = 1-\beta$) when process is out of control. So the in-control ARL_0 and the out-of-control ARL_1 can be expressed in terms of the probabilities of type I error and type II error, respectively:

$$ARL_0 = \frac{1}{\alpha}, \tag{2-16}$$

$$ARL_1 = \frac{1}{1-\beta}. \tag{2-17}$$

For a two-sided Shewhart chart, the probabilities of type I error and type II error are calculated using Equations (2-3) and (2-4).

Steady State and Zero State

Generally speaking, two modes of process states are distinguished when calculating *ARL* or *ATS*: the zero-state mode and steady-state mode. The zero-state mode means that the process always falls out of control from the beginning of a sampling interval; while the steady-state mode implies that the process has operated in a normal condition for a long time and then a shift may occur any time (Reynolds *et al.* 1990). The steady-state *ARL* is computed assuming that the quality statistic has reached its steady-state or stationary distribution condition by the random time point that the

change occurs (Reynolds & Stoumbos 2004*a*, *b*).

The *ARL* values under different modes will be different. For instance, the steady-state *ARL* of CUSUM chart is usually smaller than the zero-state *ARL* since its CUSUM statistic C_t has a value that could already be on the way to the control limit when process shift occurs (Hawkins and Olwell 1998).

Since the steady-state mode allows the shift to occur randomly, the *ARL* computed under this mode is more accurate (Nenes and Tagaras 2008). The steady-state *ATS* is also used in Reynolds and Stoumbos' studies (2004*a*, 2004*b*, 2005). Furthermore, since production processes often operate in in-control condition for most or relatively long periods of time (Montgomery 2009), the steady-state mode is therefore more realistic than the zero-state mode. In light of this, the thesis always assumes that the process is in a steady-state before a shift occurs.

2.3.3 Design of Control Charts

The goals of designing the control charts include making a chart effective for detecting process shifts of different sizes, sensitive to both mean and variance shifts, maintaining a low false alarm rate, simple to use and interpret, and capable of indicating the type and direction of the shift. Meanwhile, the design procedure should be as simple as possible. Usually, one chart outperforms another only in one or some aspects. Thus these multiple goals must be balanced with each other. Since control chart is plotted with sample data, its performance is determined by the sample size, control limit, sampling frequency and other parameters which will allow the chart to maximally realize the design goals of interest. The charts designed for different goals or purposes have different parameters.

Currently there are three general approaches to design a control chart (Saniga 1989). The first one, likely the most popular one, is through the use of heuristics such as Shewhart's. This method begins from the Shewhart control chart with "three sigma" control limits and takes a rational subgroup. It can be applied to many types of control charts.

The statistical design is another method to design the control chart. This usually

involves selecting the sample size, sampling interval, control limits and other charting parameters so that the out-of-control *ATS* of the chart for detecting a process shift is minimized and the in-control ATS_0 is equal to or larger than a specified value.

The third approach, the economic design, originated in Duncan' s study (1956) in which the sample size, sampling interval and control limits of a Shewhart $\overline{X}$ chart were determined in order to acquire a maximum average net income. Lorenzen and Vance (1986) generalized Duncan's model to make it applicable to most types of control charts. Later, it is rapidly applied to the design of all kinds of control charts (Elsayed and Chen 1994, Chou *et al.* 2000, Serel and Moskowitz 2008).

Economic design considers the economic factors involved in operating the control chart. Mostly it considers the costs of maintaining control charts related to a whole production cycle, such as sampling cost, inspection cost, false alarm cost, and correction cost, *etc.* However, it receives many criticisms for excluding the statistical features. Woodall *et al.* (1986) remarked that since the only aim of designing a chart in the Duncan-type economic model was to pursue a minimum total expected cost, it might cause high false alarm and bring extra variability into the process. Besides, including all the costs related to operating a control chart often makes it difficult to determine the specifications for the chart design. Other obstacles come from the shortage of hardware/software and the professionals in the shop floor to implement the economical design, because these applications are complex and require special algorithm (Keats *et al.* 1997).

Adding some statistical constraints pertaining to some statistical properties, such as the probabilities of type I error and type II error, to the economic model can improve the chart performance (Montgomery 2009). Such improvement could be found in the studies of the joint economic-statistical design of $\overline{X}$ and *R* charts, where the constraints on in-control and out-of-control *ATS* are used (Saniga 1989, McWilliams 1994, Saniga *et al.* 1995).

Del Castillo *et al.* (1996) made another improvement. They simplified the Duncan-type economic model by considering only the sampling and inspection cost in the design of

the $\overline{X}$ chart. However, they set three objective functions to be minimized simultaneously: expected number of false alarms, average time to signal, and sampling and inspection cost. A non-linear multiple-objective optimization algorithm was employed to approximate the weighting of the three objectives through analyzing the preference information, which was provided by decision maker. Thereafter the optimal values of sample size, sample interval and control limits were determined. This method is complicated as it has to mediate three objective functions and a relatively subjective result is obtained by introducing the preference information.

At present, the statistical design method dominates the designs of control charts. However, there is an increasing tendency to include the economic factors into the statistical design. In this thesis, chapters 3 and 4 will contain economic considerations when designing a control chart by statistical method.

2.3.4 Phase I and Phase II Operation

To apply a control chart to monitoring the process parameters, Phase I and Phase II operations are distinguished. In phase I, preliminary samples are collected and preliminary control chart is established to testify if the process is in control. The mean and variance of the quality statistics are acquired based on the data of the preliminary samples, and the corresponding control limits are constructed. Judgment about the process status is made using the preliminary control chart. If the process is thought to be out-of-control, those data that fall outside of the preliminary control limits will be investigated and deleted, and new preliminary control chart is established. This procedure is repeated until the process is thought to be in-control. This is referred to as the retrospective test of control charts. In Phase II, the final control chart that has passed the retrospective test is used to monitor the forthcoming samples drawn from the process.

If there are not sufficient data in Phase I, then the resulting charts to be used in Phase II may not work as well as expected. To transit from Phase I to Phase II, much work, process understanding and process information are often required (Woodall 2000).

For a traditional control chart, it is recommended that 20 to 30 preliminary samples

with size of four to five be used to estimate the process parameters (Montgomery 2009). Jensen *et al.* (2006) suggested that more data in Phase I are needed than typically recommended in order to achieve performance comparable with the known parameters cases. In particular, for the CUSUM chart, the number of preliminary samples should be in the hundred scales rather than the dozen scales as used by Shewhart chart (Hawkins and Olwell 1998). For example, Quesenberry (1993) recommended that at least 100 samples of size five be used in Phase I for CUSUM chart. It is because that the CUSUM chart is sensitive to small shifts and any random error in the estimated parameter will tend to cause deviated in-control and out-of-control performance.

2.3.5 Control Charts for Monitoring Mean and/or Variance

When a quality characteristic is a random variable follows a probability distribution, it can be characterized by two distribution parameters: the mean and variance. Thus, these are two kinds of process shifts that control charts are designed to detect. Usually, one chart is specialized for detecting one type of process shift. However, if properly designed, a single control chart is also able to detect both mean and variance shifts.

To detect shifts with wide ranges, two or more control charts can be applied simultaneously. It is also called the multi-chart schemes in the thesis. For instance, Lucas (1982) proposed the combined application of a CUSUM chart and a $\overline{X}$ chart which is effective over a wide range of mean shifts. Other researchers (Sparks 2000, Zhao *et al.* 2005) recommended using two or three CUSUM charts simultaneously to detect a wide range of mean shifts, in which each individual CUSUM chart detects a specific sub-range of shift. Reynolds and Stoumbos (2004*a*) proposed another CUSUM scheme consisting of three separate CUSUM charts for detecting both mean and variance shifts.

Many researchers have made effort to design a single chart to detect both mean and variance shifts. White and Schroeder (1987) first introduced a chart to monitor both process mean and variance of an electronic component. The control limits of this chart are determined by the median and a spread called the *Q*-spread. Domangue and Patch (1991) developed some omnibus EWMA schemes based on the exponential of the absolute value of the standardized sample mean of observations. A Max chart (Chen

and Cheng 1998) plots the maximum absolute values of the standardized mean and standard deviation. It is effective in detecting large shifts in the process mean and/or standard deviation. Chen *et al.* (2001) proposed the Max-EWMA chart which is effective in detecting small shifts. These charts can figure out which parameter has shifted as well as the direction of the shift when an out-of-control case occurs. A comprehensive review about the single chart in monitoring process mean and variance can be found in Cheng and Thaga' study (2006).

2.3.6 Adaptive Control Chart

An adaptive control chart allows its parameters to change based on the observed values of sample statistics which indicate the current process status. Typical adaptive charts include the variable sample sizes (*VSS*) chart, the variable sampling intervals (*VSI*) chart and the variable sample sizes and variable sampling intervals (*VSSI*) chart (Tagaras 1998, Wu and Luo 2004). Adaptive charts can be more efficient than the fixed sample size and sampling interval (FSS) control charts because they determine the next sampling strategy based on the current samples.

Reynolds *et al.* (1988) proposed the VSI $\overline{X}$ chart to monitor the process mean. The sampling interval between two samples depends on what is observed in the current sample. The sampling interval is short if sample mean $\overline{X}$ is close to the control limit; while a longer sampling interval is applied if $\overline{X}$ is close to the target value. These VSI charts could be employed with run rules. It achieves better performance than the charts with fixed sample interval. Reynolds *et al.* (1988) suggested using two different sampling intervals. Subsequently, the VSI procedure for CUSUM chart was also studied (Reynolds *et al.* 1990).

Runger and Pignatiello (1991) proposed a "dual waiting time" strategy to adapt the sampling interval between successive samples based on the results observed in each sample. Flaig (1991) studied the adaptive Shewhart $\overline{X}$ chart with variable sample size for detecting process mean shifts. The area between the central line and control limits is divided into three zones. The sample size to be taken in the next sample depends on the zone the current sample point falls in.

Daudin (1992) proposed a double sampling $\overline{X}$ chart. A second sample of larger size is taken if the mean of the first sample falls between a warning limit and the control limit. A comparative study shows that this scheme generally outperforms the Shewhart chart, EWMA chart and CUSUM chart in detecting process shifts.

Prabhu *et al.* (1993) also proposed a VSS Shewhart chart. Its performance is superior to that of the standard Shewhart control chart, particularly for small shifts. In 1994, Prabhu *et al.* introduced a VSSI $\overline{X}$ chart which made sufficient improvement in performance over the standard Shewhart chart, VSI chart or VSS chart.

Zimmer *et al.* (1998) studied the three-state adaptive control chart to detect process mean under both steady state and zero state. Unlike the two-state chart, the three-state chart has two additional threshold limits in each side of the center line, and therefore divides the region between two control limits into six zones. There are three different sample sizes. As the process moves away from the center line, the sample size increases. The average sample size is equal to the sample size of a conventional Shewhart chart. Since it is found that this chart is only slightly better than the two-state adaptive chart, the two-state adaptive strategy is recommended for most applications.

Jensen *et al.* (2008) investigated the impact of parameter estimation on the performance of a VSSI chart. He used a dual sampling scheme with two sampling intervals and two sample sizes. The threshold limit is closer to the center line than to the control limits. When a point falls within the threshold limits, a smaller sample size and a larger sampling interval are used. When a point falls outside the threshold limits but still within the control limits, a larger sample size and a smaller sampling interval are adopted. Their results show that an adaptive control chart should be used only when sufficient amount of Phase I data have been obtained to ensure an accurate estimation of process distribution parameters.

Costa and Maysa (2007) studied the non-central chi-square statistic (NCS) chart for monitoring both process mean and variance, in which all of the design parameters are adaptable (the sample size, the sampling interval, and the control limit coefficient). Their chart is not only operationally simpler than the joint $\overline{X}$ and R charts with

variable parameters, but also more sensitive to process shifts in mean and variance.

In general, the adaptive control chart has higher detection effectiveness than the conventional FSS chart.

2.3.7 Control Charts for Multiple Variables

In work shop floors, it is common that more than one quality characteristics on a same product are required to be inspected simultaneously. It is inappropriate to control them separately as these characteristics may have interaction. For example, if three distinct control charts are used independently to control a process featured by three related quality characteristics, the probabilities of type I error and type II error are not equal to their advertised levels for the individual control charts.

The multivariate control chart is specially devised for such problems. In 1947, Hotelling used a multivariate Shewhart chart to solve a bombsights problem during World War II. This kind of charts are most helpful in many chemical and process plants and semiconductor industry, where quality data on hundreds of variables need to be dealt with routinely.

One approach to constructing a multivariate control chart is to form a single control statistic from the multivariate data in each sample. This quality statistic would usually be a quadratic form involving summary statistics for each variable. The most common multivariate control chart is the Hotelling T^2 control chart for monitoring the mean vector of the process. The resulting control chart has the disadvantage as the Shewhart-type charts, both are inefficient for detecting small and moderate shifts**.**

To construct a multivariate chart which is sensitive to small shifts, the EWMA or CUSUM statistic for each variable is recorded, and then the quadratic form of these individual univariate statistics is generated as a single control statistic. It is the single statistic that is plotted on a control chart.

2.4 CUSUM Control Chart

2.4.1 Forms of CUSUM Chart

There are two forms to represent a CUSUM chart, one is the *V*-mask form of the CUSUM, and another is the tabular (or algorithm) CUSUM (Montgomery 2009).

_V_-mask CUSUM

V-mask CUSUM was proposed by Barnard in 1959, and is used when the quality characteristic is in its standardized form.

Hawkins and Olwell (1998) gave a detailed explanation about how a *V*-mask CUSUM works. Suppose an increasing mean shift δ_μ occurs at time t, then from the point (t, C_t) on a CUSUM chart, a line with slope k (reference parameter) can be drawn. If the future points fall below the line, the mean has not shifted; if a future point is above the line with at least a distance of H (control limit), it is explained as the occurrence of a process shift. Similar principle works for detecting a decreasing mean shift.

Using the above procedure, a *V*-mask CUSUM has two legs and a flat front end with a height of $2H$. Figure 3-1 shows the shape of a *V*-mask (Montgomery 2009). From the front end, one line with slope k and passing through $(t, C_t - H)$ can detect increasing shift, and another line with slope $-k$ and passing through $(t, C_t + H)$ can detect decreasing shift. When a new cumulative sum is computed, align the center of the front edge with the point just plotted. If all previous points fall within the legs, then the process is in control.

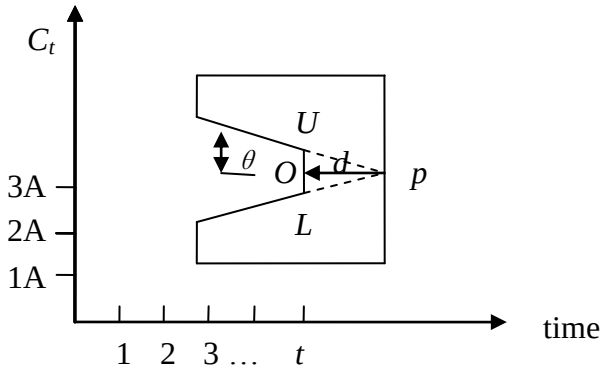

Figure 2-4. A Typical *V*-mask

Despite of its convenient usage in application, the *V*-mask CUSUM is rejected by most

researchers (Montgomery 2009). Some reasons can account for this. First of all, the head start feature which improves the performance of CUSUM chart cannot be expressed in this form. Secondly, it is unclear how far the legs of the *V*-mask should extend. As a result, it is difficult to determine whether a point falls inside or outside of the legs. Thirdly, the probabilities of type I error and type II error are statistical quantities and are not appropriate to judge a single sample as the application in *V*-mask CUSUM.

Tabular CUSUM

The tabular CUSUM chart reorganizes the mathematic expression of statistic C_t (equation (2-12)), and uses a table to manipulate the cumulative sum in two directions, *i.e.*, deviations that are above and below the target value μ_0. The statistic C^+ accumulates the deviation above the target and therefore is used in the one-sided upper CUSUM (or high-sided CUSUM); and C^- is correspondingly used in the one-sided lower CUSUM (or low-sided CUSUM). To monitor the process mean, the statistics C_t^+ and C_t^- for the *t*th sample are computed as follows (Montgomery 2009):

$$C_t^+ = \max\left[0, x_t - (\mu_0 + k) + C_{t-1}^+\right], \tag{2-18}$$

$$C_t^- = \max\left[0, (\mu_0 - k) - x_t + C_{t-1}^-\right], \tag{2-19}$$

where the starting values are $C_0^+ = C_0^- = 0$, and the reference parameter k is often chosen as halfway between the target mean μ_0 and a specific out-of-control mean μ_1. When the mean value is expressed in a standardized form, k is usually one-half of the magnitude of the process shift.

An example of the tabular form CUSUM is shown in Table 2-1, where k is set as 0.5 and the target value $\mu_0 = 5.0$.

Table 2-1. The Tabular CUSUM

Period *t*	x_t	(*a*)			(*b*)		
		$x_t - (\mu_0 + k)$	C_t^+	N_t^+	$(\mu_0 - k) - x_t$	C_t^-	N_t^-
1	5.23	-0.27	0	0	-0.73	0	0
2	3.96	-1.54	0	0	0.54	0.54	1
3	3.45	-2.05	0	0	1.05	1.59	2
4	3.69	-1.81	0	0	0.81	2.4	3

The quantities N^+ and N^- indicate the number of consecutive periods that the CUSUMS C_t^+ and C_t^- have been nonzero. The tabular CUSUM will signal when either C_t^+ or C_t^- exceeds the control limits.

In practice, C_t^- may have a different form.

$$C_t^- = \min\left[0, x_t - (\mu_0 - k) + C_{t-1}^-\right]. \tag{2-20}$$

The difference between the two expressions of C_t^- is that one ranges from 0 to H in Equation (2-19), and the other ranges from 0 to $-H$ in Equation (2-20).

One disadvantage of the tabular CUSUM comes from a property that each variable has two cumulative sums, thus the difficulty for generalizing to a multivariate procedure is increased.

To complement this, Crosier (1986) proposed a two-sided CUSUM scheme:

$$\begin{aligned} &C_t = \left|S_{t-1} + x_t - \mu_0\right|, \\ &S_t = 0, \qquad\qquad \text{if } C_t \le k\sigma, \\ &S_t = \left(S_{t-1} + x_t - \mu_0\right)(1 - k\sigma / C_t), \qquad \text{if } C_t > k\sigma, \end{aligned} \tag{2-21}$$

where $S_0 = 0$. The scheme signals an increasing mean shift if $S_t > H\sigma$ or a decreasing mean shift when $S_t < -H\sigma$.

Furthermore, Uys and Lombard (2007) proposed a new scheme which has substantially smaller out-of-control *ARL* than either the standard two-sided scheme or Crosier's scheme (1986) for small mean shifts. It works as follows:

$$Y_t = sign(x_1 + \cdots + x_{t-1}) \times x_t \qquad t = 2, 3, \ldots, \tag{2-22}$$

$$\begin{aligned} &D_1 = 0, \\ &D_t = \max(0, D_{t-1} + Y_t - k). \end{aligned} \tag{2-23}$$

However, it loses much of the advantage for large shifts.

One- and Two-Sided CUSUM

When the focus is to detect increasing or decreasing shift, a one-sided upper or lower CUSUM chart can be applied. In fact, it is partly the form of the two-sided CUSUM

chart. In a process with target mean μ_0 and standard deviation σ_0, the cumulative statistic to detect an upward mean shift is updated by:

$$\begin{aligned} C_0^+ &= 0, \\ C_t^+ &= \max(0,\ C_{t-1}^+ + x_t - u_0 - k). \end{aligned} \tag{2-24}$$

Or, in the standardized form:

$$\begin{aligned} C_0^+ &= 0, \\ C_t^+ &= \max(0,\ C_{t-1}^+ + z_t - k), \end{aligned} \tag{2-25}$$

where z_t is the standardized value of x_t which is the *t*th sample value. When C_t^+ is larger than the upper control limit *H*, the chart signals an upward shift.

Similarly, to detect a downward shift in mean, the CUSUM is updated by

$$\begin{aligned} C_0^- &= 0, \\ C_t^- &= \min(0, C_{t-1}^- + x_t - u_0 + k). \end{aligned} \tag{2-26}$$

Or, in the standardized form:

$$\begin{aligned} C_0^- &= 0, \\ C_t^- &= \min(0,\ C_{t-1}^- + z_t + k). \end{aligned} \tag{2-27}$$

It signals if $C_t^- < -H$.

It is noted that a 3-sigma Shewhart $\overline{X}$ chart is essentially a CUSUM scheme with *k* = 3 and *H* = 0. And it signals an upward shift if $C_t^+ > 0$.

To detect process variance shift, Hawkins (1981, 1993) used a new standardized quantity

$$v_t = \frac{\sqrt{|z_t|} - 0.822}{0.349}. \tag{2-28}$$

He observed that v_t is more sensitive to variance shifts than mean changes. A two-sided CUSUM chart to detect variance changes is established as follows:

$$\begin{aligned} S_t^+ &= \max(0, v_t - k + S_{t-1}^+), \\ S_t^- &= \max(0, -v_t - k + S_{t-1}^-), \end{aligned} \tag{2-29}$$

where $S_0^+ = S_0^- = 0$ and the values of reference parameter *k* and control limit *H* are

selected in the same way as that of the CUSUM chart for process mean.

Even though the CUSUM chart is inferior to the Shewhart $\overline{X}$ chart in detecting large shift, it is generally more effective than the latter in detecting process shifts from an overall viewpoint, because the $\overline{X}$ chart only uses the process information contained in the last sample point and ignores information given by the entire sequence of points (Montgomery 2009).

2.4.2 Improved CUSUM Chart

Many researchers (Sparks 2000, Reynolds and Stoumbos 2004*a*, Shu and Jiang 2006) pointed out that a control chart must have an excellent overall performance, being effective for detecting small as well as large process shifts of different combinations of δ_μ (mean shift in terms of the in-control standard deviation σ_0) and δ_σ (standard deviation shift in terms of σ_0), as the magnitude and type of future shifts are unknown in most of the cases.

In order to make the CUSUM chart effective in a broad domain of shifts, one possible approach is to combine it with other charts. It includes the $\overline{X}$ &CUSUM chart (Lucas 1982), the generalized likelihood ratio (*GLR*) chart (Siegmund and Venkatraman 1995), and the 3-CUSUM chart (Lorden and Eisenbergre 1973, Dragalin 1997, Sparks 2000, Reynolds and Stoumbos 2004*a*). Another possibility is to use the adaptive features for the CUSUM procedure when one-step-ahead forecast of process can be made efficiently (Sparks 2000).

$\overline{X}$ &CUSUM Chart

The $\overline{X}$ &CUSUM chart was proposed by Lucas (1982). This chart plots two quality statistics. One is the *t*th sample mean $\overline{x}_t$ from the process which represents a single reading or the average value of *n* observations. The other is the cumulative sum C_t^+ or C_t^-. The chart issues a signal when any or both x_t and C_t^+ (or C_t^-) falls outside of the corresponding control limit.

In Lucas's design, the mean shift of interest ranges from 0.0 to 5.0 (in terms of standard deviation σ_0). Three values (3.0, 3.5 and 4.0) of the upper control limit *UCL*

of the $\overline{X}$ chart are examined, because *UCL* smaller than 3.0 has short in-control ARL_0 while *UCL* greater than 4.0 has little effect on the $\overline{X}$ &CUSUM chart performance. When the reference parameter k is set around 0.5 and the control limit H between four and five, the CUSUM chart could produce a desired in-control ARL_0. Lucas found that the chart has a large in-control ARL_0 and a short out-of-control *ARL* for all mean shifts larger than 2.0σ or 2.5σ.

As mentioned in section 2.4.1, $\overline{X}$ chart is actually a special CUSUM chart. In this regard, the $\overline{X}$ &CUSUM chart is a special case of the 2-CUSUM chart. A general 2-CUSUM chart is running two CUSUM charts concurrently in which each sub-CUSUM chart is designed to detect a specified shift size. Correspondingly, it has two reference parameters k_1 and k_2, and two control limits H_1 and H_2. The superiority of a 2-CUSUM chart in performance has been demonstrated by Lorden and Eisenberger (1973) and Dragalin (1997). They found that it has higher effectiveness to detect moderate and large shifts.

3-CUSUM Scheme

It is reasonable to apply several CUSUM statistics simultaneously with different levels of memory. A signal is given if any of these CUSUM statistics exceeds its respective control limit.

Some researchers (Sparks 2000, Zhao *et al.* 2005) recommended using three CUSUM charts simultaneously. Sparks (2000) proposed a 3-CUSUM scheme detecting mean shifts. This combination consists of three separate CUSUM charts which are operated simultaneously. The scheme has six charting parameters, *i.e.*, the reference parameters k_1, k_2, k_3 and control limits H_1, H_2, H_3 for the three separate CUSUM charts. As a result, it would be extremely difficult to carry out an optimal design for the 3-CUSUM scheme. Sparks suggested to make the three sub-CUSUM charts sensitive to the shifts $\delta_{\mu 1}$ (= 0.75), $\delta_{\mu 2}$ (= 1.00), and $\delta_{\mu 3}$ = (1.50), respectively, for a nominal mean shift range between ($\delta_{\mu,\min} = 0.60$) and ($\delta_{\mu,\max} = 1.75$). The control limit for each sub-CUSUM chart is determined so that each sub-CUSUM chart has the same in-control ARL_0 when applied individually and meanwhile the 3-CUSUM scheme as a whole has an ARL_0 equal to a specified value τ.

Reynolds and Stoumbos (2004*a*) proposed another 3-CUSUM scheme for detecting both mean and variance shifts. It has four charting parameters, H_X (the control limits for mean shift), H_X^2 (the control limit for square of mean shift), plus the two reference parameters k^X and k^{X^2}. The performance of this chart has to be evaluated by simulation.

To differentiate these two 3-CUSUM schemes, the one proposed by Sparks (2000) is called 3-CUSUM(μ) scheme and the one devised by Reynolds and Stoumbos (2004*a*) is named as 3-CUSUM($\mu+\sigma$) scheme in this thesis.

Adaptive CUSUM Chart

Sparks (2000) proposed an adaptive CUSUM chart, namely ACUSUM chart, which adjusted the reference parameter *k* according to the on-line estimated value $\hat{\delta}_\mu$ of the mean shift. This adaptive feature could make the ACUSUM chart more efficient in signaling a range of future expected but unknown mean shifts from a holistic viewpoint. The *ARL* of the ACUSUM charts is evaluated using Monte Carlo simulation.

Shu and Jiang (2006) simplified the design and implementation of the ACUSUM chart. Particularly, they developed a two-dimensional Markov procedure to evaluate the *ARL* of the ACUSUM chart and formulated a more applicable algorithm to compute the control limit.

$$H \approx \frac{\ln[1+2k^2 \cdot ARL_0 + 2.332k]}{2k} - 1.166. \qquad (2\text{-}30)$$

Both Sparks (2000) and Shu and Jiang (2006) used an EWMA procedure to estimate the mean shift $\hat{\delta}$, and then set the reference parameter *k* equal to $0.5\hat{\delta}$.

A CUSUM chart with a "dual sample size" scheme was studied by Annadi *et al.* (1995). This chart has a similar adaptive feature as the one proposed by Prabhu *et al.* (1993) (see section 2.3.6) and could detect small shifts in the process mean more quickly. In this chart, two sample sizes n_1 and n_2 ($n_1 < n_2$) and a threshold limit *w* are manipulated so that the average sample size is n_0 when the process is in control. Here n_0 is the

specified sample size for the chart using a fixed sampling scheme. The limit w determines the switch between sample sizes n_1 and n_2. The next sample size would be n_1 if the CUSUM statistic is less than w and n_2 if it is greater than w.

Zhang and Wu's (2007) proposed an adaptive CUSUM chart based on weighted loss function (*WL*) to detect process mean and variance.

$$\begin{aligned} C_0 &= 0, \\ C_t &= \max(0, C_{t-1} + WL_t - k), \end{aligned} \tag{2-31}$$

where $WL_t = \lambda s_t^2 + (1-\lambda)(\bar{x}_t - \mu_0)^2$. In this formula, $\bar{x}_t$ and s_t are the sample mean and sample standard deviation of the tth sample and λ is the weighting parameter between (0, 1). This chart has a warning limit w and a control limit H, which divides the chart into three zones: the central zone (0, w), the warning zone (w, H) and the action zone (H, ∞). If the statistic C_t falls into the central zone, a relax sample with a smaller sample size n_1 is adopted for the next sample. On the other hand, if C_t falls into the warning zone, an alert sample with a larger sample size n_2 should be chosen. They found that the chart is usually more powerful than other charts in the whole shift domain, especially in the moderate and large shift regions.

CUSUM Chart with Head Start

This feature was devised by Lucas and Crosier (1982) to improve the sensitivity of a CUSUM chart at process start-up especially when the process is in fact out of control from the beginning. The fast initial response (*FIR*) or head start essentially sets the starting values C_0^+ and C_0^- equal to some nonzero value, typically one-half of control limits. If the process starts in control, C_0^+ and C_0^- will quickly drop to zero and the head start will have little effect on the performance of the CUSUM procedure. However, if the process starts at some level different from the target value, the head start will allow the CUSUM to detect deviation more quickly, resulting in shorter out-of-control *ARL* value. Usually, the out-of-control *ARL* are 30 to 40 percent shorter when a FIR CUSUM is used.

A FIR CUSUM can be designed to have an equivalent in-control ARL_0 and a smaller out-of-control *ARL* compared to a standard CUSUM by increasing H slightly to compensate for the decrease in ARL_0 caused by the head start.

2.4.3 Evaluation of *ATS* for CUSUM Chart

It is difficult to interpret the probability of a false alarm for a control chart, such as CUSUM chart, which combines information over time (Woodall 1990). In addition, the *ARL* of CUSUM chart cannot be calculated directly from the probabilities of type I and type II errors as for the Shewhart chart in section 2.3.2.

Generally, there are three approaches to calculate the *ARL* of a CUSUM chart: simulation, integral-equation approach, and Markov-chain procedure (Chen and Chen 2007).

The integral-equation approach calculates *ARL*s more accurately than the Markov-chain approach, but it is less versatile. The Markov-chain approach can calculate both the *ARL* and the distribution of run length. It has also been used to calculate the properties of different modified CUSUM schemes as showed in the following chapters.

Simulation Method

It has been mentioned in section 2.3.2 that process status has two modes. In order to calculate the steady-state properties, a number of P initially in-control samples are taken to imitate the steady state operation before the process shift occurs. In this phase, the simulation might issue some false alarms before the process shifts. There are two methods dealing with this problem. The first is to discard the whole simulated observations and recount the number of samples from the beginning, so that there are always P samples before the shift occurs. Another method is to reset the cumulative sum back to its initial value, and keep counting the samples. After the P in-control samples are obtained, the subsequent out-of-control samples are taken to imitate a random shift. The quality characteristic C_t is updated and compared against the control limit. When it falls beyond the control limit, the process is thought to be out-of-control. If C_t is smaller than the control limit, another sample is taken. The procedure repeats again and again until the process is judged to be out-of-control. If the zero-state *ATS* is of interest, the simulation is carried out by generating out-of-control samples from the beginning (*i.e.* $P = 0$).

Integral Equation Method

The integral equation was originally derived by Page (1954) for a one-sided CUSUM scheme. It is based on Fredholm's integral equation. A general description of the construction of one-sided and two-sided CUSUM procedures was given by Van Dobben De Bruyn (1968). Various expressions for the exact run length distribution and its parameters were given for the one-sided CUSUM procedure by Ewan and Kemp (1960), Brook and Evans (1972), and Woodall (1983). Lorenzen and Vance (1986) evaluated the upper-sided ARL^+, and lower-sided ARL^-, using the similar equations as Page's. Woodall and Adams (1993) recommended the *ARL* approximation given by Siegmund (1985). Hawkins and Olwell (1998) provided a table of constants that simplify the calculation of the integral equation and ensure an accuracy within 1-3% of the true *ARL* value.

Markov Chain Procedure

Brooke and Evans (1972) gave the form of the probability transition matrix for one-sided CUSUM scheme. Woodall (1984), Lucas and Crosier (1982) extended it to a two-sided CUSUM chart. Suppose the CUSUM statistic experiences m in-control transitional states $S_0, S_1, \ldots, S_{m-1}$ before being absorbed into the out-of-control state S_m. The width of the interval of each state is given by

$$d = H / (m - 0.5), \tag{2-32}$$

where H is the control limit. The center, O_i, of state i is given by

$$O_i = i \cdot d \qquad i = 0, 1, \ldots, m\text{-}1. \tag{2-33}$$

Let p_{ij} be the transition probability from state i to state j. Then for the CUSUM form $C_0 = 0,\ C_t = \max(0, C_{t-1} + x - k)$ for monitoring the mean of x with a normal distribution ~ $N(\mu, \sigma^2)$,

$$p_{ij} = \begin{cases} \Pr[O_i + x_t - k \le 0.5d] = F[(0.5 - i)d + k], & \text{for } j = 0, \\ \Pr[O_j - 0.5d \le O_i + x_t - k \le O_j + 0.5d] & \\ \quad = F[(j - i + 0.5)d + k] - F[(j - i - 0.5)d + k], & \text{for } j > 0, \end{cases} \tag{2-34}$$

where the cumulative probability function $F()$ is calculated as follows:

$$F(Y) = \Pr(x_t \le Y) = \Phi\left(\frac{Y - \mu}{\sigma}\right), \tag{2-35}$$

where $\Phi()$ is the cumulative probability function of the standard normal distribution.

In order to evaluate the in-control ARL_0, $F()$ must be calculated by using in-control mean and standard deviation. Based on p_{ij}, the transition probability matrix $\boldsymbol{R_0}$ can be established. It is a $m \times m$ matrix excluding the elements associated with the absorbing (out-of-control) state:

$$\boldsymbol{R_0} = \begin{bmatrix} p_{00} & p_{01} & \cdots & p_{0,m-1} \\ p_{10} & p_{11} & \cdots & p_{1,m-1} \\ \vdots & \vdots & \vdots & \vdots \\ p_{m-1,0} & p_{m-1,1} & \cdots & p_{m-1,m-1} \end{bmatrix}. \tag{2-36}$$

Finally, the zero-state ARL_0 is equal to the first element of vector $\boldsymbol{V}$ given by the following expression.

$$\boldsymbol{V} = (\boldsymbol{I} - \boldsymbol{R_0})^{-1}\, \boldsymbol{1}, \tag{2-37}$$

where $\boldsymbol{I}$ is an identity matrix and $\boldsymbol{1}$ is a vector of ones.

The transition probability matrix $\boldsymbol{R}$ for calculating out-of-control *ARL* can be established similarly as $\boldsymbol{R_0}$ except that the transition probability p_{ij} of $\boldsymbol{R}$ must be evaluated by using the out-of-control μ (= $\mu_0 + \delta_\mu \sigma_0$) and σ (= $\delta_\sigma \sigma_0$). Under the steady-state mode, it is assumed that the statistic C_t has reached its stationary distribution at the time when the process shift occurs and that the random time of process shift has a uniform distribution within the sampling interval (Reynolds *et al.* 1990). Thus, the out-of-control *ARL* is calculated as follows:

$$ARL = \boldsymbol{B}^T [(\boldsymbol{I} - \boldsymbol{R})^{-1}\, \boldsymbol{1} - \boldsymbol{1} / 2], \tag{2-38}$$

where $\boldsymbol{B}$ is the steady-state probability vector. It is obtained by first normalizing $\boldsymbol{R_0}$ and then solving the following equation:

$$\boldsymbol{B} = \boldsymbol{R_0^T}\, \boldsymbol{B}, \tag{2-39}$$

subject to

$$\mathbf{1}^{\mathrm{T}}\, \boldsymbol{B} = 1. \tag{2-40}$$

2.5 Summary

This chapter begins with the introduction to quality and quality control, and reviews various topics related to control charts. Then it expatiates the origin of CUSUM chart and its initial formation, such as V-mask CUSUM and tabular CUSUM. Different approaches for improving the performance of CUSUM charts are discussed subsequently. It includes adding another type of chart (such as Shewhart $\overline{X}$ chart to form a combination of $\overline{X}$ &CUSUM chart), using multiple CUSUM charts, using adaptive features and setting a head start.

From the above literature review, it could be found that:

(1) There is no consistent procedure and guideline for chart design. The charting parameters of many charts are determined based on heuristic, rather than using an analytical or optimal algorithm. There is a need to provide a general design method for control chart.

(2) The adaptive CUSUM chart using the reference parameter k as the adaptive parameter does not work quite efficiently. In this thesis, an adaptive CUSUM chart with new adaptive parameters will be explored to enhance the performance of the CUSUM chart.

(3) There is a trend to devise complicated statistics to achieve the high detection effectiveness of control chart. For example, Reynolds and Stoumbos (2004*a*) developed the most effective chart, the 3-CUSUM ($\mu+\sigma$) chart, to detect both mean and variance shifts. However, this chart is very complicated in design and implementation since three sub-CUSUM charts have to be dealt with. It is preferable to develop some single charts which use only one statistic. These single charts are much simpler in design and implementation, and may be as effective as those complicated charts.

(4) Including all the costs related to the implementation of a control chart complicates the design of control chart, and is not practical. That may be the reason why the economic design is not popular in SPC applications. However, economic consideration is unavoidable in the application of control chart. This thesis will explore the statistic chart designs that take key economic factors into consideration.

The following two chapters will focus on the development of new CUSUM schemes. It is assumed that the quality characteristic x has an independent and identical normal distribution with in-control process mean μ_0 and variance σ_0^2. In this thesis, it is assumed that μ_0 and σ_0 are known a priori. In practice, they may be estimated from the historic data. When process shift occurs, the mean μ and standard deviation σ will change:

$$\mu = \mu_0 + \delta_\mu \sigma_0, \quad \sigma = \delta_\sigma \sigma_0, \tag{2-41}$$

where δ_μ and δ_σ are the mean and standard deviation shifts, respectively, in terms of the in-control standard deviation σ_0. When the process is in control, $\delta_\mu = 0$ and $\delta_\sigma = 1$.

In order to facilitate the designs and discussions, the quality characteristic x is converted to z which follows a standard normal distribution when the process is in control.

$$z = \frac{x - \mu_0}{\sigma_0}. \tag{2-42}$$

In addition, throughout this thesis, it is assumed that the process shift is sustained. It will last until being detected by the control chart. It is because that sustained shifts occur in many process and most SPC practitioners would probably give higher priority to detecting them (Reynolds and Stoumbos 2004*a*). From the same perspective, the shift ranges and in-control ARL_0 (ATS_0) are also specified based on common practice and conventions that are traditionally adopted in SPC literature.

Chapter 3

CUSUM Charts for Detecting Mean Shift

Since the first control chart, Shewhart $\overline{X}$ chart, was proposed to deal with process mean shift, people have been developing and applying this type of control charts. Researchers have also found that the control charts dealing with only process mean shifts can be easily extended to the applications in which both process mean and variance are to be monitored. In view of this, this chapter will focus on the investigation of the control charts that merely monitor process mean. Two new charts, an optimal *X*&CUSUM chart and an adaptive CUSUM chart, are proposed for this purpose. An optimal design is introduced and applied in this chapter and throughout this thesis, in which an overall performance measure acts as the objective function. The performance of the two charts is compared with other five CUSUM charts. The results show that the two proposed charts have high detection effectiveness and advantage of simplicity in design and implementation. In the final part of this chapter, the effect of sampling cost on chart design and performance is discussed.

3.1 $\overline{X}$ & CUSUM Chart

This section improves the design of the Lucas' $\overline{X}$ &CUSUM chart (Lucas, 1982) by using an optimization algorithm. First of all, it introduces the steps to the implementation of a high-sided *X*&CUSUM chart. Subsequently, the measures for overall performance over a shift range are discussed. The optimal $\overline{X}$ &CUSUM chart is designed based on an overall performance measure. While the optimal design effectively improves the overall performance of the $\overline{X}$ &CUSUM chart, it does not increase the difficulty for understanding and implementing this combined chart.

3.1.1 Introduction

Over decades, many new charts and their applications have been proposed and studied by SPC practitioners and researchers in engineering, management and statistics (Zeifman and Ingman 2005, Shu *et al*. 2007, Jarrett and Pan 2007, Messaoud *et al*. 2008, Shu *et al*. 2008, Riaz and Does 2008). Among all the charts, the $\overline{X}$ (or *X*) chart and CUSUM chart are used most widely in industry and have attracted great research effort

(Luceño and Puig-Pey 2002, Yi *et al*. 2006, Liu *et al*. 2006).

In SPC implementation, it is quite difficult to predict the actual types and magnitudes of process shifts for most of the applications. In order to make the control scheme effective over a wide range of process shifts (*e.g.* mean shifts), some researchers (*e.g.* Sparks 2000, Zhao *et al.* 2005) recommended using two or three CUSUM charts simultaneously. Lucas (1982) proposed the combined scheme of $\overline{X}$ &CUSUM chart. In this scheme, the CUSUM feature will quickly detect small and moderate shifts while the addition of the $\overline{X}$ chart increases the speed of detecting large shifts. Lucas also commented that the $\overline{X}$ &CUSUM chart is almost as easy to use as a single CUSUM chart. According to the study of many researchers (*e.g.* Reynolds and Stoumbos 2004*a*), the CUSUM chart that uses a sample size of (n = 1) is most effective from an overall viewpoint. In this section, (n = 1) will be used for the $\overline{X}$ &CUSUM chart, thus it becomes the *X*&CUSUM chart.

Usually, two symmetrical CUSUM charts and one *X* chart with symmetrical lower and upper control limits are used together for detecting two-sided mean shifts. However, this section focuses on the studies of the combination of a high-sided CUSUM chart and an *X* chart with an upper control limit (*UCL*) for detecting increasing mean shifts. The symmetrical low-sided counterparts can be built similarly. The statistic C_t to be updated for the high-sided CUSUM chart is as follows:

$$\begin{aligned} C_0 &= 0, \\ C_t &= \max(0,\ C_{t-1} + (x_t - \mu_0) - k), \end{aligned} \tag{3-1}$$

where k is the reference parameter. The difference (x_t - μ_0) is a sample value of the mean shift $\delta_\mu\sigma_0$. Since only δ_μ is handled, $\sigma \equiv \sigma_0$ in this chapter. The *X*&CUSUM combination will produce an out-of-control signal if C_t becomes larger than the control limit H of the CUSUM chart or x_t falls beyond the upper control limit *UCL* of the *X* chart.

Using Equation (2-42) to convert the quality characteristic x to a standardized normal variable z, the mean shift is δ_μ and Equation (3-1) is standardized as:

$$C_0 = 0,$$
$$C_t = \max(0,\ C_{t-1} + z_t - k). \tag{3-2}$$

It is noted that the value of k in Equation (3-2) is different from the value of k in Equation (3-1). For a low-sided CUSUM chart for detecting decreasing mean shifts, the updating formula for C_t is slightly different (see Equation (2-26) and (2-27)).

3.1.2 Implementation

The implementation of a high-sided *X*&CUSUM chart is outlined below.

(1) Initialize the statistic C_0 in Equation (3-2) as zero.
(2) Take a sample value x_t of the quality characteristic.
(3) Convert x_t to z_t using Equation (2-42).
(4) Update C_t using $C_t = \max(0, C_{t-1} + z_t - k)$.
(5) If $C_t \le H$ and $x_t \le UCL$, the process is thought to be in control, and go back to step (2) for the next sample.
(6) Otherwise (i.e., $C_t > H$ and/or $x_t > UCL$), the *X*&CUSUM chart produces an out-of-control signal, and the process is stopped immediately for investigation.

The above steps can also serve as the pseudo code for developing an operational program for the computer-aided implementation of the *X*&CUSUM chart.

3.1.3 Performance Measure

In the designs of many control charts, the users have to determine a special value δ_μ of the process shift. The out-of-control *ATS* will be minimized at δ_μ. However, the values of process shifts are quite difficult to be predicted in most applications. A control chart should have excellent performance over the whole process shift range (Wu *et al*. 2004). In order to compare the overall performance of two or more charts, researchers (Reynolds and Stoumbos 2004*a*, *b*) usually examine the corresponding out-of-control *ATS* values of the charts at some discrete points of process mean shifts (δ_μ) within the shift range. For most of the cases, no chart will give the best *ATS* performance for all the shifts (Reynolds and Stoumbos 2006). However, as long as one chart has smaller out-of-control *ATS* values at more points and/or to a larger degree, this chart is thought to be more effective than others.

In order to have a more accurate and objective procedure for performance comparison between the charts, the above heuristic is expressed as a numerical measure called the Average Ratio of *ATS* (*ARATS*). This measure is an integration over the process shift range ($\delta_{\mu,\min}$, $\delta_{\mu,\max}$).

$$ARATS = \frac{1}{\delta_{\mu,\max} - \delta_{\mu,\min}} \cdot \int_{\delta_{\mu,\min}}^{\delta_{\mu,\max}} \frac{ATS(\delta_\mu)}{ATS_{\text{benchmark}}(\delta_\mu)} \cdot d\delta_\mu \,, \tag{3-3}$$

where $ATS(\delta_\mu)$ is produced by a chart at δ_μ and $ATS_{\text{benchmark}}(\delta_\mu)$ is generated by another chart that acts as the benchmark. In some situations when the sampling interval is set as the time unit, *ATS* in Equation (3-3) can be replaced by *ARL*. Thus

$$ARARL = \frac{1}{\delta_{\mu,\max} - \delta_{\mu,\min}} \cdot \int_{\delta_{\mu,\min}}^{\delta_{\mu,\max}} \frac{ARL(\delta_\mu)}{ARL_{\text{benchmark}}(\delta_\mu)} \cdot d\delta_\mu \,. \tag{3-4}$$

If the *ARATS* value of a chart is smaller than one, this chart should have smaller *ATS* values at larger portion of the shift range and/or to a larger degree and therefore will be more effective than the benchmark, and *vice versa*.

The maximum mean shift $\delta_{\mu,\max}$ and the minimum mean shift $\delta_{\mu,\min}$ in Equation (3-3) define the process shift range. In practice, the values of $\delta_{\mu,\max}$ may be determined based on the knowledge about the process (e.g., the maximum possible process shift in a process) or based on the shift range the users are interested to investigate. $\delta_{\mu,\min}$ may be set as zero in many studies. However, in some applications, $\delta_{\mu,\min}$ is set larger than zero so that process shifts smaller than $\delta_{\mu,\min}$ is ignored. The purpose is to avoid over-correction that may introduce extra variability into the process (Woodall 1985). It is because the data of out-of-control cases are sparse, and the distribution of δ_μ not only very difficult in practice to estimate the probability distribution of process shift δ_μ, differs case by case but also varies continuously over time. As a result, it is hard to find any study in the literature that designs or evaluates a control chart based on known or estimated distribution of δ_μ. Instead, as pointed out by Siddall (1983), if one has complete uncertainty about a random variable except for its bounds, then it leads to a uniform distribution. In fact, it is generally assumed explicitly (Domangue and Patch 1991, Sparks 2000) or implicitly (Reynolds and Stoumbos 2004*a*, *b*) that all process shifts occur with equal probability, a uniform distribution with a density function of

$(1/(\delta_{\mu,\max} - \delta_{\mu,\min}))$ is thus used for δ_μ in Equation (3-3). Later a study in section 4.7 of Chapter 4 will show that the relative performance of the charts is only slightly influenced by the probability distribution of δ_μ.

Another possible measure of the overall effectiveness is the *Average Extra Quadratic Loss* (*AEQL*). The quadratic loss function (Taguchi and Wu 1980) is widely used as a design criterion for the designs of many control charts (Chou *et al*. 2000, Reynolds and Stoumbos 2004*b*, Wu and Tian 2005, Chen and Chen 2007, Serel and Moskowitz 2008). The loss L incurred during an out-of-control case due to a process mean shift δ_μ is calculated by

$$L(\delta_\mu) = \ell(\delta_\mu) \cdot N(\delta_\mu), \tag{3-5}$$

where N is the average number of units produced in an out-of-control case and ℓ is the extra quadratic loss (the quadratic loss due to (δ_μ) minus the quadratic loss when process is in control) per unit.

$$N(\delta_\mu) = g \cdot ATS(\delta_\mu), \tag{3-6}$$

$$\ell(\delta_\mu) = K_c[\sigma_0^2 + (\mu - \mu_0)^2] - K_c\sigma_0^2 = K_c\sigma_0^2\delta_\mu^2, \tag{3-7}$$

where g is the production rate (*i.e.* number of units produced per unit time) and K_c is a constant depending on individual process. By taking all different δ_μ within the shift range $(\delta_{\mu,\min}, \delta_{\mu,\max})$ into consideration, *AEQL* can be calculated as an integration:

$$\begin{aligned} AEQL &= \frac{1}{\delta_{\mu,\max} - \delta_{\mu,\min}} \int_{\delta_{\mu,\min}}^{\delta_{\mu,\max}} L(\delta_\mu) d\delta_\mu \\ &= \frac{gK_c\sigma_0^2}{\delta_{\mu,\max} - \delta_{\mu,\min}} \int_{\delta_{\mu,\min}}^{\delta_{\mu,\max}} \delta_\mu^2 ATS(\delta_\mu) d\delta_\mu. \end{aligned} \tag{3-8}$$

The constant term of $gK_c\sigma_0^2$ can be omitted for the sake of simplicity as it has no influence on the performance comparison and the optimal solution. As such,

$$AEQL = \frac{1}{\delta_{\mu,\max} - \delta_{\mu,\min}} \cdot \int_{\delta_{\mu,\min}}^{\delta_{\mu,\max}} \delta_\mu^2 ATS(\delta_\mu) d\delta_\mu. \tag{3-9}$$

It is noted that the index *AEQL* is actually the weighted average *ATS* across the mean shift range using the square of mean shift δ_μ^2 as the weight. It is justifiable as quality is inversely proportional to variability (Montgomery 2009). If a chart has a smaller *AEQL*

value, its out-of-control *ATS* value at each δ_μ point is generally smaller compared with other charts. Consequently, a minimum *AEQL* will achieve the best overall statistical performance.

The method of Legendre-Gauss Quadrature can be used to carry out the integration in Equation (3-3) and (3-9). In practice, a summation can also be used to approximate the integration

$$AEQL = \frac{1}{M}\sum_{i=1}^{M} \delta_{\mu,i}^2 \cdot ARL(\delta_{\mu,i}), \tag{3-10}$$

where M is the number of shift points which equally divide the shift range ($\delta_{\mu,\max}$ - $\delta_{\mu,\min}$).

Unlike *ARATS*, the calculation of the *AEQL* does not require a predetermined benchmark chart. Moreover, *AEQL* takes into consideration of both *ATS* and loss per unit time for different process shifts. Thus *AEQL* will be used as the objective function in the optimal designs of control charts. It also avoids a problem suffered by the index of *ARATS*, that is, the results may differ to some degree when different charts are selected as the benchmark.

Reynolds and Stoumbos (2004*a*, *b*) found that *ARATS* and *AEQL* usually reach the same conclusion in chart comparison. It has also been confirmed by the results obtained in this thesis. This indicates that both *AEQL* and *ARATS* are feasible and trustworthily measures of the overall effectiveness of the control charts. Some may suspect that *AEQL* is biased to large process shifts as it is a quadratic function of process shift. It may not be true, because the relative effectiveness of the charts is measured not only by *AEQL* but also confirmed by *ARATS* in this thesis, and the latter is not particularly sensitive to large shifts.

3.1.4 Optimal design

An algorithm for the optimal design of the *X*&CUSUM chart is proposed in this study to improve Lucas' basic design algorithm. In this new algorithm, the optimal values of the charting parameters *k* (reference parameter of the CUSUM chart), *H* (control limit of the CUSUM chart) and *UCL* (upper control limit of the *X* chart) are searched in order

to minimize *AEQL* of the combined *X*&CUSUM chart. The minimization of *AEQL* leads to the reduction of loss in quality (or the cost, or the damage) incurred in the out-of-control cases. Moreover, the gain in overall detection effectiveness is acquired without sacrificing the simplicity for implementation.

The optimal design of an *X*&CUSUM chart requires the specifications of (1) τ, the minimum allowable in-control ATS_0, (2)$\delta_{\mu,\min}$, the lower bound of mean shift, and (3) $\delta_{\mu,\max}$, the upper bound of mean shift. The specification of τ is decided by the requirement on the false alarm rate. If the handling of the false alarm is very difficult, τ should be large. Otherwise, τ may be set to a lower value in order to increase the detection effectiveness. The bounds of $\delta_{\mu,\min}$ and $\delta_{\mu,\max}$ are required for calculating *AEQL* as shown in Equations (3-8) and (3-9). They are specified implicitly or explicitly in any performance evaluation and comparison (Lucas 1982, Reynolds and Stoumbos 2004*a*), because the charts cannot be accessed and compared in an infinitely large range.

Based on the specifications, the charting parameters of a *X*&CUSUM chart will be determined by the following optimization model:

Objective function: $AEQL$ = minimum (3-11)

Constraint function: $ATS_0 \geq \tau$ (3-12)

Design variables: k, H, UCL (3-13)

The optimization search aims to find the optimal values of these design variables so that the objective function *AEQL* is minimized over the entire mean shift range and the constraint of ($ATS_0 \geq \tau$) is satisfied. The *X*&CUSUM chart designed by this method is called optimal *X*&CUSUM chart.

Since *AEQL* is an integral result over the whole shift range, the optimal *X*&CUSUM chart should have the best performance from an overall viewpoint. It is noteworthy that the optimization algorithm is just to find the optimal values of the charting parameters rather than changing the features and operational rules of the charts. While it improves the overall performance of the charts, it does not, in any sense, increase the complexity

for implementation.

Any nonlinear optimization program can be used to search the optimal solution of the design variables. The search method takes *UCL* and *k* as independent variables, and *H* as the dependent variable. That is, the optimal values of *UCL* and *k* are searched to find a minimum *AEQL*. For each given set of values of *UCL* and *k*, *H* is adjusted to make the ATS_0 of the optimal *X*&CUSUM combination equal to τ. It usually takes only about one minute of CPU time to find the optimal solution in a computer program. The actual optimal design is conducted through a two-level searching. The top level searches the optimal *UCL* and the bottom level searches the optimal *k*. The dependent variable, the control limit *H*, is then adjusted to meet the constraint function.

In each of the two levels, the search starts from a starting value of *UCL* or *k* based on the best guess, and then explores into both directions (increasing and decreasing directions) with a predetermined step size. The *AEQL* value at the current design point will be calculated and compared with the previous minimum. If the current *AEQL* value is smaller, it will be used to replace the previous minimum, and the corresponding values of *UCL*, *k* and *H* are stored as the temporary optimal solutions. The search direction will change to the opposite only when current *AEQL* is larger and the current *UCL* or *k* is within one step away from the starting point. The search in either direction will be continued until the objective function *AEQL* cannot be further reduced. By this way, the optimal values of the charting parameters can be identified within a given range.

The adjustment of *H* is to satisfy the constraint function (Equation (3-12). Bracket method, halfing method and linear interpolation are adopted to determine the *H* value so that $ATS = \tau$.

In the optimal design, changing *UCL* is to allocate the probability of type I error (or power) of the optimal *X*&CUSUM combination between the *X* chart and the CUSUM chart. If *UCL* is small, *H* must be enlarged for ($ATS_0 = \tau$). This will allocate more power to the *X* chart and make the optimal *X*&CUSUM chart more sensitive to large mean shifts. On the other hand, if *UCL* is increased, *H* will be tightened, and the optimal *X*&CUSUM chart will be more powerful for detecting small shifts. Furthermore, the

reference parameter k is no longer determined to minimize the *ATS* value for a particular mean shift, instead it is optimized so that the optimal *X*&CUSUM chart is most effective for signalling mean shifts across the entire range.

Even though a global solution is highly desirable in all applications, it is usually difficult to be identified and located. Additionally, a general nonlinear problem, either constrained or unconstrained, may possess local solutions that are not the global solutions (Nocedal & Wright 1999). Usually, in the optimal design of a control chart, there is only one to three independent design variables within a feasible region, and the reliable exhaustive search using powerful computer can be employed to search for the close solutions for objective and constraint functions, which may be completed in a few seconds or minutes of CPU time. In almost all of the cases, an optimal or near-optimal solution can be identified. Similar to all the optimization strategies employed in SPC, the design algorithm of the optimal *X*&CUSUM chart makes no attempt to secure a global optimal solution. Instead, it focuses on deriving a convenient and systematic procedure for identifying a local optimum that has satisfactory performance and could be adopted in practice (Duncan 1956).

3.1.5 Calculation of *ATS*

The *ATS* of the optimal *X*&CUSUM chart is calculated using the following Markov chain procedure. It is a modification based on the earlier formulae for calculating the *ATS* of the standard CUSUM chart (see more details in section 2.4.3).

Suppose that the statistic C_t in Equation (3-2) experiences m different transitional states before being absorbed into the out-of-control state. States 0 to (m–1) are in-control states and state m is an out-of-control state. The width d of the interval of each in-control state and the center, O_i, of state i are given as follows.

$$d = H / (m - 0.5), \tag{3-14}$$

$$O_i = i \cdot d \qquad i = 0, 1, \ldots, m\text{-}1. \tag{3-15}$$

Let p_{ij} be the transition probability from state i to state j.

$$p_{ij} = \int_{\Omega} f(z_t) \cdot dz_t = \int_{\Omega} \frac{1}{\sqrt{2\pi}} \cdot \exp\left[-0.5 \cdot (z_t - \mu)^2\right] \cdot dz_t, \tag{3-16}$$

where $f(z_t)$ is the density function of z_t, and Ω is the intersection of the following two

domains Ω_1 and Ω_2:

(1) Ω_1:$z_t \le UCL$ (3-17)

It is the region for which the *X* chart in the *X*&CUSUM combination indicates an in-control process.

(2) Ω_2:$lb \le z_t \le ub$ (3-18)

It is the region for which the statistic C_t of the CUSUM chart will fall in the *j*th state, given that C_{t-1} is in the *i*th state.

$$Q_L < z_t < Q_U, \quad if \quad j > 0 \tag{3-19}$$

or

$$-\infty < z_t < Q_U, \quad if \quad j = 0 \tag{3-20}$$

where

$$Q_L = (O_j - 0.5d - O_i) + k, \qquad Q_U = (O_j + 0.5d - O_i) + k. \tag{3-21}$$

Therefore the lower bound *lb* and upper bound *ub* of z_t in region Ω_2 are determined as follows:

$$lb = \begin{cases} -\infty, & if \ j = 0, \\ Q_L, & if \ j > 0, \end{cases} \tag{3-22}$$

and

$$ub = Q_U. \tag{3-23}$$

The transition probability p_{ij} in Equation (3-16) can be actually computed by

$$p_{ij} = \begin{cases} \Phi(\min(ub, UCL) - \mu) - \Phi(lb - \mu), & if \ \min(ub, UCL) > lb \\ 0, & otherwise \end{cases} \tag{3-24}$$

where $\Phi(\ )$ is the standard normal cumulative distribution function.

Based on p_{ij}, the transition probability matrices $\boldsymbol{R_0}$ (Equation (2-36)) (for calculating in-control ATS_0) and $\boldsymbol{R}$ (for calculating out-of-control *ATS*) can be established. The in-control ATS_0 and out-of-control *ATS* can be solved using Equations (2-37) to (2-40). It is noted that the out-of-control *ATS* is required for the calculation of the objective function *AEQL* in Equation (3-11).

3.2 Adaptive CUSUM chart (ACUSUM II)

The adaptive CUSUM charts, referred to as ACUSUM charts, have attracted much research attention. By adjusting the reference parameter *k* dynamically, an ACUSUM chart may achieve better performance over a range of mean shifts than conventional CUSUM charts that are designed for maximal detection effectiveness at a particular level of process shift. This session studies a new feature of the ACUSUM chart related to an additional charting parameter *w*, *i.e.*, the exponential of the sample mean shift in $(x_t - \mu_0)^w$. The ACUSUM chart can be enhanced by adapting this parameter (w) according to the on-line estimated value of mean shift, in conjunction with the adaption of the reference parameter *k*. The statistic for the new ACUSUM chart is presented first, followed by the implementation of this chart. Subsequently, an optimization algorithm is proposed to assist the designs of this chart.

3.2.1 Introduction

A conventional CUSUM chart often determines the reference parameter *k* based on a special mean shift δ_μ. As a result, it performs optimally when the mean shift is equal to this δ_μ value. However, it is very difficult, if not impossible, to predict the actual magnitude of δ_μ for most of the applications (Reynolds and Stoumbos 2004*a*). As a result, there is no guarantee that the conventional CUSUM chart can always perform well during the operation. A probably better alternative is to apply an adaptive control chart which employs changeable parameters according to the recent values of sample statistic.

As mentioned in section 2.4.2, Sparks (2000) and Shu and Jiang (2006) proposed an ACUSUM (adaptive CUSUM) chart which adjusts the reference parameter *k* according to the on-line estimated value $\hat{\delta}_\mu$ of the mean shift. Meanwhile, it is found that an exponential *w* will influence the sensitivity of the CUSUM chart to mean shifts δ_μ (Reynolds and Stoumbos 2004*a*, Jiao and Helo 2008). Based on this finding, an enhanced ACUSUM chart is proposed in this thesis, in which both *k* and *w* are adapted dynamically in accordance with the current estimated value $\hat{\delta}_\mu$ of the mean shift. To differentiate from the version of Sparks (2000) and Shu and Jiang (2006) which is called the ACUSUM I chart, the one proposed in this section is referred to as the

ACUSUM II chart. The roman numerals I and II also indicate the respective number of adaptable charting parameters. It is noted that the ACUSUM I chart can be regarded as a special case of the ACUSUM II chart, whereby w is equal to one.

3.2.2 Quality Statistic

For the purpose of detecting increasing mean shifts, the statistic C_t in the ACUSUM II chart will be updated by

$$\begin{aligned} &C_0 = 0, \\ &C_t = \max\left(0,\ C_{t-1} + q - k\right). \end{aligned} \tag{3-25}$$

$$q = \begin{cases} z_t^w, & if \quad z_t \geq 0, \\ -(-z_t^w), & if \quad z_t < 0, \end{cases} \tag{3-26}$$

where the parameters k, w and q all depend on the current sample value z_t (standardized normal value of x_t). The statistic C_t may increase or decrease depending on whether the sample value z_t is larger or smaller than zero (or whether x_t is larger or smaller than μ_0). However, C_t is always shrunk toward zero by the reference parameter k. When an increasing mean shift occurs (*i.e.* $z_t > 0$, or $x_t > \mu_0$), C_t is likely to become larger and larger. Sooner or later, a subsequent sample point will exceed the control limit H of the ACUSUM II chart, and thereby produce an out-of-control signal.

This study focuses on the high-sided ACUSUM II chart, however, a symmetrical counterpart to detect decreasing means shifts can be built similarly.

$$\begin{aligned} &C_0^- = 0, \\ &C_t^- = \min\left(0,\ C_{t-1}^- + q + k\right), \end{aligned} \tag{3-27}$$

where q is also determined by Equation (3-26).

Studies on VSSI (variable sample size and sampling interval) CUSUM charts discover that merely using M (M = 2 or 3) sets of sample sizes and sampling intervals may gain most of the benefits that can be reached by a VSSI CUSUM chart (Yu and Wu 2004, Zhang and Wu 2006), and are relatively easier to design and implement. It suggests that, when implementing an ACUSUM II chart, one may use only M different sets of k_i and w_i (i = 1, 2, …, M) and each set is best for detecting a particular discrete value of $\delta_{\mu,\,i}$ ($\delta_{\mu,\min} < \delta_{\mu,\,1} < \ldots < \delta_{\mu,\,M} < \delta_{\mu,\max}$). Here, $\delta_{\mu,\min}$ and $\delta_{\mu,\max}$ are the lower and upper bounds.

Jointly, the M set of (k_i, w_i) will optimize the overall performance of the ACUSUM II chart over the entire mean shift range. The ACUSUM II chart keeps on switching among the M different sets of (k_i, w_i) depending on which $\delta_{\mu,\,i}$ is closest to the current estimated $\hat{\delta}_{\mu,\,t}$. At any moment one, and only one, set of (k_i, w_i) that is best for detecting $\hat{\delta}_{\mu,\,t}$ is in use (or active). Or in other words, the parameters k and w in Equations (3-25) and (3-26) will take the values of k_i and w_i, respectively. For the ACUSUM II chart, (M = 2) is always used because of its ease for design and implementation. The results of numerical studies demonstrate that there is little difference in the *ATS* performance of the ACUSUM II charts for (M = 2) and (M = 3).

Each of the M discrete $\delta_{\mu,\,i}$ is set at the center of one of the M equal intervals between $\delta_{\mu,\,\min}$ and $\delta_{\mu,\max}$, that is,

$$\delta_{\mu,\,i} = \delta_{\mu,\min} + (i - 0.5)\cdot D \quad i = 1, 2, \cdots, M,$$
$$D = (\delta_{\mu,\max} - \delta_{\mu,\min}) / M, \tag{3-28}$$

where D is the distance between two discrete values $\delta_{\mu,\,i}$ and $\delta_{\mu,\,i+1}$. When the current estimated $\hat{\delta}_{\mu,\,t}$ is closest to a particular $\delta_{\mu,i}$, the corresponding set of (k_i, w_i) is in use and Equations (3-25) and (3-26) become

$$C_0 = 0,$$
$$C_t = \max(0,\ C_{t-1} + q_i - k_i), \tag{3-29}$$

$$q_i = \begin{cases} z_t^{w_i}, & if\ z_t \geq 0, \\ -(-z_t)^{w_i}, & if\ z_t < 0. \end{cases} \tag{3-30}$$

Like an ACUSUM I chart, an ACUSUM II chart updates $\hat{\delta}_{\mu,\,t}$ by an EWMA procedure.

$$\hat{\delta}_{\mu,\,0} = \delta_{\mu,\,1},$$
$$\hat{\delta}_{\mu,\,t} = \left\| (1-\lambda)\hat{\delta}_{\mu,\,t-1} + \lambda z_t \right\|. \tag{3-31}$$

The operator $\| \ \|$ makes $\hat{\delta}_{\mu,\,t}$ equal to one of the M discrete $\delta_{\mu,\,i}$, whichever is closest to $((1-\lambda)\hat{\delta}_{t-1} + \lambda z_t)$. Then the corresponding set of (k_i, w_i) is selected to update C_t using Equations (3-29) and (3-30). If the smoothing parameter λ in Equation (3-31) equals one, $\hat{\delta}_{\mu,\,t}$ is completely determined by z_t; otherwise $\hat{\delta}_{\mu,\,t}$ also depends on the

information in the sequence of the sample points. It is noted that the values of k_i and w_i depend on z_t, or may be presented explicitly as the functions, $k_i(z_t)$ and $w_i(z_t)$, of z_t.

For example, suppose M = 2, λ = 0.4, $\delta_{\mu,\,\min}$ = 1 and $\delta_{\mu,\,\max}$ = 3, then, Equation (3-28) gives D = 1, $\delta_{\mu,1}$ = 1.5 and $\delta_{\mu,2}$ =2.5. Now, suppose $\hat{\delta}_{\mu,\,t-1} = \delta_{\mu,1}$ and z_t =3.0,

$$\hat{\delta}_{\mu,\,t} = \|(1-0.4)\times 1.5 + 0.4\times 3.0\| = \|2.1\| = \delta_{\mu,2}. \tag{3-32}$$

Thus, the set of (k_2, w_2) will be activated to update C_t, that is

$$C_t = \max\left(0,\ C_{t-1} + z_t^{w_2} - k_2\right). \tag{3-33}$$

3.2.3 Implementation

An ACUSUM II chart is implemented through the following steps:

(1) Initialize $\hat{\delta}_{\mu,\,0}$ as $\delta_{\mu,\,1}$ and the statistic C_0 in Equation (3-25) as zero (note, $\hat{\delta}_{\mu,0}$ is the initial value of the estimated mean shift when t = 0; and $\delta_{\mu,1}$ is the first one of the M discrete mean shift values determined in Equation (3-28)).

(2) Take a sample value x_t of the quality characteristic.

(3) Standardize x_t to z_t.

(4) Update $\hat{\delta}_{\mu,\,t}$ by Equation (3-31).

(5) If $\hat{\delta}_{\mu,\,t} = \delta_{\mu,i}$, select the charting parameters k_i and w_i to update C_t using Equations (3-29) and (3-30).

(6) If $C_t \le H$, the process is thought in control, and go back to step (2) for the next sample.

(7) Otherwise (*i.e.*, $C_t > H$), the ACUSUM II chart produces an out-of-control signal, and the process is stopped immediately for investigation.

3.2.4 Optimal design

To design an ACUSUM II chart, three parameters need be specified as for the optimal *X*&CUSUM chart in section 3.1.4: (1) τ, the minimum allowable in-control ATS_0 for a one-sided ACUSUM II chart, (2) $\delta_{\mu,\min}$, the lower bound of mean shift, and (3) $\delta_{\mu,\max}$, the upper bound of mean shift. The above three specifications are also required for the design of an ACUSUM I chart (Sparks 2000), as well as for many other charts.

Based on the specifications, the design variables of an ACUSUM II chart will be determined using the following design model.

Objective function: $AEQL$ = minimum (3-34)

Constraint function: $ATS_0 \geq \tau$ (3-35)

Design variables: k_i, w_i (i =1, 2, …, M), λ, H (3-36)

where H is the control limit of the ACUSUM II chart. When M = 2, there are in total six design variables. Among them, k_1, w_1, k_2, w_2 and λ are optimized so that the objective function $AEQL$ is minimized. The value of the last variable H is adjusted so that ATS_0 is equal to τ.

It is noted that the objective function (Equation (3-34)) and constraint function (Equation (3-35)) are the same as that for the optimal design for the X&CUSUM chart in section 3.1.4. In fact, these objective and constraint functions are always used in the optimal design in this thesis, in which $AEQL$ is to be minimized.

3.2.5 Calculation of *ATS*

The in-control ATS_0 and out-of-control ATS of an ACUSUM II chart will be computed using Markov chain procedure. The ACUSUM II chart can be described by a two-dimensional Markov chain (Shu and Jiang 2006). Suppose that the statistic C_t in Equation (3-25) experiences m different transitional states before being absorbed into the out-of-control state. States 0 to (m–1) are in-control states and state m is an out-of-control state. The width of the interval of each state and the center, O_j, of state j are determined using Equations (3-14) and (3-15), respectively.

As aforementioned, (M = 2) is used for the ACUSUM II chart. Then, two set of parameters of (k_i, w_i) are employed corresponding to two discrete mean shifts $\delta_{\mu,1}$ and $\delta_{\mu,2}$.

$$\delta_{\mu,i} = \delta_{\mu,min} + (i - 0.5)\, D \qquad i = 1, 2, \tag{3-37}$$

where

$$D = (\delta_{\mu,max} - \delta_{\mu,min}) / 2 \tag{3-38}$$

is the distance between these discrete mean shift values.

In a two-dimensional Markov chain, a point (i, j) represents a status in which the ith set

of (k_i, w_i) is in use and the statistic C_t is equal to O_j. Let $p_{ij\text{-}uv}$ be the transition probability from point (i, j) to point (u, v).

$$p_{ij-uv} = \int_{\Omega} f(z_t) \cdot dz_t = \int_{\Omega} \frac{1}{\sqrt{2\pi}} \cdot \exp\left[-0.5 \cdot (z_t - \mu)^2\right] \cdot dz_t, \tag{3-39}$$

where $f(z_t)$ is the density function of z_t, and Ω is the intersection of the following two domains Ω_1 and Ω_2:

(1) Ω_1: $LB \le z_t \le UB$. (3-40)

It is the region that the chart will use the uth set of (k_u, w_u) for the tth sample, given that the ith set of (k_i, w_i) is employed for the (t-1)th sample. Referring to Equations (3-31) and (3-37), the lower bound LB and upper bound UB of the region Ω_1 can be determined as follows:

$$LB = \begin{cases} -\infty, & if \quad u = 1, \\ \left[\delta_u - 0.5D - (1-\lambda)\delta_i\right] / \lambda, & if \quad u > 1, \end{cases} \tag{3-41}$$

$$UB = \begin{cases} \left[\delta_u + 0.5D - (1-\lambda)\delta_i\right] / \lambda, & if \quad u < M, \\ +\infty, & if \quad u = M. \end{cases} \tag{3-42}$$

(1) Ω_2: $lb \le z_t \le ub$. (3-43)

It is the region for which the statistic C_t will be closest to O_v, given that $C_{t\text{-}1}$ is equal to O_j. To make this transition (see Equations (3-25), (3-26) and (3-15)),

$$Q_L < q < Q_U, \quad if \;\; v > 0, \tag{3-44}$$

or

$$-\infty < q < Q_U, \quad if \;\; v = 0, \tag{3-45}$$

where

$$Q_L = (O_v - 0.5d - O_j) + k_u, \qquad Q_U = (O_v + 0.5d - O_j) + k_u, \tag{3-46}$$

Then, since

$$z_t = \begin{cases} q^{1/w_u}, & if \;\; q \ge 0, \\ -(-q)^{1/w_u}, & if \;\; q < 0, \end{cases} \tag{3-47}$$

therefore the lower bound lb and upper bound ub of z_t in the region Ω_2 are determined as follows:

$$lb = \begin{cases} -\infty, & if \quad v = 0, \\ Q_L^{1/w_u}, & if \quad v > 0 \;\; and \;\; Q_L \ge 0, \\ -(-Q_L)^{1/w_u}, & if \quad v > 0 \;\; and \;\; Q_L < 0, \end{cases} \tag{3-48}$$

and

$$ub = \begin{cases} Q_U^{1/w_u}, & if \quad Q_U \geq 0, \\ -(-Q_U)^{1/w_u}, & if \quad Q_U < 0. \end{cases} \tag{3-49}$$

The transition probability $p_{ij\text{-}uv}$ in Equation (3-39) can be actually computed by

$$p_{ij-uv} = \begin{cases} \Phi(\min(ub, UB) - u) - \Phi(\max(lb, LB) - u), & if \quad \min(ub, UB) > \max(lb, LB), \\ 0, & \text{otherwise.} \end{cases} \tag{3-50}$$

Based on $p_{ij\text{-}uv}$, the transition probability matrix $\boldsymbol{R_0}$ (Equation (2-36)) for calculating in-control ATS_0 and $\boldsymbol{R}$ for calculating out-of-control *ATS* can be established. Then, the in-control ATS_0 and out-of-control *ATS* can be acquired using formulae (2-37) to (2-40).

Again, any nonlinear optimization program can be used to search the optimal solution. In our study, the simple, yet reliable, Hooke-Jeeves procedure is employed (Siddall 1982). It can complete the design of an ACUSUM II chart in a few CPU seconds with a personal computer.

3.3 Performance Evaluation and Comparison

This section conducts a systematic performance comparison among seven CUSUM charts for monitoring process mean, including the optimal *X*&CUSUM chart and ACUSUM II chart proposed in this chapter. The optimization algorithm is used to assist the designs of all the CUSUM charts. The results demonstrate that the optimal design can significantly improve the performance of all CUSUM charts over the entire process shift range. The testing cases reveal that the ACUSUM II chart not only outperforms the ACUSUM I chart to a substantial degree, but also works as well as the most effective 3-CUSUM(μ) scheme. The optimal *X*&CUSUM chart also outperforms the Lucas' *X*&CUSUM chart. Furthermore, the two new charts proposed in this chapter are easier to design and implement in a computerized environment compared with some other combined schemes.

3.3.1 Charts to be Compared

The performance of the two new charts, the optimal *X*&CUSUM and ACUSUM II charts, proposed in this chapter, will be compared with that of other five CUSUM control charts in this section. For the convenience of comparison, all the charts are studied as one-sided charts with an upper control limit for detecting increasing mean shifts.

(1) The conventional CUSUM chart

The design of a conventional CUSUM chart aims at minimizing the out-of-control *ATS* at a specified mean shift level which is usually set as one σ_0, and consequently the reference parameter *k* is equal to $0.5\sigma_0$ (Lucas 1982, Sparks 2000).

(2) The optimal CUSUM chart

This chart is similar to a conventional CUSUM chart in operation. However, this CUSUM chart is designed by an optimization algorithm in which the design variables *k* and *H* are optimized using *AEQL* as the objective function and ($ATS_0 \geq \tau$) as the constraint function.

Objective function: $AEQL$ = minimum (3-51)

Constraint function: $ATS_0 \geq \tau$ (3-52)

Design variables: k, H (3-53)

This optimal design model is very similar to that for the optimal X&CUSUM chart in section 3.1.4 and the ACUSUM II chart in section 3.2.4, except that it

includes only one independent variable *k* and one dependent variable *H*.

(3) The ACUSUM I chart

This is the adaptive CUSUM chart with *k* being adjusted during the operation. Here, the model developed by Shu and Jiang (2006) is adopted, in which the mean shift for the *t*th sample is estimated by the following EWMA procedure:

$$\hat{\delta}_{\mu,\,0} = Q_0,$$

$$\hat{\delta}_{\mu,t} = \begin{cases} \delta_{\mu,\min}, & \text{if} \quad \xi < \delta_{\mu,\min}, \\ \xi, & \text{if} \quad \delta_{\mu,\min} \le \xi \le L, \\ L, & \text{if} \quad \xi > L, \end{cases} \tag{3-54}$$

$$\xi = (1-\lambda)\hat{\delta}_{\mu,\,t-1} + \lambda z_t,$$

where λ ($0 \le \lambda \le 1$) is the smoothing parameter, Q_0 is the initial value of $\hat{\delta}_{\mu,\,t}$, and L is an upper limit of $\hat{\delta}_{\mu,\,t}$. Shu and Jiang (2006) set L as four with the belief that an out-of-control signal will be produced before $\hat{\delta}_{\mu,\,t}$ reaches L. The two upper limit $\delta_{\mu,\max}$ and L are different. The former is the limit of the real mean shift of the process and the latter is the limit for the estimate $\hat{\delta}_{\mu,\,t}$. In this study, the charting parameters λ, Q_0 and the control limit H of an ACUSUM I chart are optimized so that *AEQL* is minimized subject to ($ATS_0 \ge \tau$).

(4) The ACUSUM II chart proposed in section 3.2

(5) The Lucas' *X*&CUSUM chart

Lucas (1982) suggested a design algorithm for the *X*&CUSUM chart. The reference parameter *k* of the CUSUM chart is set as 0.5, the upper control limit *UCL* of the *X* chart is selected between 3.5 and 4 (in this study, *UCL* is set as 3.75). Finally, the control limit *H* of the CUSUM chart is adjusted to produce a desired in-control ATS_0). Lucas found that the *X*&CUSUM chart designed by this algorithm has a larger in-control ATS_0 and a shorter out-of-control *ATS* for all mean shifts larger than 2.0σ or 2.5σ.

(6) The optimal *X*&CUSUM chart proposed in section 3.1

(7) The 3-CUSUM(μ) scheme (Sparks 2000)

As introduced in section 2.4.2, in this scheme, three separate CUSUM charts will be operated simultaneously for detecting mean shifts. Its *ATS* may have to be evaluated using simulation. Moreover, since this scheme has six design variables,

it would be extremely time consuming to carry out an optimal design for the 3-CUSUM(μ) scheme. Sparks suggested a template with three discrete δ_i* values (δ_1* = 0.75, δ_2* = 1.00, δ_3* = 1.50) for a nominal mean shift range between ($\delta_{\min}$* = 0.60) and ($\delta_{\max}$* = 1.75). For other different shift ranges bracketed by $\delta_{\min}$ and $\delta_{\max}$, the discrete $\delta_{\mu,i}$ values may be mapped to Sparks' template by

$$\delta_{\mu,i} = \delta_{\mu,\min} + \frac{\delta_{\mu,\max} - \delta_{\mu,\min}}{\delta_{\mu,\max}^* - \delta_{\mu,\min}^*} \cdot (\delta_i^* - \delta_{\mu,\min}^*) \qquad i = 1, 2, 3. \tag{3-55}$$

Then, the reference parameter k_i is set as $0.5\delta_{\mu,i}$. Finally, as suggested by Sparks (2000), the control limit H_i for each of the three separate CUSUM charts is determined so that each separate CUSUM chart has the same in-control ATS_0 when applied individually and, meanwhile, the 3-CUSUM(μ) scheme as a whole has an ATS_0 equal to τ.

Among the above seven charts, the first four are single-chart schemes using only one CUSUM chart, whereas the last three charts are multi-chart schemes, each of which consists of two or three separate control charts and all of these separate charts have to be handled simultaneously throughout the operation.

3.3.2 Comparison under a General Condition

The first comparison is carried out under a general condition with (τ = 740, $\delta_{\mu,\min}$ = 0.5, $\delta_{\mu,\max}$ = 4). The specification of (τ = 740) ensures that the resultant false alarm rate is identical to that of a typical 3-sigma $\bar{X}$ chart when two symmetrical CUSUM charts are used simultaneously to detect the two-sided mean shifts. With these specifications, the seven control charts are designed. The *ATS* values are summarized in Table 3-1 and the charting parameters are displayed in Table 3-2 for case 0. There are several interesting findings as below:

(1) The in-control ATS_0 values of the seven charts are very close to 740. Since the *ATS* values for the 3-CUSUM(μ) scheme is evaluated by simulation, its ATS_0 value is slightly smaller than others.
(2) If comparing the ACUSUM II chart with each of the single-chart schemes (the conventional CUSUM, the optimal CUSUM and the ACUSUM I charts), the out-of-control *ATS* values of the ACUMUM II chart are smaller for most of the

mean shift δ_μ. The ACUSUM II chart is less effective than the ACUSUM I chart only for detecting very small δ_μ (*i.e.*, when δ_μ is close or equal to $\delta_{\mu,\min}$). And it is inferior to the conventional CUSUM chart when $\delta_\mu \leq 1.5$. On the other hand, the ACUSUM II chart is less sensitive than the optimal CUSUM chart only within a small region of mean shifts (*i.e.*, when $1.5 \leq \delta_\mu \leq 2.5$). Comparing the ACUSUM II chart with the three multi-chart schemes, it is found that the single ACUSUM II chart usually outperforms the Lucas' *X*&CUSUM chart when mean shift is relatively large (*i.e.*, when $\delta_\mu > 1.5$), and it outperforms the optimal *X*&CUSUM chart except for a few shift points in the middle of the shift range. However, the ACUMUM II chart is always slightly less effective than the 3-CUSUM(μ) scheme.

(3) Comparing the optimal *X*&CUSUM chart with the single-chart schemes, it is found that its *ATS* values are often either equal or close to the minimum across the shift range. For example, the Lucas' *X*&CUSUM chart produces larger out-of-control *ATS* values than the optimal *X*&CUSUM chart in most shift points. The combination of the *X* and CUSUM charts plus the optimal design makes this scheme very effective from an overall viewpoint. On the other hand, the Lucas' *X*&CUSUM chart is more effective than the conventional and optimal CUSUM charts due to the combined effect of the *X* chart and CUSUM chart. Its *ATS* values are also smaller than that of the ACUSUM I chart. However, as the ACUSUM II chart, the optimal *X*&CUSUM chart is always slightly inferior to the 3-CUSUM(μ) scheme.

Table 3-1. *ATS* Comparison among Seven CUSUM Charts

($\delta_{\mu,\min} = 0.5$, $\delta_{\mu,\max} = 4.0$)

δ_μ	con CUSUM	opt CUSUM	ACUSUM I	ACUSUM II	opt *X*&CUSUM	Lucas' *X*&CUSUM	3-CUSUM (μ)
0.00	739.42	739.48	739.66	739.16	740.36	739.99	736.85
0.50	33.73	54.59	26.44	40.15	43.91	34.13	38.55
1.00	9.19	11.13	10.54	10.14	10.05	9.25	10.02
1.50	5.06	4.98	6.10	5.22	5.05	5.07	5.18
2.00	3.53	3.17	4.10	3.38	3.33	3.50	3.30
2.50	2.75	2.36	3.02	2.42	2.44	2.66	2.34
3.00	2.29	1.92	2.38	1.85	1.88	2.11	1.79
3.50	1.99	1.62	1.97	1.48	1.51	1.71	1.45
4.00	1.79	1.40	1.68	1.24	1.26	1.42	1.23
AEQL	16.759	15.375	17.341	14.398	14.575	15.292	14.087
$\frac{AEQL}{AEQL_{\text{ACUSUM II}}}$	1.164	1.068	1.204	1.000	1.012	1.062	0.978
ARATS	1.116	1.074	1.164	1.000	1.013	1.038	0.978

Table 3-2. Charting Parameters of Seven CUSUM Charts

Case No.	$\delta_{\mu,\min}$	$\delta_{\mu,\max}$	con CUSUM	opt CUSUM	ACUSUM I	ACUSUM II	opt *X*&CUSUM	Lucas' *X*&CUSUM	3-CUSUM(μ)
0	0.5	4.0	$k = 0.500$ $H = 4.774$	$k = 0.825$ $H = 3.048$	$Q_0 = 3.417$ $H = 1.706$ $\lambda = 0.400$	$H = 6.898$, $\lambda = 0.456$ $k_1 = 0.594$, $k_2 = 1.154$ $w_1 = 1.435$, $w_2 = 1.750$	$k = 0.625$ $H = 4.167$ $UCL = 3.334$	$k = 0.5$ $H = 4.167$ $UCL = 3.75$	$k_1 = 0.478$, $k_2 = 0.859$ $k_3 = 1.620$, $H_1 = 5.794$ $H_2 = 3.384$, $H_3 = 1.645$
1	0.25	3.0	$k = 0.500$ $H = 4.774$	$k = 0.613$ $H = 4.015$	$Q_0 = 1.625$ $H = 1.481$ $\lambda = 0.100$	$H = 5.853$, $\lambda = 0.488$ $k_1 = 0.518$, $k_2 = 1.008$ $w_1 = 1.150$, $w_2 = 1.450$	$k = 0.613$ $H = 4.071$ $UCL = 3.639$	$k = 0.5$ $H = 4.167$ $UCL = 3.75$	$k_1 = 0.304$, $k_2 = 0.603$ $k_3 = 1.201$, $H_1 = 8.222$ $H_2 = 4.670$, $H_3 = 2.339$
2	0.25	5.0	$k = 0.500$ $H = 4.774$	$k = 0.913$ $H = 2.760$	$Q_0 = 4.208$ $H = 1.749$ $\lambda = 0.150$	$H = 7.373$, $\lambda = 0.640$ $k_1 = 0.563$, $k_2 = 0.563$ $w_1 = 1.465$, $w_2 = 2.110$	$k = 0.613$ $H = 4.361$ $UCL = 3.251$	$k = 0.5$ $H = 4.167$ $UCL = 3.75$	$k_1 = 0.435$, $k_2 = 0.951$ $k_3 = 1.984$, $H_1 = 6.350$ $H_2 = 3.086$, $H_3 = 1.251$
3	0.75	3.0	$k = 0.500$ $H = 4.774$	$k = 0.738$ $H = 3.392$	$Q_0 = 1.500$ $H = 1.365$ $\lambda = 0.400$	$H = 4.925$, $\lambda = 0.280$ $k_1 = 0.692$, $k_2 = 1.142$ $w_1 = 1.260$, $w_2 = 1.425$	$k = 0.738$ $H = 3.492$ $UCL = 3.447$	$k = 0.5$ $H = 4.167$ $UCL = 3.75$	$k_1 = 0.522$, $k_2 = 0.766$ $k_3 = 1.255$, $H_1 = 5.196$ $H_2 = 3.656$, $H_3 = 2.175$
4	0.75	5.0	$k = 0.500$ $H = 4.774$	$k = 0.938$ $H = 2.687$	$Q_0 = 3.583$ $H = 1.682$ $\lambda = 0.950$	$H = 8.722$, $\lambda = 0.500$ $k_1 = 0.839$, $k_2 = 0.839$ $w_1 = 1.840$, $w_2 = 1.840$	$k = 0.638$ $H = 4.205$ $UCL = 3.250$	$k = 0.5$ $H = 4.167$ $UCL = 3.75$	$k_1 = 0.652$, $k_2 = 1.114$ $k_3 = 2.038$, $H_1 = 4.388$ $H_2 = 2.566$, $H_3 = 1.182$

It is well known that, for most of the cases, no chart will give a better performance than other charts for all the shifts points (Reynolds and Stoumbos 2006). Consequently, it is more appropriate to compare their overall performance in order to make an accurate and objective conclusion about the relative effectiveness among the charts. The following three holistic measures are evaluated are enumerated at the bottom of Table 3-1 as well as in case 0 in Table 3-3:

(1) *AEQL* (Equation (3-8));

(2) *AEQL* / $AEQL_{\text{ACUSUM II}}$, ($AEQL_{\text{ACUSUM II}}$ is the *AEQL* value of the ACUSUM II chart);

(3) *ARATS* (Equation (3-3) in which the ACUSUM II chart is used as the benchmark).

The values of these holistic measures indicate that:

(1) In terms of *AEQL* values, the rankings of the seven charts are read as 3-CUSUM(μ), ACUSUM II, optimal *X*&CUSUM, Lucas' *X*&CUSUM, optimal CUSUM, conventional CUSUM and ACUSUM I charts, with 3-CUSUM(μ) scheme being the most powerful one and ACUSUM I being the least effective one. The ACUSUM II chart convincingly outperforms all of the single-chart schemes. It even excels the Lucas' *X*&CUSUM and optimal *X*&CUSUM charts, and is only slightly inferior to the 3-CUSUM(μ) scheme.

(2) From Table 3-1, the values of *AEQL* / $AEQL_{\text{ACUSUM II}}$ and *ARATS* of each chart are often fairly close to each other. Specifically, both measures give the same ranking of the chart effectiveness.

Table 3-3. Holistic Measures of Seven CUSUM Charts

Case No.	$\delta_{\mu,\min}$	$\delta_{\mu,\max}$		con CUSUM	opt CUSUM	ACUSUM I	ACUSUM II	opt *X*&CUSUM	Lucas' *X*&CUSUM	3-CUSUM (μ)
0	0.5	4.0	*AEQL*	16.759	15.375	17.341	14.398	14.575	15.292	14.087
			$\frac{AEQL}{AEQL_{\text{ACUSUM II}}}$	1.164	1.068	1.204	1.000	1.012	1.062	0.978
			ARATS	1.116	1.074	1.164	1.000	1.013	1.038	0.978
1	0.25	3.0	*AEQL*	12.922	12.725	16.288	12.305	12.493	12.618	11.850
			$\frac{AEQL}{AEQL_{\text{ACUSUM II}}}$	1.050	1.034	1.324	1.000	1.015	1.025	0.963
			ARATS	1.028	1.033	1.246	1.000	1.022	1.012	0.956
2	0.25	5.0	*AEQL*	19.778	17.010	24.791	16.037	16.197	16.969	15.780
			$\frac{AEQL}{AEQL_{\text{ACUSUM II}}}$	1.233	1.061	1.546	1.000	1.010	1.058	0.984
			ARATS	1.161	1.085	1.430	1.000	1.019	1.034	0.984
3	0.75	3.0	*AEQL*	13.873	13.174	13.697	12.888	12.992	13.505	12.680
			$\frac{AEQL}{AEQL_{\text{ACUSUM II}}}$	1.076	1.022	1.063	1.000	1.008	1.048	0.984
			ARATS	1.055	1.019	1.048	1.000	1.011	1.032	0.983
4	0.75	5.0	*AEQL*	21.011	17.537	17.795	16.922	16.787	17.924	16.589
			$\frac{AEQL}{AEQL_{\text{ACUSUM II}}}$	1.242	1.036	1.052	1.000	0.992	1.059	0.980
			ARATS	1.182	1.039	1.041	1.000	0.989	1.040	0.980
Grand Averages			*AEQL*	16.869	15.164	17.983	14.510	14.609	15.262	14.197
			$\frac{AEQL}{AEQL_{\text{ACUSUM II}}}$	1.163	1.045	1.239	1.000	1.007	1.052	0.978
			ARATS	1.109	1.050	1.186	1.000	1.011	1.031	0.976

3.3.3 Comparison in a 2^k Experiment

Next, the effectiveness of the seven charts is further compared through a factorial 2^2 experiment with four different cases of $\delta_{\mu,\min}$ and $\delta_{\mu,\max}$: (1) $\delta_{\mu,\min} = 0.25$, $\delta_{\mu,\max} = 3.0$; (2) $\delta_{\mu,\min} = 0.25$, $\delta_{\mu,\max} = 5.0$; (3) $\delta_{\mu,\min} = 0.75$, $\delta_{\mu,\max} = 3.0$; (4) $\delta_{\mu,\min} = 0.75$, $\delta_{\mu,\max} = 5.0$.

The experimental results show that the relative *ATS* performance of the seven charts in these four cases are similar to that under the general condition (case 0 in section 3.3.2). In view of this, only the *AEQL* and *ARATS* values of the charts are listed in Table 3-3. The parameters of the charts are displayed in Table 3-2.

It is found that the ranking of the charts based on the *AEQL* values in each of the four cases is nearly the same as the ranking in case 0 with only a few exceptions as elaborated below (see Table 3-3):

(1) The ACUSUM I chart becomes superior to the conventional CUSUM chart when $\delta_{\mu,\min}$ is great (= 0.75).
(2) The optimal *X*&CUSUM chart slightly outperforms the ACUSUM II chart when both $\delta_{\mu,\min}$ and $\delta_{\mu,\max}$ are great ($\delta_{\mu,\min} = 0.75$, $\delta_{\mu,\max} = 5.0$).
(3) The optimal CUSUM chart slightly outperforms the Lucas' *X*&CUSUM chart when both $\delta_{\mu,\min}$ is great ($\delta_{\mu,\min} = 0.75$).

3.3.4 Discussion on Detection Effectiveness

Finally, the grand average $\overline{AEQL}$ of *AEQL* and the grand average $\overline{ARATS}$ of *ARATS*, as well as $\overline{AEQL/AEQL_{\text{ACUSUM II}}}$, of the charts over the five cases in Table 3-3 are calculated and listed at the bottom of Table 3-3. It is found that,

(1) In terms of detection effectiveness, the overall rankings based on $\overline{AEQL/AEQL_{\text{ACUSUM II}}}$ of the seven charts from highest performance to lowest performance are 3-CUSUM(μ), ACUSUM II, optimal *X*&CUSUM, optimal

CUSUM, Lucas' *X*&CUSUM, conventional CUSUM and ACUSUM I chart.

(2) Owing to an additional adaptable parameter *w*, the ACUSUM II chart developed in this PhD project has achieved the goal of improving the detection effectiveness of the earlier adaptive ACUSUM I chart. Since the ACUSUM I chart is simply a special case of the ACUSUM II chart, the ACUSUM II chart will be at least equally effective as the ACUSUM I chart if using ($w_1 = w_2 = 1$). It is very likely that the ACUSUM II chart has the optimal values of w_i different from one and, therefore, outperforms the ACUSUM I chart. Based on the values of ($\overline{AEQL/AEQL_{\text{ACUSUM II}}}$) resulting from different combinations of δ_μ, $\delta_{\mu,\min}$ and $\delta_{\mu,\max}$, it is found that the ACUSUM II chart is more effective than the ACUSUM I chart (by 23.9%), the conventional CUSUM chart (by 16.3%), the optimal CUSUM chart (by 4.5%), the Lucas' *X*&CUSUM chart (by 5.2%) and the optimal *X*&CUSUM chart (by 0.7%). It is only inferior to the 3-CUSUM(μ) chart by 2.2%. The two exponentials w_1 and w_2 of the ACUSUM II charts are larger than one. It is consistent with the results found by Jiao and Helo (2008) that the optimal value of *w* of a CUSUM chart is always greater than one. Moreover, the optimal values of w_1 and w_2 of an ACUSUM II chart often increase along with the increase of the mean shift range.

(3) The conventional CUSUM chart is substantially less effective than other charts from an overall viewpoint. The conventionally adopted value of ($k = 0.5$) seems too small. It makes the CUSUM chart very insensitive to moderate or large mean shifts. The optimal CUSUM chart also uses a fixed *k*, but its *k* value is optimized. As a result, the overall performance has been significantly improved. The optimal CUSUM chart outperforms the conventional counterpart by 11.8% in terms of *AEQL*. This indicates that the optimal design is an effective way to enhance the CUSUM chart for detecting process shifts over a shift range. In table 3-2, the optimal value of *k* of the optimal CUSUM chart is much larger than the conventional setting of ($k = 0.5$).

(4) The optimal design is also very important for the *X*&CUSUM charts. It not only

optimizes the chart parameters but also optimize the allocation of detection power between the *X* chart element and CUSUM chart element. The optimal *X*&CUSUM chart is more effective than the Lucas' *X*&CUSUM chart by 4.5%. The fact that the overall performance of the Lucas' *X*&CUSUM chart is even lower than that of the optimal CUSUM chart indicates that if we simply put an *X* chart and a CUSUM chart together without optimizing the charting parameters, this combination may not be necessarily superior to a single CUSUM chart.

(5) The overall performance of the ACUSUM I chart proposed by Shu and Jiang (2006) is unsatisfactory. The reason may be that, during the initial in-control period, the estimated $\hat{\delta}_{\mu,t}$ is often very close to $\delta_{\mu,\min}$ as it uses $\delta_{\mu,\min}$ as the lower bound. As a result, the reference parameter *k* is also very small because of ($k = 0.5\hat{\delta}_{\mu,t}$). When a mean shift occurs, the EWMA mechanism will take a long time to push up $\hat{\delta}_{\mu,t}$ and *k*, and consequently leads to a large out-of-control *ATS*, especially for large mean shifts. If a lower bound larger than $\delta_{\mu,\min}$ is used for $\hat{\delta}_{\mu,t}$, the performance of the ACUSUM I chart may be improved.

(6) The values of *AEQL* and *ARATS* show that the multi-chart schemes usually have higher detection effectiveness than the single-chart schemes. Among the multi-chart schemes, the 3-CUSUM(μ) scheme has the highest detection effectiveness. The single ACUSUM II chart is second only to the 3-CUSUM(μ) scheme. From a practical viewpoint, however, the difference in overall detection effectiveness is minor between the multi-scheme charts and the single ACUSUM II chart.

(7) It is likely that the detecting effectiveness of the multi-chart schemes will be improved when more individual (or separate) charts are involved. For example, the 3-CUSUM(μ) scheme is more effective than the 2-CUSUM chart by 4% and the latter is more sensitive than the optimal CUSUM chart by about 4% (the details have not been presented in this thesis). However, people seldom consider the 4-CUSUM or 5-CUSUM chart because of the increase in the complexity for design

and implementation. In a recent paper, Reynolds and Stoumbos (2006) preferred a two-chart combination ($EWMA_X$ and $EWMA_X^2$) to a three-chart combination ($EWMA_X$, $EWMA_X^2$ and $\overline{X}$), even though the three-chart combination produces a smaller out-of-control *ATS*. They believe that the improved detection effectiveness of the three-chart combination is not sufficient to outweigh the increase in complexity. Likewise, the minor superiority of the 3-CUSUM(μ) scheme over the ACUSUM II chart and optimal *X*&CUSUM chart in *ATS* performance can hardly outweigh the increase in the difficulty for implementation and design, as to be discussed shortly.

3.3.5 Discussion on Simplicity in Design and Implementation

In addition to detection effectiveness, the considerations pertaining to the ease of design and implementation are also quite important for selecting a control chart, especially when the *ATS* performance of the charts is very close. In view of the simplicity in design and implementation, the optimal CUSUM chart seems most promising. Generally speaking, the multi-chart schemes have higher detection effectiveness than the single-chart schemes, but they are more difficult to be designed and implemented. The following discussion is more focused on the comparison among the two new charts (optimal *X*&CUSUM chart, ACUSUM II chart) and 3-CUSUM(μ) scheme.

(1) Considering the number of charting parameters. The optimal *X*&CUSUM chart is simpler than the ACUSUM II chart and 3-CUSUM(μ) scheme. As shown in Table 3-2, the *X*&CUSUM chart has only three charting parameters, while the other two charts have six. Moreover, people in workshop floor are more familiar with the procedure of *X* chart and CUSUM chart.

(2) The *ATS* of the ACUSUM II chart and the optimal *X*&CUSUM chart can be evaluated by a Markov procedure. As a result, the design of these two charts can be completed in a few minutes of CPU time. In contrast, due to the interaction of the three separate CUSUM charts, the *ATS* of a 3-CUSUM(μ) scheme has to be evaluated by simulation. Consequently, the design of a 3-CUSUM(μ) scheme may

take about one hour, or longer, of CPU time even if the number of simulation runs is set as 100,000. If using 1,000,000 runs in simulation as suggested by some researchers (Reynolds and Stoumbos 2006), much longer CPU time is required.

(3) In a computerized SPC environment, the operation of all charts is almost equally easy. The operators only have to key in the reading of each sample, and the computer will carry out all computation and adaption automatically. However, the operators will feel more comfortable to observe an ACUSUM II chart than the multi-chart schemes on a computer monitor and to decide the process status. Figure 3-1 shows the computer displays of a 3-CUSUM(μ) scheme (Figure 3-1(*a*)), an ACUSUM II chart (Figure 3-1(*b*)), and an optimal *X*&CUSUM chart (Figure 3-1(*c*)) for monitoring the two-sided mean shifts of a same process. The process starts with an in-control status with $\delta_\mu = 0$ (or $\mu = \mu_0$) until the tenth sample when a sustained increasing mean shift of ($\delta_\mu = 0.8\sigma$) occurs. Then between the 17^{th} and 18^{th} samples, the process status changes again due to a sustained decreasing mean shift of ($\delta_\mu = -\sigma$). On the computer monitor, the display of the single ACUSUM II chart is large and clear. It is easy for the operators to figure out whether the process is in control or out of control. In contrast, the two separate charts of an optimal *X*&CUSUM chart and the three separate CUSUM charts of a 3-CUSUM(μ) scheme are quite crowded and messy for the operators to observe. They have to check all the seperate charts at the same time in order to decide the process status.

(4) The location of the changing point (the time when a process shift occurs) usually provides most useful diagnostic information to facilitate the identification of the assignable cause. Most of the practical users of the CUSUM charts take the point from which onward the sample points are invariably larger (or smaller) than zero as the estimated change point (Nishina 1992). When using an ACUSUM II chart or any other single-chart scheme, it is straightforward to use this heuristic method to estimate the changing point. On the other hand, each of the two separate charts of an optimal *X*&CUSUM chart and the three separate CUSUM charts of a 3-CUSUM(μ) scheme may suggest different change points and therefore bring

about confusion for the estimation of the change point.

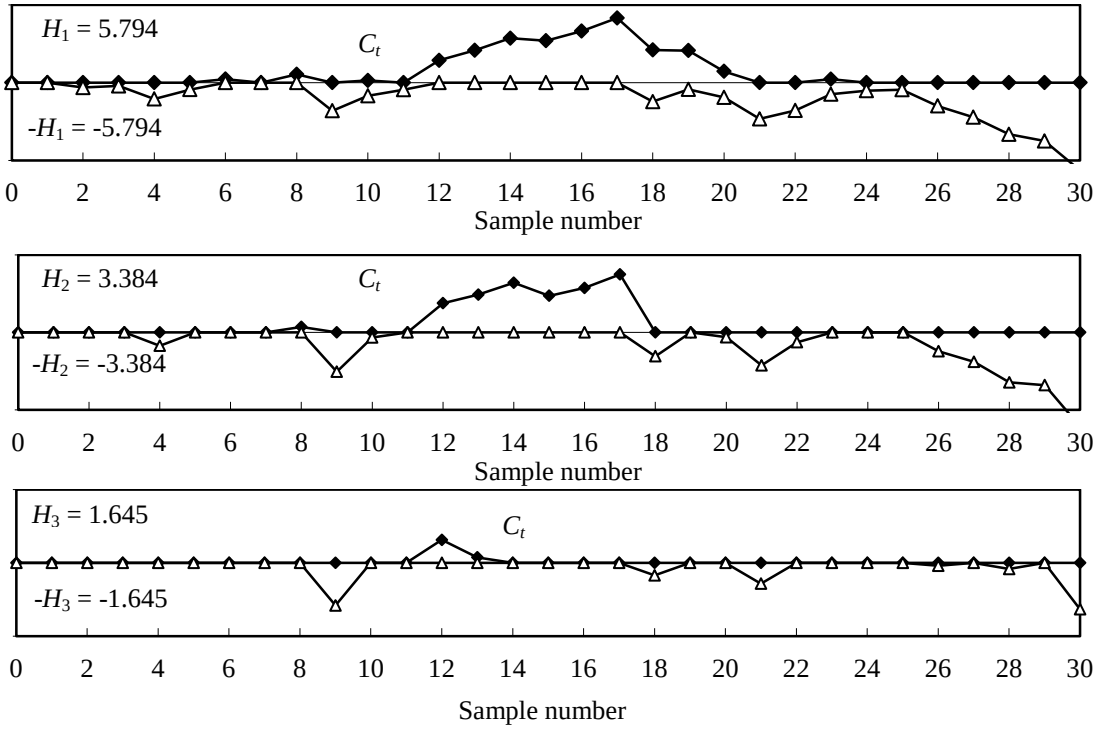

(*a*) 3-CUSUM(μ) Scheme

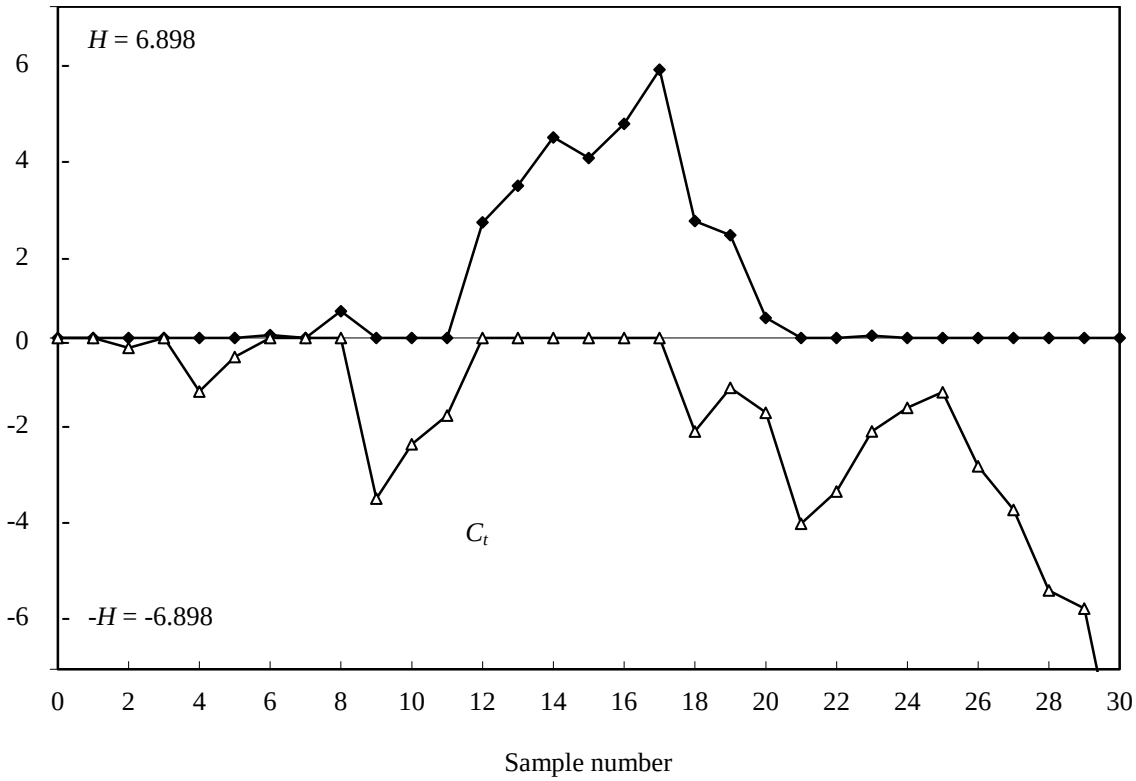

(*b*) ACUSUM II Chart

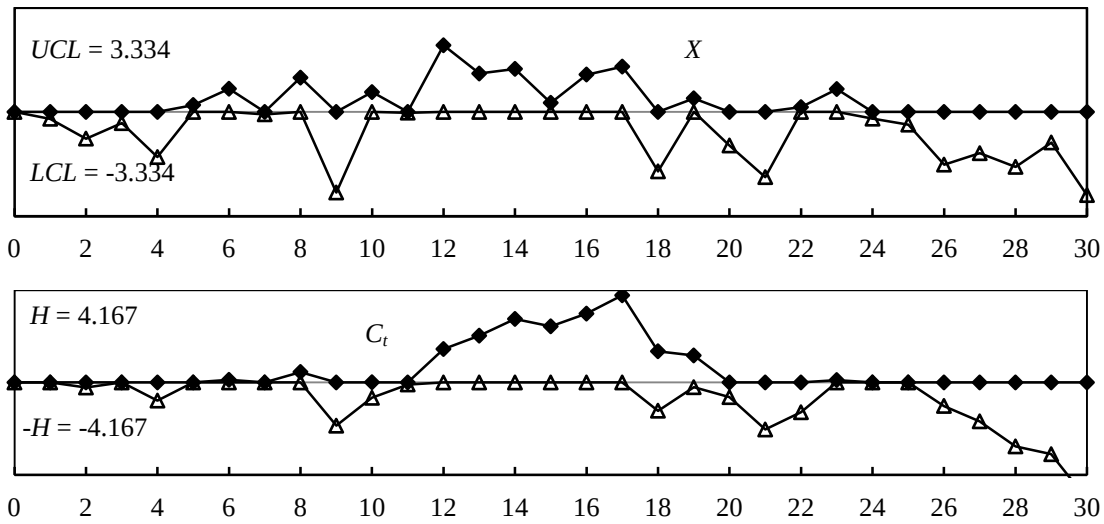

(*c*) Optimal *X*&CUSUM Chart

Figure 3-1. Computer Displays of Three Charts

3.3.6 Summary Comments

Section 3.3 has studied the performance of the proposed optimal *X*&CUSUM chart and ACUSUM II chart by reporting a systematic comparative study of seven CUSUM charts for detecting mean shifts under different conditions.

The five cases with different mean shift ranges ($\delta_{\mu,\min} \leq \delta_{\mu} \leq \delta_{\mu,\max}$) should be sufficiently representative to cover most SPC scenarios in practice. The charting parameters of the seven CUSUM charts for these five cases are summarized in Table 3-2. A QA engineer can choose a case that is most analogous to his particular application and then deploys the corresponding charting parameters from Table 3-2.

The ACUSUM II chart proposed in this PhD thesis will provide one more alternative for the SPC users and may arouse more research interests in the topic of adaptive control charts. The high detection effectiveness of the ACUSUM II chart is attributed to the on-line adaption of an additional charting parameter *w* and the optimized design of all charting parameters. The ACUSUM II chart is not only the best single-chart scheme in terms of the overall detection effectiveness, but also outperforms many multi-chart schemes (*e.g.* the *X*&CUSUM charts). Even though the ACUSUM II chart

is slightly inferior to the 3-CUSUM(μ) scheme in detection effectiveness, it is simpler than the latter for implementation, and, especially, for design.

The ACUSUM II chart retains most of the advantages of the single-chart schemes in the simplicity for design and implementation, such as the high speed in *ATS* computation through a Markov procedure, the clearness and clarity of the computer display for the operator to observe, to decide the process status and to estimate the changing point. The implementation of the ACUSUM II chart is very simple in a computer-aided SPC system which has been widely available in modern industries.

The optimal *X*&CUSUM chart is slightly inferior to the ACUSUM II chart and the 3-CUSUM(μ) scheme. Its performance is enhanced greatly by the optimal design compared with the Lucas' *X*&CUSUM chart. It outperforms Lucas' *X*&CUSUM chart, ACUSUM I chart and the conventional and optimal CUSUM charts. Without the optimal design, the Lucas' *X*&CUSUM chart is even slightly less effective than the single optimal CUSUM chart if measured by *AEQL*. Additionally, the statistic of the optimal *X*&CUSUM chart is simpler than that of the ACUSUM II chart and 3-CUSUM(μ) scheme, and its *ATS* can be calculated by a Markov procedure. Furthermore, people in the work floor may be more familiar with the procedure of *X* chart and CUSUM chart. Given these advantages, the optimal *X*&CUSUM chart is also a good choice for many applications.

3.4 Example

A manufacturing factory produces a specific type of bearings. The diameter x of the bearing is a key dimension and specified as 80±0.008 *mm*. The process mean can be easily adjusted to the nominal value (80 *mm*) at the center between the lower and upper specification limits. In phase I operation, it is found that the distribution of the diameter can be well approximated by a normal distribution and the standard deviation σ is estimated as 0.00217 *mm*. The QA engineer specifies the minimum allowable ATS_0 as 370 (same as that of a conventional 3-sigma $\bar{X}$ chart), and requires that two-sided mean shifts be detected. This means that the specified value of τ for the design of a one-sided CUSUM chart should be 740. Moreover, based on his experience with the process, the QA engineer believes that adjusting the process for a mean shift smaller than 0.25σ may cause over-adjustment and that mean shifts larger than 5.0σ seldom occur. Consequently, the lower and upper bounds of mean shift are determined as 0.25σ and 5.0σ, respectively. In order to standardize the design and operation, the diameter x is converted to z conforming to a standard normal distribution.

$$z = \frac{x - 80}{0.00217}.$$

The diameter is previously monitored by a conventional CUSUM chart with k = 0.5 by means of an on-site computer. A possible way to improve the overall performance is to turn to the more effective charts, such as the optimal *X*&CUSUM chart, ACUSUM II chart, and 3-CUSUM(μ) scheme. Based on the specifications of τ = 740, $\delta_{\mu,\min}$ = 0.25 and $\delta_{\mu\ \max}$ = 5.0, the above four charts can be designed. The charting parameters can be obtained from Table 3-2.

Conventional CUSUM chart: k = 0.5, H = 4.774, $AEQL$ = 19.778.

Optimal *X*&CUSUM chart: k = 0.613, H = 4.361, UCL = 3.251, $AEQL$ =16.197

ACUSUM II chart: H = 7.373, λ = 0.640, k_1 = 0.563, k_2 = 0.563, w_1 = 1.465, w_2 = 2.110, $AEQL$ = 16.037.

3-CUSUM(μ) scheme: $k_1 = 0.435$, $k_2 = 0.951$, $k_3 = 1.984$, $H_1 = 6.350$, $H_2 = 3.086$, $H_3 = 1.251$, $AEQL$ =15.780.

The *ATS* performance of these charts is similar to that shown in Table 3-1. The ACUSUM II chart has achieved better overall *ATS* performance than all other charts except that it is slightly inferior to the 3-CUSUM(μ) scheme. In view of its ease in design and implementation, the QA engineer finally selects the ACUSUM II chart. The running of this ACUSUM II chart is illustrated in Figure 3-1(*b*). The operator can easily decide the process status and estimate the changing point by checking the pattern of the sample points on the computer screen.

3.5 Effect of Sampling Cost on the Design and Performance of Control Charts

The $\overline{X}$ and CUSUM control charts are most widely used to monitor the mean of a quality characteristic *x*. This section studies the sample sizes of control charts in the domain of statistical design. It takes the important sampling inspection cost (including the variable and fixed cost components) into consideration. The chart performance will be measured by *AEQL*. There are two comparative studies. One compares the performance of control charts that use conventional sample sizes; the other studies the performance of the charts using optimal sample sizes. There are two important findings based on the results of this study: (1) The $\overline{X}$ chart becomes more statistically effective for detecting mean shifts when the fixed sampling cost cannot be neglected and/or when the mean shift range is small. (2) The optimal sample sizes $n_{\overline{X}}$ (for the $\overline{X}$ chart) and n_{CUSUM} (for the CUSUM chart) depend on the range of the mean shift and the ratio between the fixed and variable sampling costs.

3.5.1 Introduction

Many new charts and techniques in SPC have been proposed in recent years (Liu *et al*. 2007, Yu *et al*. 2007, Costa *et al*. 2009, Magalhães *et al*. 2009). Generally, there are two different methods to design the control charts. The statistical method (Lucas 1982, Reynolds *et al*. 1990, Castagliola *et al*. 2008, Costa *et al*. 2009) aims at achieving the best statistical performance (e.g. the minimum out-of-control *ATS*) and the economic method (Duncan 1956, Rahim and Lashkari 1982, Zhang *et al*. 2008, Torng *et al*. 2009, Ho *et al*. 2009) attempts to minimize the SPC cost (e.g. the average cost per time unit). The economic designs have some weaknesses. For example, the resultant charts may have poor statistical performance and the calculated cost savings may be misleading (Woodall 1986). As a result, almost all of the control charts nowadays used in practice are designed by statistical methods. Among them, the $\overline{X}$ chart and CUSUM chart are the two most popular charts for variables. The $\overline{X}$ chart checks the sample mean $\bar{x}_t$ which is defined as follows:

$$\bar{x}_t = \frac{x_1 + x_2 + \cdots x_i + \cdots + x_{n_{\bar{x}}}}{n_{\bar{x}}}, \tag{3-56}$$

where x_i is the ith observed value of the quality characteristic x in the tth sample. An $\bar{X}$ chart produces an out-of-control signal when an $\bar{x}_t$ value falls below the lower control limit *LCL* or above the upper control limit *UCL*. On the other hand, the statistic C_t to be updated for an upper-sided CUSUM chart is

$$\begin{aligned} &C_0 = 0, \\ &C_t = \max\left(0,\ C_{t-1} + (\bar{x}_t - \mu_0) - k\right), \end{aligned} \tag{3-57}$$

The CUSUM chart signals an out-of-control status when C_t is larger than the control limit H.

The $\bar{X}$ chart usually uses a sample size $n_{\bar{x}}$ = 4, 5 or 6 and the CUSUM chart often works best with a sample size n_{CUSUM} = 1 (Montgomery 2009). The numerical results obtained by Reynolds and Stoumbos (2004*a*) further show that, from an overall viewpoint, the CUSUM charts with (n_{CUSUM} = 1) generally outperforms the Shewhart charts with ($n_{\bar{X}}$ = 4) for detecting mean shifts. However, these findings are obtained by only considering the variable sampling inspection cost c, but neglecting the impact of the fixed sampling inspection cost b. As a result, the sampling interval h is proportional to the sample size n and the use of large sample size has little advantage.

This section will study and compare the performance of the $\bar{X}$ chart and CUSUM chart, as well as their combination (i.e. the $\bar{X}$ &CUSUM chart), for detecting mean shift δ. All of the three charts are designed by statistical method, but taking the sampling cost (including both the variable and fixed components) into consideration.

3.5.2 Sampling Cost

In a sampling inspection, the sampling cost consists of a fixed component b and a variable component c. While b is the cost per sample and is independent of the sample

size n, c is the cost per unit and is proportional to n (Duncan 1956, Montgomery 2009). The fixed component b represents all overhead cost for taking a sample. It includes the cost (or time) for shutting down and restarting a process, walking a distance, cleaning hands and platform, setting the equipment, switching the computer, and so on. The following widely adopted model expresses the total sampling cost C as (Duncan 1956, Montgomery 2009),

$$C = cn + b. \tag{3-58}$$

Let A be the resources (in terms of dollars) available for sampling inspection in a unit of time. Then, to make full use of the resources, we have

$$A = \frac{C}{h} = \frac{cn + b}{h}, \text{ or } \quad h = \frac{cn + b}{A} \tag{3-59}$$

where h is the sampling interval. If b is expressed in terms of c (*i.e.*, $b = Bc$, where B is the fixed sampling cost in terms of c), then from Equation (3-59),

$$h = \frac{c}{A}(n + B). \tag{3-60}$$

The constant term of c/A in Equation (3-60) can be dropped as it can be considered as the time unit or a scaling for the sampling interval. Thus,

$$h = n + B. \tag{3-61}$$

If the fixed sampling cost is negligible (i.e. $B = 0$),

$$h = n. \tag{3-62}$$

It is noted that the fixed sampling cost B exists in most applications, and ($B = 0$) just represents a rare or special case. As a result, studying the impact of B on the performance of control charts has both practical and research significance. When ($B > 0$), the total cost for taking a sample does not increase proportionally along with an increase of the sample size n, and the sampling interval h increases more slowly in terms of percentage. For example, if $B = 0$, h is increased four times when n increases from one to four. However, if $B = 2$, h is only doubled with the same increment of n. As a result, a larger B value encourages the use of a relatively larger sample size in order to acquire a higher detection power.

3.5.3 Comparative Studies when Charts Using Fixed *n*

In this section, the control charts use the fixed sample sizes which are determined according to the conventions in literature. Consequently, they are called conventional charts in this study. Three conventional charts, $\overline{X}$, CUSUM and $\overline{X}$ &CUSUM charts, are compared for three shift ranges: a small one with $\delta_{\mu,\max} = 2$ (Castagliola *et al*. 2008), a medium one with $\delta_{\mu,\max} = 4$ (Montgomery 2009) and a large one with $\delta_{\mu,\max} = 6$. The lower bound $\delta_{\mu,\min}$ is fixed as zero in this section. The specification τ for the in-control ATS_0 is set as 740. The cost parameter B takes six different values (0, 0.5, 1, 3, 6, 10). It is the ratio between the overhead sampling cost and the cost for inspecting a single unit, and its value can be determined easily and accurately by a field test.

The key charting parameters of the conventional charts are set with reference to the studies by Lucas (1982), Reynolds and Stoumbos (2004*a*) and Montgomery (2009).

$\overline{X}$ chart: $n_{\overline{X}} = 4$.

CUSUM chart: $n_{\text{CUSUM}} = 1$, $k = 0.25, 0.5, 0.75$ for $\delta_{\mu,\max} = 2, 4, 6$, respectively.

$\overline{X}$ &CUSUM chart: $n_{\overline{X}\&\text{CUSUM}} = 1$, $k = 0.25, 0.5, 0.75$ for $\delta_{\mu,\max} = 2, 4, 6$, respectively,

$UCL = 3.5$ (for the $\overline{X}$ element).

The upper control limit UCL of the $\overline{X}$ chart, the control limit H of the CUSUM chart and the control limit H of the CUSUM element in the $\overline{X}$ &CUSUM combination are adjusted so that ATS_0 equals τ. The sampling interval h is determined based on the sample size n and the fixed sampling cost B using Equation (3-61).

Table 3-4 shows the performance comparison of the three charts. It displays the charting parameters, the *AEQL* value (Equation 3-9 in section 3.1.3), the *AEQL*/ $AEQL_{\overline{X}}$ ratio, and the *ARATS* value (using the $\overline{X}$ chart as the benchmark, Equation 3-3 in section 3.1.3) of each chart under different $\delta_{\mu,\max}$ and B values.

Let us first study the cases in which $\delta_{\mu,\max} = 4$. Here, the mean shift range ($0 < \delta_\mu \leq 4$) is

considered as a nominal setting (Montgomery 2009). It can be seen that, along with the increase in *B*, the $\overline{X}$ chart becomes increasingly more effective in terms of *AEQL* compared with the CUSUM chart. This is because a larger *B* value makes the sampling interval *h* of the $\overline{X}$ chart increase less in terms of percentage and thus helps to shorten the *ATS* of this chart. The CUSUM chart outperforms the $\overline{X}$ chart only when *B* is zero. It is the case studied in many published works. However, ($B = 0$) is a rare case. For all other *B* values, even when *B* is as small as 0.5, the $\overline{X}$ chart outperforms the CUSUM chart. As an example, when $B = 3$, the *AEQL* of the CUSUM chart is larger than that of the $\overline{X}$ chart by 46%. Consequently, the out-of-control *ATS* of the CUSUM chart is generally larger than that of the $\overline{X}$ chart over the shift range. As illustrated in Figure 3-2, the normalized *ATS* (i.e. $ATS_{\text{CUSUM}}/ ATS_{\overline{X}}$) is larger, or substantially larger, than one as long as $\delta_\mu \geq 0.5$. The highest ratio of $ATS_{\text{CUSUM}}/ ATS_{\overline{X}}$ is 2.33 at $\delta_\mu = 1.8$.

Next, for the cases where $\delta_{\mu,\max} = 2$, the relative effectiveness of the $\overline{X}$ chart is even higher. Even for a small fixed sampling cost such as $B = 0.5$, the *AEQL* value of the $\overline{X}$ chart is 8% smaller than that of the CUSUM chart. When $B = 3$, the *AEQL* value of the $\overline{X}$ chart is 67% lower.

Table 3-4. Comparison of Conventional Charts

$\delta_{\mu,\max}$	*B*	Chart	*n*	*h*	*UCL*	*k*	*H*	*AEQL*	$AEQL/AEQL_{xbar}$	*ARATS*
2	0	xbar	4	4.0	1.27	-	-	10.81	1.00	1.00
		CUSUM	1	1.0	-	0.25	8.01	9.26	0.86	0.95
		xbar&CUSUM	1	1.0	3.50	0.25	8.31	9.34	0.86	0.95
	0.5	xbar	4	4.5	1.25	-	-	11.45	1.00	1.00
		CUSUM	1	1.5	-	0.25	7.24	12.35	1.08	1.17
		xbar&CUSUM	1	1.5	3.50	0.25	7.42	12.35	1.08	1.17
	1	xbar	4	5.0	1.24	-	-	12.06	1.00	1.00
		CUSUM	1	2.0	-	0.25	6.71	15.08	1.25	1.33
		xbar&CUSUM	1	2.0	3.50	0.25	6.83	15.02	1.25	1.33
	3	xbar	4	7.0	1.17	-	-	14.35	1.00	1.00
		CUSUM	1	4.0	-	0.25	5.46	23.95	1.67	1.70
		xbar&CUSUM	1	4.0	3.50	0.25	5.50	23.81	1.66	1.68
	6	xbar	4	10.0	1.11	-	-	17.42	1.00	1.00
		CUSUM	1	7.0	-	0.25	4.51	34.11	1.96	1.91
		xbar&CUSUM	1	7.0	3.50	0.25	4.53	33.95	1.95	1.90
	10	xbar	4	14.0	1.04	-	-	21.13	1.00	1.00
		CUSUM	1	11.0	-	0.25	3.79	44.82	2.12	2.01
		xbar&CUSUM	1	11.0	3.50	0.25	3.79	44.68	2.11	2.00
4	0	xbar	4	4.0	1.27	-	-	14.82	1.00	1.00
		CUSUM	1	1.0	-	0.5	4.77	12.49	0.84	0.90
		xbar&CUSUM	1	1.0	3.50	0.5	4.91	11.14	0.75	0.84
	0.5	xbar	4	4.5	1.25	-	-	16.31	1.00	1.00
		CUSUM	1	1.5	-	0.5	4.38	16.99	1.04	1.11
		xbar&CUSUM	1	1.5	3.50	0.5	4.45	15.27	0.94	1.04
	1	xbar	4	5.0	1.24	-	-	17.78	1.00	1.00
		CUSUM	1	2.0	-	0.5	4.09	21.01	1.18	1.26
		xbar&CUSUM	1	2.0	3.50	0.5	4.15	19.11	1.07	1.18
	3	xbar	4	7.0	1.17	-	-	23.59	1.00	1.00
		CUSUM	1	4.0	-	0.5	3.43	34.35	1.46	1.56
		xbar&CUSUM	1	4.0	3.50	0.5	3.44	32.80	1.39	1.52
	6	xbar	4	10.0	1.11	-	-	32.13	1.00	1.00
		CUSUM	1	7.0	-	0.5	2.90	49.92	1.55	1.71
		xbar&CUSUM	1	7.0	3.50	0.5	2.90	49.93	1.55	1.71
	10	xbar	4	14.0	1.04	-	-	43.32	1.00	1.00
		CUSUM	1	11.0	-	0.5	2.49	66.98	1.55	1.75
		xbar&CUSUM	1	11.0	3.50	0.5	2.49	66.98	1.55	1.75
6	0	xbar	4	4.0	1.27	-	-	26.75	1.00	1.00
		CUSUM	1	1.0	-	0.75	3.34	13.23	0.49	0.68
		xbar&CUSUM	1	1.0	3.50	0.75	3.41	12.22	0.46	0.65
	0.5	xbar	4	4.5	1.25	-	-	29.86	1.00	1.00
		CUSUM	1	1.5	-	0.75	3.07	18.07	0.61	0.84
		xbar&CUSUM	1	1.5	3.50	0.75	3.10	17.30	0.58	0.82
	1	xbar	4	5.0	1.24	-	-	32.95	1.00	1.00
		CUSUM	1	2.0	-	0.75	2.88	22.59	0.69	0.95
		xbar&CUSUM	1	2.0	3.50	0.75	2.89	22.20	0.67	0.94
	3	xbar	4	7.0	1.17	-	-	45.27	1.00	1.00
		CUSUM	1	4.0	-	0.75	2.43	39.05	0.86	1.20
		xbar&CUSUM	1	4.0	3.50	0.75	2.43	39.05	0.86	1.20
	6	xbar	4	10.0	1.11	-	-	63.63	1.00	1.00
		CUSUM	1	7.0	-	0.75	2.07	61.55	0.97	1.35
		xbar&CUSUM	1	7.0	3.50	0.75	2.07	61.55	0.97	1.35
	10	xbar	4	14.0	1.04	-	-	87.98	1.00	1.00
		CUSUM	1	11.0	-	0.75	1.79	89.71	1.02	1.42
		xbar&CUSUM	1	11.0	3.50	0.75	1.79	89.71	1.02	1.42

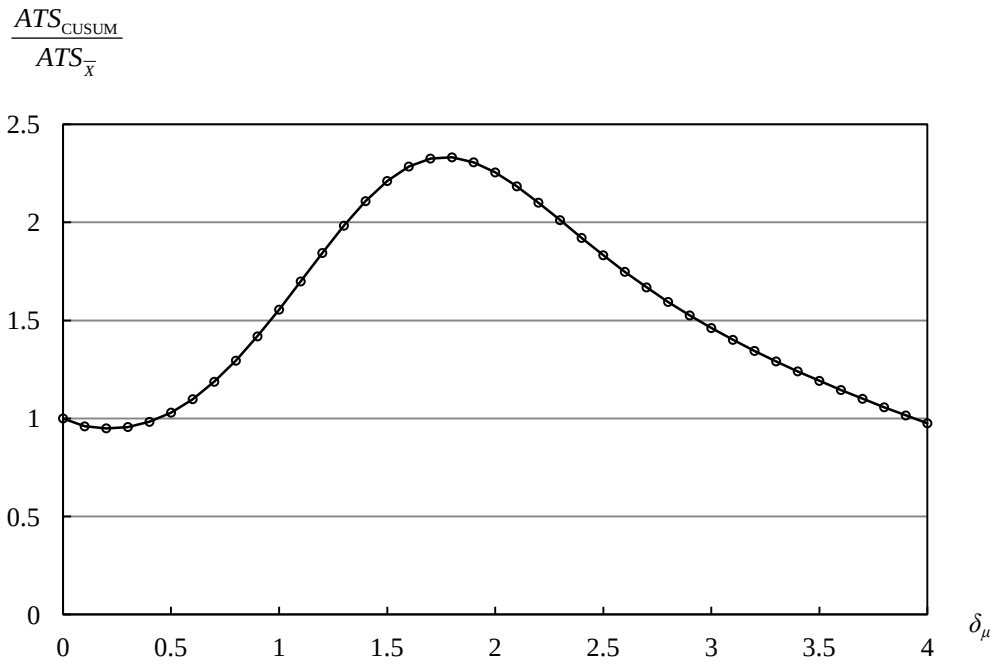

Figure 3-2. $ATS_{\text{CUSUM}}/ATS_{\bar{X}}$ vs. δ_μ

Finally, if $\delta_{\mu,\max} = 6$ (Table 3-4), the performance of the $\bar{X}$ chart is still improved when *B* increases. But its *AEQL* value is larger than that of the CUSUM chart until (*B* = 10). However, when $B \geq 6$, the difference in *AEQL* values between the two charts becomes smaller than 3%.

Comparing with the $AEQL/AEQL_{\bar{X}}$ ratio, the *ARATS* measure (the rightmost column in Table 3-4) is generally more in favor of the $\bar{X}$ chart. For example when $\delta_{\mu,\max} = 2$, even if *B* = 0, the *ATS* value of the $\bar{X}$ chart is, on average, only 5% longer than that of the CUSUM chart. Even for $\delta_{\mu,\max} = 6$, the $\bar{X}$ chart considerably outperforms the CUSUM chart in terms of *ARATS* when $B \geq 3.0$.

The results in Table 3-4 reveal that the general belief that the overall statistical performance of the CUSUM chart with ($n_{\text{CUSUM}} = 1$) is often superior to that of the $\bar{X}$ chart with ($n_{\bar{X}} = 4$) may not be true even when the fixed sampling cost *B* is just slightly larger than zero. If the simplicity in design and implementation is taken into consideration, the $\bar{X}$ chart may be more attractive for many applications. It is also observed that the $\bar{X}$ &CUSUM chart always has a better, or at least equal, operating

characteristic compared with the CUSUM chart, especially when B is small. This is indicated by both *AEQL* and *ARATS* values.

3.5.4 Comparative Studies when Charts Using Optimal *n*

In this section, the same specifications are used for τ, $\delta_{\mu,\max}$ and B as in the last section. However, all the three charts will be optimized by the following model as in section 3.1.4. Therefore, they are called the optimal control charts in this study.

Objective function: $AEQL$ = minimum. (3-63)

Constraint function: $ATS_0 \geq \tau$. (3-64)

Design variables: charting parameters. (3-65)

During the optimal design, the optimal values of the independent design variables are searched in order to minimize *AEQL*. The dependent variables are the sampling interval h (determined by Equation (3-61)) and the control limits. The control limits are adjusted so that the constraint function on ATS_0 (Equation (3-64)) is satisfied.

For an $\bar{X}$ chart, the only independent variable is the sample size n, and the dependent variables are the sampling interval h and control limit *UCL*. For a CUSUM chart, the independent variables are the sample size n and reference parameter k, and the dependent variables are the sampling interval h and control limit H. The $\bar{X}$ &CUSUM chart has two control limits *UCL* and H for the $\bar{X}$ and CUSUM elements, respectively. These two control limits are adjusted simultaneously so that the detection power of the $\bar{X}$ &CUSUM combination is allocated between the $\bar{X}$ and CUSUM elements in an optimal manner and the in-control ATS_0 of the whole $\bar{X}$ &CUSUM chart is equal to τ.

Table 3-5 displays the results of the comparison among the three optimal control charts. The values of the charting parameters are the optimal ones. Some similar conclusions can be reached as those for the conventional charts. That is, the

performance of the $\overline{X}$ chart is enhanced along with an increase in B and/or a decrease in $\delta_{\mu,\max}$, and the $\overline{X}$ &CUSUM chart always outperforms the CUSUM chart.

However, the results for the comparison of the optimal charts reveal some new findings. For example, the overall effectiveness of the CUSUM chart has been improved to a considerable degree. As a result, it outperforms the $\overline{X}$ chart in all of the cases in Table 3-5. However, when $B \geq 3.0$, the difference in *AEQL* values between the two charts is relatively insignificant, always smaller than 10%.

From Table 3-5, it is also found that, for most of the cases, the optimal value of the sample size $n_{\overline{X}}$ is smaller than four, except for $\delta_{\mu,\max} = 2$. However, this shift range of $(0 < \delta \leq 2)$ seems too small for most applications. The optimal value of n_{CUSUM} is likely to be larger than one except for $B \leq 1$ when $\delta_{\mu,\max} = 6$. Usually, $(\delta_{\mu,\max} = 6)$ represents a quite large mean shift range. The optimal values of the sample sizes $n_{\overline{X}}$ and n_{CUSUM} depend on both $\delta_{\mu,\max}$ and B. They always increase along with an increase in B and/or a decrease in $\delta_{\mu,\max}$. A practical user may select a set of charting parameters from Table 3-5 for his particular application based on the values of $\delta_{\mu,\max}$ and B.

As a general guideline for the nominal setting $(0 < \delta_{\mu} \leq 4)$, the optimal $n_{\overline{X}}$ is either 3 or 4, for both $(B = 0)$ and $(B > 0)$. This indicates that, for the best overall statistical performance, $n_{\overline{X}}$ should be set beyond the commonly recommended range of 4 to 6, or at the lower end of this range. For $(0 < \delta_{\mu} \leq 4)$, the optimal n_{CUSUM} is either 2 or 3, larger than the widely adopted value of one.

Table 3-5. Comparison of Optimal Charts

$\delta_{\mu,\max}$	*B*	Chart	*n*	*h*	*UCL*	*k*	*H*	*AEQL*	$AEQL/AEQL_{xbar}$	*ARATS*
2	0	xbar	7	7.0	0.89	-	-	8.92	1.00	1.00
		CUSUM	5	5.0	-	0.41	0.84	7.61	0.85	0.87
		xbar&CUSUM	5	5.0	1.21	0.28	1.34	7.42	0.83	0.85
	0.5	xbar	7	7.5	0.88	-	-	9. 34	1.00	1.00
		CUSUM	6	6.5	-	0.38	0.71	8.09	0.87	0.87
		xbar&CUSUM	6	6.5	1.06	0.26	1.14	7.94	0.85	0.86
	1	xbar	8	9.0	0.80	-	-	9.75	1.00	1.00
		CUSUM	6	7.0	-	0.38	0.69	8.57	0.88	0.89
		xbar&CUSUM	6	7.0	1.05	0.26	1.11	8.41	0.86	0.87
	3	xbar	8	11.0	0.77	-	-	11.30	1.00	1.00
		CUSUM	7	10.0	-	0.31	0.64	10.32	0.91	0.91
		xbar&CUSUM	7	10.0	0.91	0.24	0.93	10.21	0.90	0.90
	6	xbar	8	14.0	0.73	-	-	13.56	1.00	1.00
		CUSUM	7	13.0	-	0.31	0.58	12.75	0.94	0.93
		xbar&CUSUM	7	13.0	0.87	0.20	0.98	12.65	0.93	0.92
	10	xbar	9	19.0	0.65	-	-	16.49	1.00	1.00
		CUSUM	8	18.0	-	0.29	0.48	15.79	0.96	0.95
		xbar&CUSUM	8	18.0	0.76	0.18	0.82	15.71	0.95	0.94
4	0	xbar	3	3.0	1.53	-	-	13.84	1.00	1.00
		CUSUM	2	2.0	-	0.65	1.68	10.63	0.77	0.81
		xbar&CUSUM	2	2.0	2.14	0.43	2.67	10.19	0.74	0.79
	0.5	xbar	3	3.5	1.50	-	-	15.46	1.00	1.00
		CUSUM	2	2.5	-	0.65	1.60	12.66	0.82	0.86
		xbar&CUSUM	2	2.5	2.07	0.43	2.57	12.22	0.79	0.84
	1	xbar	3	4.0	1.47	-	-	17. 06	1.00	1.00
		CUSUM	2	3.0	-	0.65	1.53	14.61	0.86	0.89
		xbar&CUSUM	2	3.0	2.03	0.43	2.46	14.18	0.83	0.87
	3	xbar	3	6.0	1.39	-	-	23.24	1.00	1.00
		CUSUM	3	6.0	-	0.54	1.02	21.15	0.91	0.90
		xbar&CUSUM	3	6.0	1.51	0.36	1.63	20.92	0.90	0.89
	6	xbar	4	10.0	1.11	-	-	32.13	1.00	1.00
		CUSUM	3	9.0	-	0.48	1.00	30.22	0.94	0.96
		xbar&CUSUM	3	9.0	1.41	0.36	1.45	30.02	0.93	0.95
	10	xbar	4	14.0	1.04	-	-	43.32	1.00	1.00
		CUSUM	3	13.0	-	0.48	0.88	41.95	0.97	0.99
		xbar&CUSUM	3	13.0	1.33	0.31	1.47	41.76	0.96	0.98
6	0	xbar	2	2.0	1.97	-	-	18.28	1.00	1.00
		CUSUM	1	1.0	-	1.0	2.52	12.74	0.70	0.77
		xbar&CUSUM	1	1.0	3.27	0.6	4.41	11.95	0.65	0.74
	0.5	xbar	2	2.5	1.92	-	-	21.74	1.00	1.00
		CUSUM	1	1.5	-	1.0	2.32	17.53	0.81	0.89
		xbar&CUSUM	1	1.5	3.12	0.6	4.11	16.69	0.77	0.86
	1	xbar	2	3.0	1.87	-	-	25.15	1.00	1.00
		CUSUM	1	2.0	-	0.9	2.42	22.02	0.88	0.96
		xbar&CUSUM	1	2.0	3.03	0.6	3.86	21.17	0.84	0.94
	3	xbar	2	5.0	1.75	-	-	38.39	1.00	1.00
		CUSUM	2	5.0	-	0.65	1.33	35.74	0.93	0.91
		xbar&CUSUM	2	5.0	1.89	0.44	2.15	35.46	0.93	0.90
	6	xbar	2	8.0	1.62	-	-	57.66	1.00	1.00
		CUSUM	2	8.0	-	0.65	1.15	55.22	0.96	0.93
		xbar&CUSUM	2	8.0	1.76	0.44	1.89	54.95	0.95	0.92
	10	xbar	2	12.0	1.51	-	-	82.83	1.00	1.00
		CUSUM	2	12.0	-	0.58	1.12	80.62	0.97	0.94
		xbar&CUSUM	2	12.0	1.65	0.37	1.90	80.39	0.97	0.93

It is interesting to find that the optimal design can improve the overall performance of all charts to a considerable or substantial degree. Figure 3-3 displays the curve of ($ATS_{\text{conventional CUSUM}}/ATS_{\text{optimal CUSUM}}$) versus δ_μ under (B = 3, $\delta_{\mu,\max}$ = 4). The conventional CUSUM chart uses a sample size of (n_{CUSUM} = 1), and the optimal CUSUM chart uses an optimal sample size of (n_{CUSUM} = 3). The value of ($ATS_{\text{conventional CUSUM}}/ATS_{\text{optimal CUSUM}}$) is obviously larger than one across the entire shift range. The curve is close to one only when δ is either very small or very large. It clearly indicates that the CUSUM chart using the optimal sample size has a much better overall performance in this case.

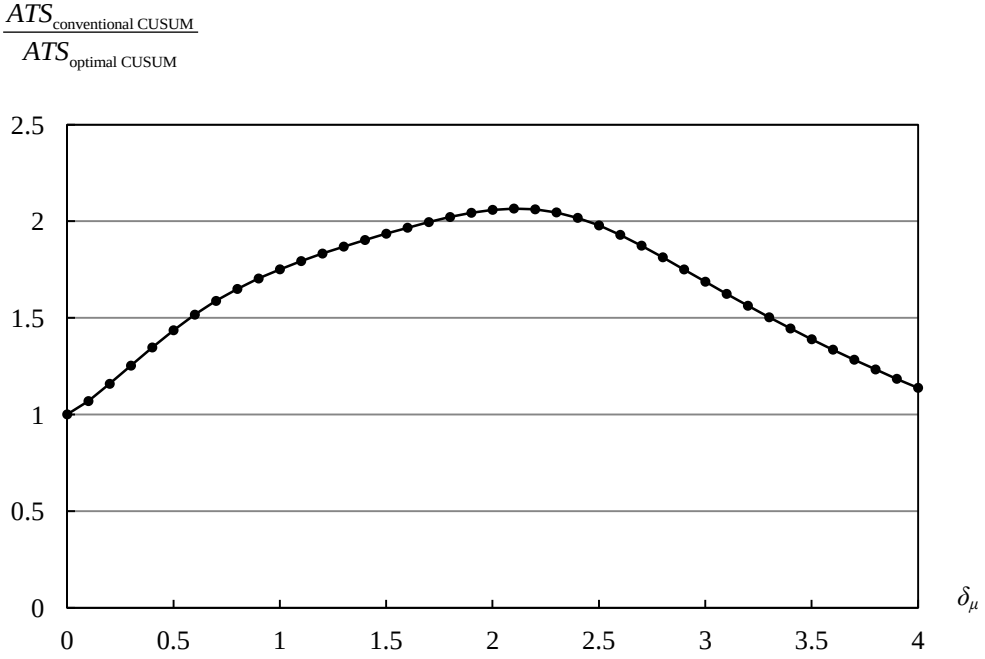

Figure 3-3. ($ATS_{\text{conventional CUSUM}}/ATS_{\text{optimal CUSUM}}$) vs. δ_μ

Table 3-6 compares the $AEQL_{\text{optimal}}$ of an optimal chart (using optimal $n_{\bar{X}}$ and n_{CUSUM}) with the $AEQL_{\text{conventional}}$ of the corresponding conventional chart (using $n_{\bar{X}}$ = 4 and n_{CUSUM} = 1) under different combinations of $\delta_{\mu,\max}$ and B. The optimal design always brings about improvement for all of the cases. The gain is quite significant for many combinations of $\delta_{\mu,\max}$ and B. For example, the optimal design can reduce the $AEQL$ of the CUSUM chart by 57% when $\delta_{\mu,\max}$ = 2 and B = 3; it reduces the $AEQL$ of the $\bar{X}$ chart by 32% when $\delta_{\mu,\max}$ = 6 and B = 0.

Table 3-6. Improvement in *AEQL* by Optimal design

$\delta_{\mu,\max}$	B	$AEQL_{optimal}/AEQL_{conventional}$		
		$\overline{X}$	CUSUM	$\overline{X}$ &CUSUM
2	0.0	0.8255	0.8222	0.7946
	0.5	0.8161	0.6554	0.6430
	1.0	0.8082	0.5681	0.5601
	3.0	0.7877	0.4309	0.4289
	6.0	0.7789	0.3737	0.3726
	10.0	0.7805	0.3523	0.3517
4	0.0	0.9339	0.8513	0.9149
	0.5	0.9483	0.7451	0.8005
	1.0	0.9593	0.6953	0.7420
	3.0	0.9852	0.6157	0.6378
	6.0	1.0000	0.6053	0.6013
	10.0	1.0000	0.6263	0.6235
6	0.0	0.6832	0.9632	0.9781
	0.5	0.7282	0.9699	0.9644
	1.0	0.7631	0.9750	0.9538
	3.0	0.8479	0.9153	0.9080
	6.0	0.9062	0.8973	0.8929
	10.0	0.9415	0.8987	0.8961

It is noted that the improvement in performance is attributable not only to the optimal sample size, but also to the optimal designs of other charting parameters, such as the reference parameter *k* of the CUSUM and $\overline{X}$ &CUSUM charts.

It is also noted that the optimal design only changes the values of the charting parameters, leaving the structure and operational rules of the charts untouched. This means that the gain in detection effectiveness is acquired without sacrificing the simplicity for implementation.

Finally, from the rightmost two columns in Table 3-5, it is interesting to find that, the $AEQL/AEQL_{\overline{X}}$ ratio and *ARATS* value of an optimal control chart are usually quite close to each other.

The optimization model proposed in this study can be used in all statistical designs for the $\overline{X}$ and CUSUM charts, and the results can be applied to general SPC applications with or without the fixed sampling cost *B*. Moreover, both the variable and fixed sampling costs dealt with in this study can be estimated easily and accurately.

3.5.5 Example

The thickness *x* of a printed circuit board is an important dimension and has to be monitored by a control chart using a sampling inspection. The two-sided mean shifts have to be detected. The thickness *x* is specified as 1.60±0.038 *mm*. The process mean can be easily adjusted to the nominal value (1.60 *mm*) at the center between the lower and upper specification limits. In phase I operation, it is found that the distribution of *x* can be well approximated by a normal distribution and the standard deviation σ_0 of *x* is very close to 0.0091 *mm*. The time for preparing a sampling inspection (fixed sampling cost *b*) is 60 seconds and the time for inspecting one circuit board (variable sampling cost *c*) is 20 seconds. Thus, the value of *B* is equal to three. An operator is assigned to spend five minutes (300 seconds) per hour to run the control chart (available resources *A* = 300 seconds per hour). Based on past experience, the Quality Assurance (QA) engineer believes that the maximum possible mean shift be no larger than $4\sigma_0$ (i.e., $\delta_{\mu,\max} = 4$). In this application, the sampling cost is proportional to the time spent on the sampling inspection, therefore the cost components of *b* and *c* are expressed in terms of seconds and the resource *A* as the allocated inspection time in seconds per working hour.

In order to standardize the design and operation, the thickness *x* is again converted to *z* conforming to a standard normal distribution.

$$z = \frac{x - 1.6}{0.0091}.$$

Since a two-sided control chart is to be designed, the τ value is set equal to 740 for the design of the upper- or lower-sided charts.

The specifications can be summarized as: $\tau = 740$, $\delta_{\mu,\max} = 4$ and $B = 3$. The charting parameters of the conventional and optimal $\bar{X}$ and CUSUM charts, as well as their *AEQL* values, can be found from Tables 3-4 and 3-5 and are listed below.

The conventional $\bar{X}$ chart: $n = 4$, $h = 7.0$, $UCL = 1.17$, $AEQL = 23.59$.

The optimal $\bar{X}$ chart: $n = 3$, $h = 6.0$, $UCL = 1.39$, $AEQL = 23.24$.

The conventional CUSUM chart: $n = 1$, $h = 4.0$, $k = 0.50$, $H = 3.43$, $AEQL = 34.35$.

The optimal CUSUM chart: $n = 3$, $h = 6.0$, $k = 0.54$, $H = 1.02$, $AEQL = 21.15$.

For detecting decreasing mean shifts, the $\bar{X}$ chart uses a lower control limit *LCL* (= -*UCL*), and the lower-sided CUSUM chart (Equation (2-27)) adopts the same values of *k* and *H* as its upper-sided counterpart.

By comparing the *AEQL* values of the charts, it can be seen that the optimal CUSUM chart has the best overall performance, followed by the optimal $\bar{X}$ chart and the conventional $\bar{X}$ chart. The conventional CUSUM chart surprisingly ranks the last.

Figure 3-4 displays the *ATS* curves of the four charts.

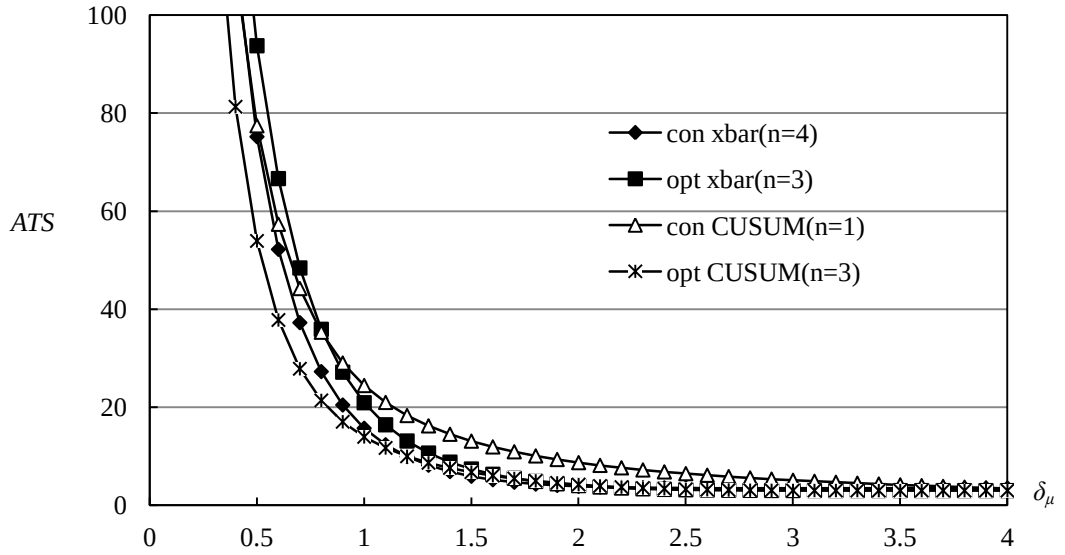

Figure 3-4 (*a*). *ATS* Comparison among Four Charts

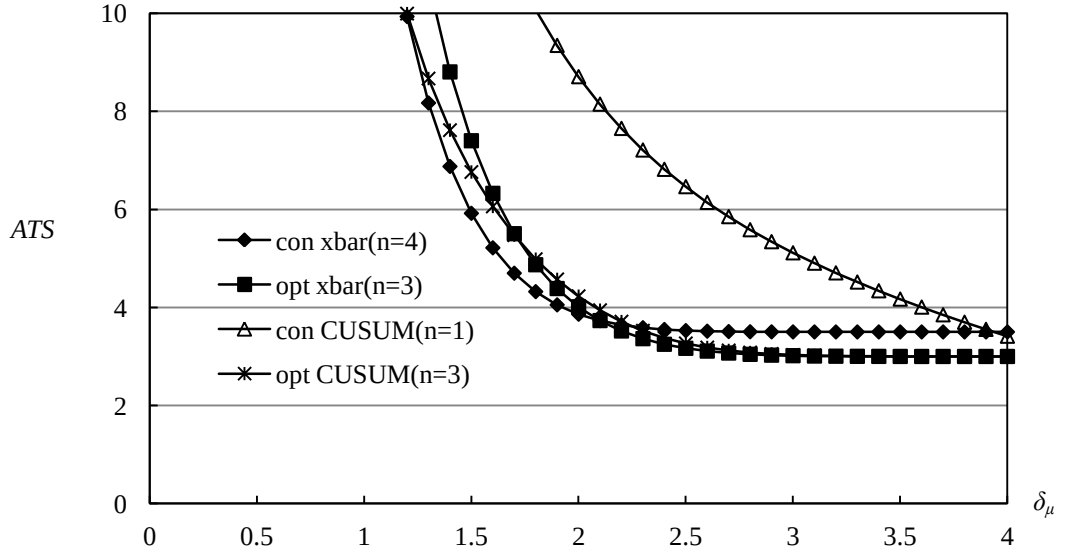

Figure 3-4 (*b*). *ATS* Comparison among Four Charts

Figure 3-4(*a*) shows the *ATS* curves over the whole shift range except for ($\delta_\mu = 0$) where the in-control ATS_0 values of all charts are equal to τ (= 740). Figure 3-4(*b*) zooms in the *ATS* curves for moderate and large mean shifts. The conventional CUSUM chart produces very large *ATS* values in this region, and consequently has a poor overall performance. The optimal CUSUM chart always produces an *ATS* value equal or close to the minimum across the shift range. The optimal $\bar{X}$ chart works best for $\delta_\mu \geq 1.8$.

3.5.6 Summary Comments

Section 3.5 studies the overall performance of the conventional and optimal $\overline{X}$ and CUSUM charts. It employs the statistical method to design the control charts, because statistical design is more realistic and used almost exclusively in today's SPC practice. However, the important sampling inspection costs including both the variable component *c* and fixed component *b* have been taken into consideration. Since the fixed sampling cost is an indispensable component of the total sampling inspection cost for most of the SPC applications and the $\overline{X}$ and CUSUM charts are the two charts used most widely in SPC practice, this study is important in research and useful for practice. The proposed approach is viable and feasible as the ratio *B* between *b* and *c* can be determined easily and accurately. The results bring about several important findings.

Firstly, it is found that the fixed sampling cost *b* significantly influences the performance of the control charts. Since the fixed sampling cost often exists, neglecting it discriminately may result in improper designs. Between the $\overline{X}$ and CUSUM charts, the former becomes relatively more effective along with an increase in *b*. When *b* is considerably large (say $b \geq 3c$), the performance difference between the two charts becomes insignificant. If the simplicity in design and implementation is a concern in an application, the $\overline{X}$ chart may be a better choice.

Secondly, the optimal design has demonstrated itself as a promising tool to improve the overall performance of all charts. Without the optimal design, a CUSUM chart may be even less effective than an $\overline{X}$ chart. Moreover, the optimal design only changes the values of the charting parameters. The implementation of an optimal chart is as easy as that of a conventional chart.

Thirdly, it is found that the optimal values of the sample sizes $n_{\overline{X}}$ and n_{CUSUM} are not four and one, respectively. This finding is generally true even regardless of the fixed sampling cost *b*. The optimal sample size for an application can be determined by the

optimal design. As a general guideline for ($0 < \delta_\mu \leq 4$), an $\overline{X}$ chart may use a sample size $n_{\overline{X}}$ of three or four; and a CUSUM chart may use a n_{CUSUM} value of two or three. Table 3-5 provides a useful reference for the designs of the $\overline{X}$ chart, CUSUM chart and their combination for different specifications of $\delta_{\mu,\max}$ and B (including the case of $B = 0$). It should cover most of the applications.

The discussions in this section are focused on the $\overline{X}$ and CUSUM charts. However, the general findings, including the influence of the sampling cost on a chart's performance and the role of the optimal design, can be applied to many other charts.

3.6 Summary of Chapter 3

This chapter proposes two new charts, the optimal *X*&CUSUM chart and ACUSUM II chart for detecting mean shift. It first presents an optimization algorithm for the design of the $\overline{X}$ &CUSUM chart based on *AEQL*. This performance measure is more comprehensive than *ARL* or *ATS*, since it considers both quality loss and the speed to signal over the range of mean shift.

Second, a new adaptive CUSUM (ACUSUM II) chart is proposed. A distinctive feature of the ACUSUM II chart is an additional adaptable parameter *w*, *i.e.*, the exponential of the sample mean shift in $(x_t - \mu_0)^w$. The ACUSUM II chart will adapt this parameter (w) according to the on-line estimated value of mean shift, in conjunction with the adaption of the reference parameter *k*.

In the performance evaluation part, the above two charts are compared with five other CUSUM charts for detecting process mean shift. The results reveal that the ACUSUM II chart not only outperforms the ACUSUM I chart and all other single-chart schemes to a substantial degree, but also works nearly equally as the most effective combined schemes, the 3-CUSUM(μ) scheme. On the other hand, the optimal *X*&CUSUM chart is more effective than the Lucas' *X*&CUSUM chart. Furthermore, both the ACUSUM II and the optimal *X*&CUSUM charts are relatively easier to implement and much simpler to design compared with the 3-CUSUM(μ) scheme.

In the last part of this chapter, the important sampling inspection cost (including the variable and fixed cost components) is taken into consideration when designing the control chart. The two most widely used charts, $\overline{X}$ and CUSUM control charts, are used to investigate the effect of the sampling cost. The results reveal that the $\overline{X}$ chart becomes more effective relatively for detecting mean shifts when the fixed sampling cost cannot be neglected and/or when the mean shift range is small. It is also found that if both $n_{\overline{X}}$ and n_{CUSUM} are determined based on some conventional wisdom as $n_{\overline{X}} = 4$

and $n_{CUSUM} = 1$, the simple $\overline{X}$ chart often outperforms the more complicated CUSUM chart from an overall viewpoint. Furthermore, under all circumstances, the overall statistical performance of both charts can be improved, or significantly improved, by the optimal design. The optimal sample sizes $n_{\overline{X}}$ and n_{CUSUM} depend on the range of the mean shift and the ratio between the fixed and variable sampling costs. In the general cases in which the mean shift $\delta_\mu \leq 4$, the best sample sizes are $n_{\overline{X}} = 3$ or 4, and $n_{CUSUM} = 2$ or 3.

Chapter 4

CUSUM Charts for Detecting Shifts in Mean and Variance

In Statistical Process Control (SPC), when dealing with a quality characteristic *x* that is a variable, it is usually necessary to monitor both the mean value and variability. As on-line measurement and distributed computing systems become a norm in today's SPC applications (Woodall and Montgomery 1999), many combined CUSUM or EWMA schemes have been developed (Serel and Moskowitz 2008, Sheu and Lu 2008). However, it is usually a complicated procedure because of the necessity of manipulating several CUSUM or EWMA charts simultaneously and designing and evaluating them by the time-consuming simulation. In this regard, this chapter will propose two simple control charts, the *X* chart and the ABS CUSUM chart, for detecting process shifts in mean and variance. Additionally, the effective but complicated 3-CUSUM(μ+σ) scheme (three combined CUSUM charts detecting process shifts in mean and variance, proposed by Reynolds and Stoumbos (2004*a*)) will be optimized to achieve a highest performance. The optimization method applied in this chapter is similar to those discussed in Chapter 3, except that the overall performance measure considers both mean and variance shifts. A comparative study among seven charts is presented subsequently. Moreover, the effect of sampling cost on the design and performance of control charts will also be investigated as in section 3.5 of Chapter 3. At the end, the effect of process shift distributions on chart design and performance will be investigated.

4.1 *X* chart

Traditionally, the $\overline{X}$ chart is used to detect process mean shift. In this section, it will be applied to detect process shifts in both mean and variance. The overall performance measure, *AEQL* and *ARATS* are again used as the objective function for the optimal design, but they need be re-defined when both mean and variance shifts are included. Additionally, this section presents the formulae to calculate the control limit and *ATS* of the $\overline{X}$ chart. Finally, the optimal sample size for $\overline{X}$ chart is discussed. The results are quite different from those based on the common sense.

4.1.1 Introduction

In SPC for variables, the main task of a control chart is to detect process shifts in mean and variance. To date, the combination of a Shewhart $\overline{X}$ chart and an *R* chart (or an *S* chart) is still adopted widely. This is obviously attributable to the simplicity of these combinations for understanding, implementation and design. A sample size *n* between 4 and 6 is usually recommended for the $\overline{X}$ &*R* (or $\overline{X}$ &*S*) combination (Montgomery 2009). When *n* = 1, an *X* chart can be combined with an MR (Moving Range) chart. Since deterioration in product quality is often the main concern, only the increasing variance shift, together with the increasing and decreasing mean shifts, is handled in most of the applications (Reynolds and Glosh 1981).

In the last ten years, some charting schemes that use a single chart to monitor both mean and variance have been proposed, as the design and implementation of a single chart is substantially simpler than those multi-chart schemes. These single charts include the *L* chart (Reynolds and Glosh 1981), the omnibus EWMA chart (Domangue and Patch 1991), the Likelihood Ratio Test (Sullivan and Woodall 1996), the *B* chart (Grabov and Ingman 1996), the MaxEWMA chart (Chen *et al.* 2001), a EWMA chart based on a non-central chi-square statistic (Costa and Rahim 2006*a*), the WLC chart (Wu and Tian 2005), a synthetic control chart based on a non-central chi-square statistic (Costa and Rahim 2006*b*) and a new Shiryaev-Roberts chart (zhang *et al*. 2011). Among them, the omnibus EWMA chart (Domangue and Patch 1991) may be the most effective one for detecting process shifts in the whole domain. Other schemes are either ineffective for detecting small shifts (*e.g.*, the Shewhart-type charts) or insensitive to large shifts (*e.g.*, the MaxEWMA chart and the WLC chart which use a sample size *n* larger than one).

A single $\overline{X}$ or *X* chart is also able to detect the two-sided mean shifts and/or an increasing variance shift (Reynolds and Stoumbos 2004*b*). In fact, many researchers pointed out that a single *X* chart outperforms the *X*&MR combination (Reynolds and Stoumbos 2004*a*). In this section, it is found that the optimal sample size for the $\overline{X}$ chart is one, rather than some value around four. It means that the simplest *X* chart is the most effective $\overline{X}$ charts for monitoring both mean and variance.

4.1.2 Performance Measure

As aforementioned in section 3.1.3, performance comparison among the charts cannot be concluded only based on the *ATS* values at one or a few process shift points, as it is usually difficult to predict the magnitudes and types of process shifts (Reynolds and Stoumbos 2004*a*, *b*). This principle is also applied to the control charts detecting both mean and variance shifts. These charts should have an excellent overall performance in a broad shift domain, that is, being effective for detecting both small and large process shifts of different combinations of mean shift δ_μ and standard deviation shift δ_σ (Reynolds and Stoumbos 2004*a*, *b*, Sparks 2000, Shu and Jiang 2006). The two overall performance measures, *AEQL* and *ARATS*, discussed in chapter 3 can be adopted here for detecting both δ_μ and δ_σ. Both measures are calculated similar to those in section 3.1.3, except that process shifts in both mean and variance need be handled. The *ARATS* is calculated by:

$$ARATS = \frac{1}{A_D} \cdot \iint_D \frac{ATS(\delta_\mu, \delta_\sigma)}{ATS_{\text{benchmark}}(\delta_\mu, \delta_\sigma)} \cdot d\delta_\mu d\delta_\sigma , \tag{4-1}$$

where $ATS(\delta_\mu, \delta_\sigma)$ is produced by a chart at $(\delta_\mu, \delta_\sigma)$ and $ATS_{\text{benchmark}}(\delta_\mu, \delta_\sigma)$ is generated by another chart that acts as the benchmark. The symbol *D* indicates the process shift domain $\left(D \in \left[\delta_\mu,\ \delta_\sigma \middle| (0 < \delta_\mu \le \delta_{\mu,\max}) \cap (1 < \delta_\sigma \le \delta_{\sigma,\max}) \right] \right)$ and A_D is its area. The shift domain *D* is determined by the maximum shifts $\delta_{\mu,\max}$ in mean and $\delta_{\sigma,\max}$ in standard deviation.

Same as those in section 3.1.3, *AEQL* can be calculated by an integration

$$AEQL = \frac{1}{A_D} \iint_D (\delta_\mu^2 + \delta_\sigma^2 - 1) ATS(\delta_\mu, \delta_\sigma) d\delta_\mu d\delta_\sigma . \tag{4-2}$$

The extra quadratic loss is (δ_μ^2) when only mean shift δ_μ is considered. It is replaced by ($\delta_\mu^2 + \delta_\sigma^2 - 1$) in Equation (4-2) when only δ_σ and δ_μ are to be detected. If both process mean shift and standard deviation shift are assumed to follow uniform distributions, a summation can be used to approximate the integration in Equation (4-2).

$$AEQL = \frac{1}{M} \sum_{i=1}^{M} (\delta_{\mu,i}^2 + \delta_{\sigma,i}^2 - 1) \cdot ATS(\delta_{\mu,i}, \delta_{\sigma,i}) , \tag{4-3}$$

4.1.3 Design of the $\bar{X}$ Chart

To design an $\bar{X}$ chart, a specification τ for the minimum allowable in-control ATS_0

needs to be determined according to the requirement on the false alarm rate. In this section, only the variable sampling cost is considered and the sampling interval h is proportional to the sample size n for a given inspection rate (Reynolds and Stoumbos 2004*a*). If the sampling interval when (n = 1) is taken as the time unit, then

$$h = n. \tag{4-4}$$

For example, when the inspection rate is ten items per hour, if the sample size n is one, the sampling interval h should be 0.1 hours. Taking 0.1 hour as the time unit, we have h = 1.

The upper control limit *UCL* of an $\bar{X}$ chart can be calculated in one step.

$$UCL = \frac{\sigma_0}{\sqrt{n}}\Phi^{-1}\left(1-\frac{0.5h}{\tau}\right)+\mu_0, \tag{4-5}$$

where $\Phi^{-1}(\ )$ is the inverse function of the cumulative probability function of the standard normal distribution. Since the lower control limit *LCL* and the upper control limit *UCL* are symmetrical with respect to μ_0,

$$LCL = 2\mu_0 - UCL. \tag{4-6}$$

4.1.4 Calculation of *ATS*

The in-control ATS_0 of an $\bar{X}$ chart is calculated by

$$ATS_0 = \frac{h}{\alpha} = \frac{h}{1+\Phi\left(\frac{LCL-\mu_0}{\sigma_0/\sqrt{n}}\right)-\Phi\left(\frac{UCL-\mu_0}{\sigma_0/\sqrt{n}}\right)}, \tag{4-7}$$

where α is the type I error probability. The steady-state out-of-control *ATS* of an $\bar{X}$ chart is evaluated by

$$ATS = \left[\frac{1}{1+\Phi\left(\frac{LCL-(\mu_0+\delta_\mu\sigma_0)}{\delta_\sigma\sigma_0/\sqrt{n}}\right)-\Phi\left(\frac{UCL-(\mu_0+\delta_\mu\sigma_0)}{\delta_\sigma\sigma_0/\sqrt{n}}\right)}-0.5\right]\cdot h\,. \tag{4-8}$$

4.1.5 Sample Size of $\bar{X}$ Chart

As a rule of thumb in SPC, a sample size n around four is commonly recommended as the best choice for an $\bar{X}$ chart and a $\bar{X}$ &R combination. Surprisingly, an $\bar{X}$ chart with n = 1 (i.e., an X chart) in fact has much better overall performance for detecting

both δ_μ and δ_σ. Table 4-1 displays the *ATS* values of an *X* chart (with $n = 1$) and an $\bar{X}$ chart (with $n = 4$) over a process shift domain of ($0 \le \delta_\mu \le 5$ and $1 \le \delta_\sigma \le 6$). The control limits of the two charts are also listed at the bottom of Table 4-1.

Table 4-1. *ATS* Values of Two $\bar{X}$ Charts ($\delta_{\mu,\max} = 5$, $\delta_{\sigma,\max} = 6$)

δ_σ	Chart	δ_μ										
		0.0	0.5	1.0	1.5	2.0	2.5	3.0	3.5	4.0	4.5	5.0
1.0	*X* chart	370	155	43.4	14.5	5.80	2.74	1.50	0.95	0.69	0.57	0.52
	$\bar{X}$ chart ($n = 4$)	370	63.7	11.7	3.93	2.32	2.03	2.00	2.00	2.00	2.00	2.00
1.5	*X* chart	21.5	16.9	10.0	5.75	3.45	2.21	1.50	1.09	0.84	0.69	0.60
	$\bar{X}$ chart ($n = 4$)	42.8	23.0	9.16	4.47	2.80	2.22	2.04	2.01	2.00	2.00	2.00
2.0	*X* chart	6.98	6.36	5.01	3.69	2.68	1.97	1.49	1.17	0.95	0.79	0.69
	$\bar{X}$ chart ($n = 4$)	17.8	13.5	7.92	4.76	3.22	2.49	2.18	2.05	2.01	2.00	2.00
2.5	*X* chart	3.84	3.68	3.25	2.72	2.22	1.80	1.47	1.21	1.02	0.88	0.77
	$\bar{X}$ chart ($n = 4$)	11.0	9.57	6.94	4.84	3.53	2.77	2.36	2.16	2.06	2.02	2.01
3.0	*X* chart	2.65	2.59	2.41	2.16	1.90	1.64	1.41	1.22	1.06	0.93	0.83
	$\bar{X}$ chart ($n = 4$)	8.11	7.50	6.13	4.76	3.71	3.01	2.56	2.29	2.14	2.06	2.03
3.5	*X* chart	2.05	2.02	1.94	1.81	1.65	1.49	1.34	1.20	1.07	0.97	0.87
	$\bar{X}$ chart ($n = 4$)	6.57	6.26	5.48	4.58	3.78	3.17	2.73	2.44	2.25	2.13	2.07
4.0	*X* chart	1.71	1.69	1.64	1.57	1.47	1.37	1.26	1.16	1.07	0.98	0.90
	$\bar{X}$ chart ($n = 4$)	5.63	5.45	4.98	4.37	3.78	3.27	2.87	2.57	2.36	2.22	2.13
4.5	*X* chart	1.48	1.47	1.44	1.39	1.33	1.26	1.19	1.12	1.04	0.97	0.91
	$\bar{X}$ chart ($n = 4$)	5.00	4.89	4.58	4.17	3.72	3.31	2.96	2.67	2.46	2.30	2.19
5.0	*X* chart	1.32	1.32	1.30	1.27	1.23	1.18	1.13	1.07	1.02	0.96	0.91
	$\bar{X}$ chart ($n = 4$)	4.55	4.48	4.27	3.97	3.64	3.31	3.01	2.75	2.55	2.39	2.26
5.5	*X* chart	1.21	1.20	1.19	1.17	1.14	1.11	1.07	1.03	0.98	0.94	0.90
	$\bar{X}$ chart ($n = 4$)	4.22	4.17	4.02	3.80	3.55	3.28	3.03	2.81	2.61	2.46	2.33
6.0	*X* chart	1.12	1.12	1.11	1.09	1.07	1.05	1.02	0.99	0.95	0.92	0.89
	$\bar{X}$ chart ($n = 4$)	3.96	3.92	3.82	3.65	3.46	3.24	3.03	2.84	2.66	2.51	2.39

	X chart	$\bar{X}$ chart ($n = 4$)
AEQL	28.6725	71.0552
$AEQL / AEQL_X$	1.0000	2.4782
ARATS	1.0000	2.3983
parameters	$UCL = 2.9997$	$UCL = 1.2744$

In this table, there are in total 120 out-of-control points (combinations of the discrete values of δ_μ and δ_σ) and one in-control point ($\delta_\mu = 0$ and $\delta_\sigma = 1$). Each point contains the *ATS* values of the two charts for a particular combination of the values of δ_μ and δ_σ. It can be observed that both charts produce the same in-control ATS_0 equal to τ (= 370). The $\bar{X}$ chart has smaller or substantially smaller *ATS* values than the *X* chart in eight out-of-control points, where both δ_μ and δ_σ are small (top-left corner in Table 4-1). However, in all other 112 out-of-control points, the *ATS* values of the $\bar{X}$ chart are greater, or much greater, than the *ATS* values of the *X* chart. The *AEQL* values of the $\bar{X}$ chart and *X* chart are 71.06 and 28.67, respectively, and the ratio $AEQL_{\bar{X}} / AEQL_X$ is

equal to 2.478. Another index *ARATS* is equal to 2.398 (note that the *X* chart is used as the benchmark in Equation (4-1)). Both $AEQL_{\overline{X}} / AEQL_X$ and *ARATS* clearly manifest that the *X* chart (with $n = 1$) outperforms the $\overline{X}$ chart (with $n = 4$) by about 140% from an overall viewpoint. The $\overline{X}$ chart is very sensitive to small process shifts, but it is too ineffective for detecting all other process shifts.

Figure 4-1 shows the results of a more systematic study on the sample size of the $\overline{X}$ chart for detecting both δ_μ and δ_σ. Here, the $\overline{X}$ charts are studied in three different process shift domains. For each shift domain, a curve of *AEQL* versus sample size *n* is displayed in Figure 4-1. All of the three curves reveal that *AEQL* is an increasing function of sample size *n*. Consequently, ($n = 1$) gives the smallest *AEQL* and is the best sample size. In Figure 4-1, the smallest shift domain studied is ($\delta_{\mu,max} = 3$, $\delta_{\sigma,max} = 4$). An even smaller shift domain is seldom considered in SPC practice.

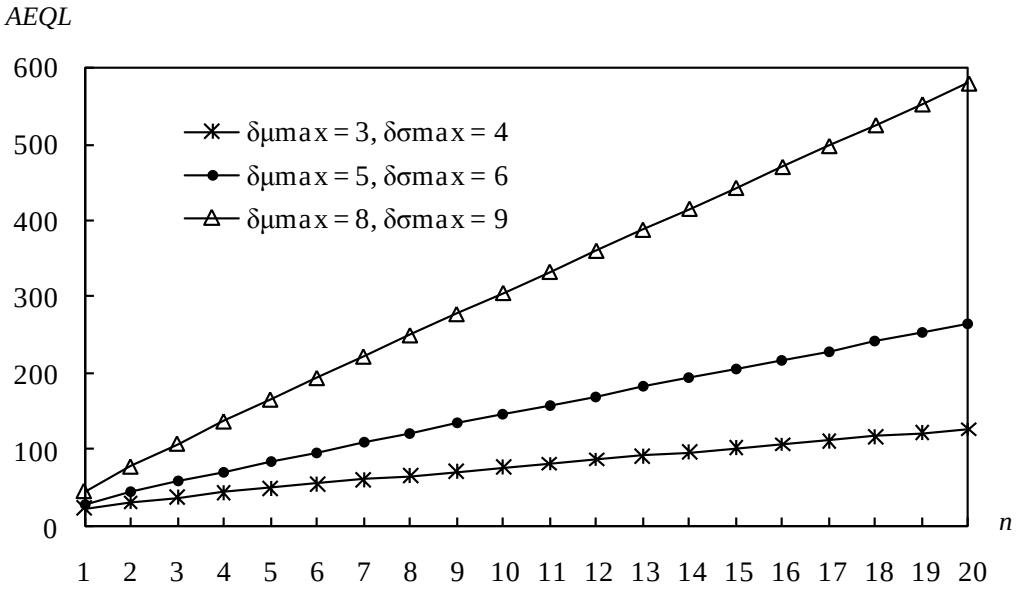

Figure 4-1. Relationship of *AEQL* and *n* in Three Shift Domains

When a larger sample size is used, the power that an $\overline{X}$ chart detects a process shift in each sample becomes higher. It is a positive effect of a large *n*, because the increased power will reduce the *ARL*, as well as *ATS*. However, since the sampling interval *h* is proportional to the sample size *n* for a given inspection rate, a large *n* also has a negative effect that increases *h*, as well as *ATS*. From a holistic viewpoint, the positive effect of a large sample size *n* may not outweigh its negative effect and, consequently, a large *n*

will result in a large *ATS* and *AEQL*. From Table 4-1, it can be observed that a large *n* is particularly helpless for detecting a standard deviation shift δ_σ.

The above discussions suggest that the simplest *X* chart is the most effective $\overline{X}$ chart for detecting δ_μ and δ_σ. The *X* chart is so simple that even the computation of the sample mean $\bar{x}$ is omitted. One can directly plot the single reading *x* of each sample on the *X* chart. When the *X* chart is adopted, the formulae for computing the control limits and *ATS* can be simplified to

$$UCL = \sigma_0 \cdot \Phi^{-1}\left(1 - \frac{0.5}{\tau}\right) + \mu_0, \qquad (4\text{-}9)$$
$$LCL = 2\mu_0 - UCL,$$

$$ATS_0 = \frac{1}{1 + \Phi\left(\frac{LCL - \mu_0}{\sigma_0}\right) - \Phi\left(\frac{UCL - \mu_0}{\sigma_0}\right)}, \qquad (4\text{-}10)$$

$$ATS = \frac{1}{1 + \Phi\left(\frac{LCL - (\mu_0 + \delta_\mu\sigma_0)}{\delta_\sigma\sigma_0}\right) - \Phi\left(\frac{UCL - (\mu_0 + \delta_\mu\sigma_0)}{\delta_\sigma\sigma_0}\right)} - 0.5. \qquad (4\text{-}11)$$

The control limits *UCL* and *LCL* can be determined manually with the help of a calculator and a table of the standard normal cumulative distribution function.

4.2 ABS CUSUM Chart

In this section, a single CUSUM chart which is able to detect two-sided mean shifts and increasing variance shifts is developed using the optimal design algorithm. This algorithm facilitates the determination of the charting parameters of the CUSUM chart for maximum overall detection effectiveness. This new CUSUM chart inspects the absolute value of sample mean shifts.

4.2.1 Introduction

A scheme using a single CUSUM chart to detect two-sided mean shifts and increasing variance shifts has been developed by Wu and Tian (2005), but this chart is not applicable to the cases in which (n = 1). Recently, Wu and Wang (2007) proposed another single CUSUM chart that uses a sample size of (n = 1) to detect both two-sided mean shifts and increasing variance shift. However, the formulae for evaluating and designing this CUSUM chart are quite complicated. In this section, a simple CUSUM chart aiming at maximizing the overall detection effectiveness against δ_μ and δ_σ of different sizes is proposed. This CUSUM chart uses the absolute value of the sample mean to update its statistic and is therefore called the ABS CUSUM chart.

4.2.2 Quality Statistic

The statistic of the ABS CUSUM chart is:

$$\begin{aligned} C_0 &= 0 \\ C_t &= \max(0,\ C_{t-1} + |z_t| - k), \end{aligned} \tag{4-12}$$

where z_t is the standardized normal value of x_t from the tth sample. The sample size for the ABS CUSUM chart is always equal to one. When C_t crosses the control limit H, it is regarded as an out-of-control signal.

4.2.3 Optimal design

The ABS CUSUM chart is designed using the following optimization model.

$$\begin{aligned} &\text{Objective function:} && AEQL = \text{minimum} \\ &\text{Constraint function:} && ARL_0 = \tau \\ &\text{Design variables:} && k, H \end{aligned} \tag{4-13}$$

In the optimal design, the optimal value of k is searched in order to produce a minimum $AEQL$ or to achieve the best trade-off between the power against small shifts and the

power against large shifts. The control limit H is adjusted to make ARL_0 equal to τ. The design of an ABS CUSUM chart can be finished in about 10 seconds of CPU time in a desktop computer.

4.2.4 Calculation of *ATS*

The ABS CUSUM chart can be described by a Markov chain. Suppose that the statistic C_t in Equation (4-12) experiences m transitional states with states 0 to (m–1) being in-control states and state m an out-of-control state. The width d of the interval of each state and the center O_i of state i are given by Equation (2-32) and (2-33), respectively.

The transition probability matrices, $\boldsymbol{R_0}$ for in-control status and $\boldsymbol{R}$ for out-of-control status, have a size of ($m \times m$). Their elements, p_{ij}, are the transition probabilities from state i to state j.

$$p_{ij} = \begin{cases} \Pr[O_i + |z_t| - k_B \le 0.5d] = F_{|z|}[(0.5 - i)d + k_B] & \text{for } j = 0 \\ \Pr[O_j - 0.5d \le O_i + |z_t| - k_B \le O_j + 0.5d] & \\ = F_{|z|}[(j - i + 0.5)d + k_B] - F_{|z|}[(j - i - 0.5)d + k_B] & \text{for } j > 0, \end{cases} \tag{4-14}$$

where the cumulative probability function $F_{|z|}()$ of $|z_t|$ is calculated by

$$F_{|z|}(Y) = \Pr(|z_t| \le Y) = \Phi\left(\frac{Y - \delta_\mu \sigma_0}{\delta_\sigma \sigma_0}\right) - \Phi\left(\frac{-Y - \delta_\mu \sigma_0}{\delta_\sigma \sigma_0}\right). \tag{4-15}$$

Then the in-control ATS_0 and out-of-control ATS can be calculated using Equations (2-37) to (2-40) in section 2.4.3.

4.3 Optimal 3-CUSUM(μ+σ) Scheme

The 3-CUSUM(μ+σ) chart proposed by Reynolds and Stoumbos (2004*a*) incorporates three individual CUSUM charts, two of which detect process mean shift δ_μ and the third one detects process standard deviation shift δ_σ. This section will use the optimal design to improve the overall performance of the 3-CUSUM(μ+σ) chart.

4.3.1 Introduction

As mentioned in section 2.4.2, Reynolds and Stoumbos (2004*a*) proposed a 3-CUSUM(μ+σ) scheme which uses three individual CUSUM charts to monitor process mean and variance. They found that the 3-CUSUM(μ+σ) scheme outperforms many other charts. They also concluded that using a sample size of (n = 1) is the best choice from an overall viewpoint, because (n = 1) makes the scheme much more effective for detecting large process shifts that may seriously impair the product quality.

The studies, so for carried out in this thesis, show that the optimal design can greatly improve the performance of many control charts. Therefore, it is expected that the optimal design can also enhance the overall detection effectiveness of the 3-CUSUM(μ+σ) scheme.

4.3.2 Quality Statistic

For a 3-CUSUM(μ+σ) scheme with a sample size of (n = 1), the three statistics to be updated and plotted are C^{X+} (for increasing mean shift), C^{X-} (for decreasing mean shift) and C^{X^2} (for increasing variance shift).

$$
\begin{aligned}
&C_0^{X+} = 0, \quad C_0^{X-} = 0, \quad C_0^{X^2} = 0,\\
&C_t^{X+} = \max(0,\ C_{t-1}^{X+}) + (x_t - \mu_0 - k^X),\\
&C_t^{X-} = \min(0,\ C_{t-1}^{X-}) + (x_t - \mu_0 + k^X),\\
&C_t^{X^2} = \max(0,\ C_{t-1}^{X^2}) + \left[(x_t - \mu_0)^2 - k^{X^2} \right].
\end{aligned}
\tag{4-16}
$$

The reference parameters k^X and k^{X^2} decide the sensitivity of the 3-CUSUM(μ+σ) scheme to different process shift. While small k^X and k^{X^2} render the scheme more sensitive to small process shifts, large k^X and k^{X^2} make the scheme nearly as effective as the Shewhart charts for detecting large shifts. If any or more of the three statistics, C^{X+}, C^{X-}, C^{X^2}, falls beyond the corresponding control limit, H_{CX}, $-H_{CX}$, or $H_{CX}{}^2$, the

3-CUSUM(μ+σ) scheme produces an out-of-control signal.

4.3.3 Optimal design

In the paper by Reynolds and Stoumbos (2004*a*), the reference parameters k^X and k^{X^2} of a 3-CUSUM(μ+σ) scheme are determined based on ζ_μ and ζ_σ (the specified values of δ_μ and δ_σ). However, it is not quite clear how to actually select the values for ζ_μ and ζ_σ. It seems that ζ_μ and ζ_σ increase along with the increase of $\delta_{\mu,\max}$ and $\delta_{\sigma,\max}$, and ζ_σ is larger than ζ_μ by about one unit.

Using the optimal design, the charting parameters of the 3-CUSUM(μ+σ) scheme can be optimized in order to improve the overall performance. The following design model may be ideal for the 3-CUSUM(μ+σ) scheme:

Objective function:	$AEQL$ = minimum	
Constraint function:	$ATS_0 \geq \tau$	(4-17)
Independent variables:	k^X, k^{X^2}, H_{CX}	
Dependent variables:	H_{CX}^2	

The *AEQL* can be calculated using Equation (4-2). The optimal values of k^X, k^{X^2} and H_{CX} are searched in order to achieve the minimum *AEQL* for the 3-CUSUM(μ+σ) scheme. For each set of the values of the independent variables, the dependent variable H_{CX}^2 is adjusted so that ($ATS_0 \geq \tau$). However, this design model is very difficult to be pursued, because this full-fledged optimal design has three independent variables k^X, k^{X^2} and H_{CX} to be searched. Even worse, the *ATS* of the 3-CUSUM(μ+σ) scheme has to be evaluated by the simulation. It is very time consuming not only for the in-control ATS_0 but also for the out-of-control *ATS*, because usually 100 initial in-control observations have to be generated before the process shift in every simulation iteration under the steady-state mode. Moreover, the evaluation of the objective function, *AEQL*, requires the computation of *ATS* at many discrete shift points. Furthermore, the inherent variability of simulation results makes it very difficult to get a convergent design solution. Reynolds and Stoumbos (2004*a*) suggested using a simulation with 1,000,000 runs to evaluate *ATS*. However, in a trial run, even the number of simulation runs is reduced to 100,000, a desktop computer takes about 130 hours of CPU time in order to

find the optimal values for the three independent variables k^X, k^{X^2} and H_{CX}.

In view of this, the following simplified optimization model is developed in this section for the optimal design of the 3-CUSUM(μ+σ) scheme:

Objective function:	$AEQL$ = minimum	
Constraint function:	$ATS_0 \geq \tau$	(4-18)
Independent variables:	ζ_μ	
Dependent variables:	k^X, k^{X^2}, H_{CX}, H_{CX}^2	

In this model, ζ_σ, k^X and k^{X^2} can be calculated based on the single independent variable ζ_μ (Reynolds and Stoumbos 2004*a*):

$$\zeta_\sigma = \zeta_\mu + 1, \qquad k^X = 0.5\zeta_\mu\sigma_0, \qquad k^{X^2} = 2\sigma_0^2 \ln \zeta_\sigma /(1-\zeta_\sigma^{-2}). \tag{4-19}$$

The 3-CUSUM(μ+σ) scheme with the k^X and k^{X^2} values being determined as above will detect the specific process shifts (ζ_μ, ζ_σ) most quickly. Finally, the control limits H_{CX} and H_{CX}^2 are determined so that the individual CUSUM charts have equal in-control ATS_0 and the overall ATS_0 of the 3-CUSUM(μ+σ) scheme is equal to the specified τ.

Since there is only one independent variable ζ_μ, the optimal design of a 3-CUSUM(μ+σ) scheme becomes relatively more feasible and tractable. If the number of simulation runs is set as 100,000, the design of a typical 3-CUSUM(μ+σ) scheme can be completed in about seven hours in a desktop computer. Unlike the conventional design procedure in which ζ_μ is specified and fixed, the optimal design searches the optimal value of ζ_μ so that a best trade-off between the power against small shifts and that against large shifts can be acquired, and the overall performance of the 3-CUSUM(μ+σ) scheme can be improved. The 3-CUSUM(μ+σ) scheme designed by this optimization algorithm is denoted as the optimal 3-CUSUM(μ+σ) scheme in this chapter.

4.4 Performance Evaluation and Comparison

This section compares the performance of five control charts for detecting both δ_μ and δ_σ: *X* chart, ABS CUSUM chart, conventional and optimal 3-CUSUM(μ+σ) schemes, and the scale CUSUM chart. These charts are designed under three different shift domains. The *ATS* values, *AEQL* and *ARATS* values of these charts are compared to give an overall picture about their detection effectiveness. The results show that the optimal 3-CUSUM(μ+σ) scheme has the highest detection effectiveness, followed by the ABS CUSUM chart, the scale CUSUM chart, and then the *X* chart. The conventional 3-CUSUM(μ+σ) scheme ranks last. Furthermore, the simplicity in design and implementation is discussed later. Since the ABS CUSUM chart is almost as effective as the optimal 3-CUSUM(μ+σ) scheme and is easier for implementation and design, this chart may be most suitable for many SPC applications in which both mean and variance of a variable have to be monitored. The simplest *X* chart may be adopted when process shift domain is large.

4.4.1 Charts to be Compared

The performance of the three charts (the *X* chart, ABS CUSUM chart and the optimal 3-CUSUM(μ+σ) scheme) proposed in this chapter will be compared with that of other two CUSUM control charts in this section.

(1) The *X* chart proposed in section 4.1

(2) The ABS CUSUM chart proposed in section 4.2

(3) The optimal 3-CUSUM(μ+σ) scheme proposed in section 4.3

(4) The conventional 3-CUSUM(μ+σ) scheme proposed by Reynolds and Stoumbos (2004*a*)

The statistics of this conventional 3-CUSUM(μ+σ) scheme are presented in Equation (4-16). The values for ζ_μ and ζ_σ in different shift domains are specified according to the recommendation by Reynolds and Stoumbos (2004*a*) as showed in Table 4-2. Correspondingly, the reference parameters k^X and k^{X^2} are calculated by Equation (4-19). The control limits H_{CX} (for C^{x+} and C^{x-}) and $H_{CX}{}^2$ (for C^{X^2}) are determined so that the individual CUSUM charts have equal in-control ATS_0 and the overall ATS_0 of the conventional 3-CUSUM(μ+σ) scheme is equal to the specified τ.

Table 4-2. Process Shift Domains

No.	Shift domain	$\delta_{\mu,\max}$	$\delta_{\sigma,\max}$	Conventional 3-CUSUM(μ+σ) scheme	
				ξ_μ	ξ_σ
1	$0<\delta_\mu\le 3,\ 1<\delta_\sigma\le 4$	3	4	0.30	1.28
2	$0<\delta_\mu\le 5,\ 1<\delta_\sigma\le 6$	5	6	0.38	1.35
3	$0<\delta_\mu\le 8,\ 1<\delta_\sigma\le 9$	8	9	0.50	1.50

(5) The scale CUSUM chart proposed by Hawkins (1981)

The scale CUSUM chart is almost the same as the ABS CUSUM chart except that the expression $|z_t|$ in Equation (4-14) will be replaced by $\sqrt{|z_t|}$ as follows:

$$C_0 = 0$$
$$C_t = \max(0,\ C_{t-1} + \sqrt{|z_t|} - k). \qquad (4\text{-}20)$$

The optimal design of the scale CUSUM chart uses the same objective and constraint functions (Equation (4-13)) as the ABS CUSUM chart. The optimal value of the only independent variable, the reference parameter *k*, is searched to obtain the minimum *AEQL*; while the dependent variable, the control limit *H*, will be adjusted to satisfy the constraint function $ATS_0 = \tau$.

4.4.2 Comparison on Detection Effectiveness

In order to have a fair comparison, all the five charts, the *X* chart, the ABS CUSUM chart, the conventional and optimal 3-CUSUM(μ+σ) schemes, and the scale CUSUM chart are designed in an optimal manner. The minimum allowable value τ of the in-control ATS_0 is set as 370. It makes the in-control performance of the control charts match that of a typical 3σ Shewhart $\bar{X}$ chart. In this section, it is assumed that both process mean shift δ_μ and standard deviation shift δ_σ follow uniform distribution. Three shift domains as shown in Table 4-2 are investigated in order to cover different situations.

Within each shift domain, the out-of-control *ATS* is evaluated at one in-control point and 120 shift points (the pairs of the discrete values of δ_μ and δ_σ).

Comparison of *ATS*

The *ATS* values of the five control charts under three shift domains are listed in Tables 4-3, 4-4 and 4-5. It is observed that:

(1) In all these tables, the conventional 3-CUSUM(μ+σ) scheme produces very small *ATS* values in a small region where both δ_μ and δ_σ are minor (in the top-left corner). But in other part of the tables, the conventional 3-CUSUM(μ+σ) scheme usually has obviously larger *ATS* values than all other charts.

(2) Generally speaking, the optimal 3-CUSUM(μ+σ) scheme produces considerably smaller *ATS* values than other charts when only minor or moderate pure mean shifts exist. However, beyond this small region, the *ATS* performance of the ABS CUSUM chart is sometimes even slightly better than that of the optimal 3-CUSUM(μ+σ) scheme. For example, in Table 4-4 where ($\delta_{\mu,\max} = 5$, $\delta_{\sigma,\max} = 6$), except in a few points in the top-left corner where ($0 < \delta_\mu \leq 4.0$ and $1 < \delta_\sigma \leq 2.5$), there is almost no observable difference in *ATS* values between the optimal 3-CUSUM(μ+σ) scheme and the ABS CUSUM chart.

(3) The out-of-control *ATS* of the ABS CUSUM chart is smaller than, or at least equal to, the *ATS* of the *X* chart and the scale CUSUM chart in almost all of the points in Tables 4-3 to 4-5.

(4) As expected, the *X* chart has larger *ATS* for minor mean and/or variance shifts. However, beyond these small regions, there are usually only insignificant differences in *ATS* values among the five charts.

(5) The *ATS* comparison is also influenced by the values of $\delta_{\mu,\max}$ and $\delta_{\sigma,\max}$. The *X* chart produces longer out-of-control *ATS* than other four charts when shift domain is small or moderate. For example, in Table 4-3 where ($\delta_{\mu,\max} = 3$, $\delta_{\sigma,\max} = 4$), the optimal 3-CUSUM(μ+σ) chart produces smaller *ATS* than the *X* chart in 119 out of 120 out-of-control points. However, in Table 4-5 where ($\delta_{\mu,\max} = 8$, $\delta_{\sigma,\max} = 9$), the former outperforms the latter in only 51 points.

Table 4-3. *ATS* Values of Five Control Charts ($\delta_{\mu,\max} = 3$, $\delta_{\sigma,\max} = 4$)

δ_σ	Chart	δ_μ										
		0.0	0.3	0.6	0.9	1.2	1.5	1.8	2.1	2.4	2.7	3.0
1.0	*X* chart	370	252	119	55.3	27.3	14.5	8.19	4.93	3.14	2.12	1.50
	ABS CUSUM	369	234	91.4	34.4	14.7	7.42	4.37	2.91	2.10	1.61	1.28
	con 3-CUSUM($\mu+\sigma$)	368	57.7	22.6	13.4	9.16	6.57	4.83	3.64	2.8	2.21	1.79
	opt 3-CUSUM($\mu+\sigma$)	371	186	58.5	20.9	9.49	5.39	3.51	2.53	1.92	1.53	1.24
	scale CUSUM	369	237	96.0	37.4	16.1	8.06	4.64	3.00	2.13	1.61	1.27
1.3	*X* chart	47.1	40.3	27.9	17.9	11.4	7.53	5.11	3.59	2.60	1.95	1.50
	ABS CUSUM	37.1	31.6	21.3	13.2	8.26	5.42	3.76	2.75	2.10	1.66	1.35
	con 3-CUSUM($\mu+\sigma$)	30.1	24.2	15.9	10.8	7.67	5.69	4.37	3.39	2.69	2.18	1.80
	opt 3-CUSUM($\mu+\sigma$)	38.1	30.5	18.9	11.1	6.92	4.61	3.30	2.48	1.95	1.57	1.30
	scale CUSUM	38.9	33.2	22.4	13.9	8.69	5.66	3.88	2.80	2.12	1.66	1.35
1.6	*X* chart	15.9	14.8	12.1	9.29	6.93	5.16	3.89	2.98	2.32	1.85	1.50
	ABS CUSUM	12.6	11.7	9.68	7.47	5.62	4.25	3.26	2.56	2.05	1.68	1.41
	con 3-CUSUM($\mu+\sigma$)	12.4	11.5	9.70	7.76	6.13	4.85	3.86	3.14	2.56	2.14	1.80
	opt 3-CUSUM($\mu+\sigma$)	12.9	11.8	9.39	7.10	5.20	3.92	3.01	2.40	1.94	1.61	1.36
	scale CUSUM	13.1	12.2	10.1	7.75	5.80	4.36	3.32	2.59	2.07	1.69	1.40
1.9	*X* chart	8.24	7.91	7.05	5.97	4.90	3.97	3.21	2.61	2.14	1.78	1.50
	ABS CUSUM	6.80	6.55	5.90	5.06	4.22	3.48	2.86	2.37	1.98	1.68	1.44
	con 3-CUSUM($\mu+\sigma$)	7.46	7.19	6.56	5.74	4.87	4.12	3.45	2.90	2.44	2.08	1.80
	opt 3-CUSUM($\mu+\sigma$)	6.91	6.63	5.91	4.97	4.12	3.35	2.75	2.27	1.91	1.62	1.40
	scale CUSUM	7.02	6.76	6.07	5.19	4.31	3.53	2.90	2.39	1.99	1.68	1.44
2.2	*X* chart	5.29	5.16	4.80	4.31	3.76	3.23	2.75	2.34	2.00	1.72	1.49
	ABS CUSUM	4.57	4.47	4.19	3.80	3.36	2.93	2.54	2.19	1.90	1.65	1.45
	con 3-CUSUM($\mu+\sigma$)	5.29	5.19	4.90	4.47	3.98	3.51	3.06	2.65	2.31	2.02	1.77
	opt 3-CUSUM($\mu+\sigma$)	4.63	4.5	4.2	3.8	3.33	2.89	2.48	2.14	1.85	1.61	1.41
	scale CUSUM	4.67	4.56	4.27	3.87	3.41	2.96	2.56	2.20	1.90	1.65	1.45
2.5	*X* chart	3.84	3.78	3.61	3.35	3.04	2.72	2.41	2.13	1.88	1.66	1.47
	ABS CUSUM	3.44	3.39	3.25	3.05	2.80	2.53	2.27	2.03	1.81	1.61	1.44
	con 3-CUSUM($\mu+\sigma$)	4.07	4.03	3.89	3.62	3.35	3.04	2.72	2.44	2.18	1.94	1.74
	opt 3-CUSUM($\mu+\sigma$)	3.47	3.41	3.26	3.05	2.79	2.51	2.25	2.00	1.78	1.59	1.42
	scale CUSUM	3.49	3.44	3.30	3.08	2.82	2.55	2.28	2.03	1.81	1.61	1.44
2.8	*X* chart	3.02	2.99	2.89	2.74	2.56	2.36	2.15	1.95	1.76	1.59	1.44
	ABS CUSUM	2.78	2.75	2.67	2.55	2.40	2.23	2.05	1.88	1.71	1.56	1.42
	con 3-CUSUM($\mu+\sigma$)	3.34	3.32	3.20	3.07	2.88	2.67	2.46	2.25	2.04	1.86	1.68
	opt 3-CUSUM($\mu+\sigma$)	2.81	2.78	2.68	2.58	2.40	2.23	2.04	1.86	1.69	1.54	1.40
	scale CUSUM	2.81	2.78	2.70	2.57	2.41	2.24	2.06	1.88	1.71	1.56	1.42
3.1	*X* chart	2.50	2.48	2.42	2.33	2.21	2.08	1.94	1.79	1.65	1.52	1.40
	ABS CUSUM	2.35	2.34	2.29	2.21	2.11	1.99	1.87	1.74	1.62	1.50	1.39
	con 3-CUSUM($\mu+\sigma$)	2.83	2.80	2.75	2.65	2.53	2.39	2.23	2.08	1.92	1.78	1.63
	opt 3-CUSUM($\mu+\sigma$)	2.36	2.36	2.30	2.23	2.12	1.99	1.86	1.74	1.61	1.48	1.37
	scale CUSUM	2.37	2.35	2.30	2.22	2.12	2.00	1.87	1.74	1.62	1.50	1.38
3.4	*X* chart	2.15	2.14	2.10	2.04	1.96	1.87	1.77	1.66	1.56	1.45	1.36
	ABS CUSUM	2.05	2.04	2.01	1.96	1.89	1.81	1.72	1.63	1.53	1.44	1.35
	con 3-CUSUM($\mu+\sigma$)	2.46	2.44	2.41	2.34	2.26	2.15	2.05	1.92	1.82	1.69	1.59
	opt 3-CUSUM($\mu+\sigma$)	2.06	2.06	2.02	1.96	1.89	1.81	1.72	1.62	1.52	1.43	1.34
	scale CUSUM	2.06	2.05	2.02	1.96	1.89	1.81	1.72	1.63	1.53	1.44	1.34
3.7	*X* chart	1.90	1.89	1.86	1.82	1.76	1.70	1.63	1.55	1.47	1.39	1.31
	ABS CUSUM	1.83	1.83	1.80	1.77	1.72	1.66	1.60	1.53	1.45	1.38	1.31
	con 3-CUSUM($\mu+\sigma$)	2.19	2.18	2.15	2.1	2.04	1.97	1.89	1.8	1.71	1.62	1.52
	opt 3-CUSUM($\mu+\sigma$)	1.84	1.83	1.81	1.77	1.72	1.66	1.60	1.53	1.45	1.38	1.30
	scale CUSUM	1.84	1.83	1.81	1.77	1.72	1.66	1.60	1.52	1.45	1.38	1.30
4.0	*X* chart	1.71	1.70	1.68	1.65	1.61	1.57	1.51	1.45	1.39	1.33	1.26
	ABS CUSUM	1.67	1.66	1.65	1.62	1.58	1.54	1.49	1.44	1.38	1.32	1.26
	con 3-CUSUM($\mu+\sigma$)	1.98	1.98	1.95	1.93	1.87	1.82	1.75	1.68	1.62	1.54	1.47
	opt 3-CUSUM($\mu+\sigma$)	1.67	1.67	1.65	1.62	1.58	1.54	1.49	1.43	1.38	1.32	1.26
	scale CUSUM	1.67	1.66	1.65	1.62	1.58	1.54	1.49	1.44	1.38	1.32	1.26

Table 4-4. *ATS* Values of Five Control Charts ($\delta_{\mu,\max} = 5$, $\delta_{\sigma,\max} = 6$)

δ_σ	Chart	δ_μ										
		0.0	0.5	1.0	1.5	2.0	2.5	3.0	3.5	4.0	4.5	5.0
1.0	*X* chart	370	155	43.4	14.5	5.80	2.74	1.50	0.95	0.69	0.57	0.52
	ABS CUSUM	370	136	30.0	8.66	3.59	1.95	1.26	0.90	0.69	0.58	0.53
	con 3-CUSUM($\mu+\sigma$)	371	28.2	11.0	6.18	3.80	2.48	1.71	1.26	0.95	0.75	0.62
	opt 3-CUSUM($\mu+\sigma$)	371	107	20.9	6.41	3.00	1.79	1.22	0.89	0.70	0.59	0.53
	scale CUSUM	370	137	30.5	8.85	3.64	1.96	1.26	0.90	0.70	0.58	0.53
1.5	*X* chart	21.5	16.9	10.0	5.75	3.45	2.21	1.50	1.09	0.84	0.69	0.60
	ABS CUSUM	17.8	14.0	8.28	4.75	2.91	1.93	1.37	1.04	0.83	0.69	0.61
	con 3-CUSUM($\mu+\sigma$)	15.4	12.1	7.62	4.93	3.34	2.36	1.74	1.33	1.05	0.86	0.73
	opt 3-CUSUM($\mu+\sigma$)	17.5	13.3	7.59	4.31	2.69	1.83	1.33	1.03	0.82	0.69	0.61
	scale CUSUM	18.1	14.2	8.38	4.80	2.93	1.94	1.37	1.04	0.83	0.69	0.61
2.0	*X* chart	6.98	6.36	5.01	3.69	2.68	1.97	1.49	1.17	0.95	0.79	0.69
	ABS CUSUM	6.04	5.53	4.42	3.31	2.45	1.84	1.42	1.13	0.93	0.79	0.69
	con 3-CUSUM($\mu+\sigma$)	6.41	5.93	4.87	3.74	2.87	2.21	1.73	1.39	1.13	0.95	0.81
	opt 3-CUSUM($\mu+\sigma$)	6.00	5.44	4.28	3.22	2.36	1.80	1.39	1.12	0.93	0.79	0.69
	scale CUSUM	6.10	5.58	4.46	3.33	2.46	1.85	1.43	1.14	0.93	0.79	0.69
2.5	*X* chart	3.84	3.68	3.25	2.72	2.22	1.80	1.47	1.21	1.02	0.88	0.77
	ABS CUSUM	3.48	3.34	2.98	2.53	2.09	1.72	1.42	1.19	1.01	0.87	0.77
	con 3-CUSUM($\mu+\sigma$)	3.97	3.82	3.42	2.96	2.48	2.04	1.69	1.41	1.20	1.03	0.89
	opt 3-CUSUM($\mu+\sigma$)	3.46	3.33	2.95	2.50	2.08	1.70	1.41	1.18	1.00	0.87	0.77
	scale CUSUM	3.50	3.36	3.00	2.54	2.10	1.73	1.42	1.19	1.01	0.87	0.77
3.0	*X* chart	2.65	2.59	2.41	2.16	1.90	1.64	1.41	1.22	1.06	0.93	0.83
	ABS CUSUM	2.47	2.42	2.27	2.05	1.82	1.59	1.38	1.20	1.05	0.93	0.83
	con 3-CUSUM($\mu+\sigma$)	2.90	2.82	2.65	2.42	2.13	1.86	1.62	1.40	1.22	1.07	0.95
	opt 3-CUSUM($\mu+\sigma$)	2.48	2.42	2.27	2.04	1.81	1.58	1.38	1.20	1.05	0.93	0.83
	scale CUSUM	2.49	2.43	2.28	2.06	1.82	1.59	1.38	1.20	1.05	0.93	0.83
3.5	*X* chart	2.05	2.02	1.94	1.81	1.65	1.49	1.34	1.20	1.07	0.97	0.87
	ABS CUSUM	1.96	1.93	1.85	1.74	1.60	1.46	1.32	1.18	1.07	0.96	0.87
	con 3-CUSUM($\mu+\sigma$)	2.30	2.27	2.18	2.04	1.88	1.70	1.53	1.37	1.22	1.09	0.99
	opt 3-CUSUM($\mu+\sigma$)	1.96	1.93	1.85	1.74	1.61	1.45	1.32	1.19	1.06	0.96	0.87
	scale CUSUM	1.97	1.94	1.86	1.74	1.61	1.46	1.32	1.19	1.07	0.96	0.88
4.0	*X* chart	1.71	1.69	1.64	1.57	1.47	1.37	1.26	1.16	1.07	0.98	0.90
	ABS CUSUM	1.65	1.63	1.59	1.52	1.44	1.34	1.25	1.15	1.06	0.97	0.90
	con 3-CUSUM($\mu+\sigma$)	1.92	1.90	1.86	1.78	1.67	1.55	1.43	1.32	1.21	1.10	1.01
	opt 3-CUSUM($\mu+\sigma$)	1.66	1.64	1.59	1.52	1.44	1.34	1.25	1.15	1.05	0.98	0.90
	scale CUSUM	1.65	1.64	1.59	1.53	1.44	1.35	1.25	1.15	1.06	0.98	0.90
4.5	*X* chart	1.48	1.47	1.44	1.39	1.33	1.26	1.19	1.12	1.04	0.97	0.91
	ABS CUSUM	1.44	1.44	1.41	1.37	1.31	1.25	1.18	1.11	1.04	0.97	0.91
	con 3-CUSUM($\mu+\sigma$)	1.68	1.67	1.63	1.58	1.52	1.44	1.35	1.26	1.18	1.09	1.02
	opt 3-CUSUM($\mu+\sigma$)	1.46	1.44	1.41	1.37	1.31	1.25	1.18	1.11	1.04	0.98	0.91
	scale CUSUM	1.45	1.44	1.41	1.37	1.31	1.25	1.18	1.11	1.04	0.97	0.91
5.0	*X* chart	1.32	1.32	1.30	1.27	1.23	1.18	1.13	1.07	1.02	0.96	0.91
	ABS CUSUM	1.30	1.29	1.28	1.25	1.21	1.17	1.12	1.06	1.01	0.96	0.91
	con 3-CUSUM($\mu+\sigma$)	1.51	1.49	1.48	1.44	1.39	1.33	1.27	1.21	1.14	1.07	1.02
	opt 3-CUSUM($\mu+\sigma$)	1.30	1.30	1.28	1.25	1.22	1.17	1.12	1.06	1.01	0.96	0.91
	scale CUSUM	1.30	1.30	1.28	1.25	1.21	1.17	1.12	1.07	1.01	0.96	0.91
5.5	*X* chart	1.21	1.20	1.19	1.17	1.14	1.11	1.07	1.03	0.98	0.94	0.90
	ABS CUSUM	1.19	1.19	1.18	1.16	1.13	1.10	1.06	1.02	0.98	0.94	0.90
	con 3-CUSUM($\mu+\sigma$)	1.36	1.36	1.34	1.32	1.29	1.25	1.20	1.15	1.10	1.05	1.00
	opt 3-CUSUM($\mu+\sigma$)	1.19	1.20	1.18	1.16	1.14	1.10	1.07	1.02	0.98	0.94	0.90
	scale CUSUM	1.20	1.19	1.18	1.16	1.13	1.10	1.06	1.02	0.98	0.94	0.90
6.0	*X* chart	1.12	1.12	1.11	1.09	1.07	1.05	1.02	0.99	0.95	0.92	0.89
	ABS CUSUM	1.11	1.11	1.10	1.08	1.07	1.04	1.01	0.98	0.95	0.92	0.89
	con 3-CUSUM($\mu+\sigma$)	1.27	1.26	1.25	1.23	1.20	1.18	1.15	1.10	1.06	1.02	0.98
	opt 3-CUSUM($\mu+\sigma$)	1.12	1.12	1.10	1.09	1.07	1.04	1.01	0.98	0.95	0.92	0.89
	scale CUSUM	1.11	1.11	1.10	1.09	1.07	1.04	1.02	0.99	0.95	0.92	0.89

Table 4-5. *ATS* Values of Five Control Charts ($\delta_{\mu,\max} = 8$, $\delta_{\sigma,\max} = 9$)

δ_σ	Chart	δ_μ										
		0.0	0.8	1.6	2,4	3.2	4.0	4.8	5.6	6.4	7.2	8.0
1.0	*X* chart	370	71.0	11.9	3.14	1.23	0.69	0.54	0.50	0.50	0.50	0.50
	ABS CUSUM	369	59.8	8.19	2.32	1.09	0.68	0.54	0.51	0.50	0.50	0.50
	con 3-CUSUM($\mu+\sigma$)	370	14.1	5.18	2.52	1.41	0.89	0.63	0.53	0.50	0.50	0.50
	opt 3-CUSUM($\mu+\sigma$)	368	48.5	6.52	2.09	1.07	0.69	0.54	0.51	0.50	0.50	0.50
	Scale CUSUM	369	62.0	8.74	2.40	1.09	0.68	0.54	0.51	0.50	0.50	0.50
1.8	*X* chart	9.96	7.30	3.97	2.20	1.34	0.91	0.69	0.58	0.53	0.51	0.50
	ABS CUSUM	8.82	6.51	3.59	2.03	1.27	0.89	0.69	0.58	0.53	0.51	0.50
	con 3-CUSUM($\mu+\sigma$)	8.18	6.26	3.73	2.28	1.50	1.05	0.80	0.64	0.56	0.53	0.51
	opt 3-CUSUM($\mu+\sigma$)	8.52	6.21	3.43	1.96	1.25	0.89	0.69	0.58	0.53	0.51	0.50
	Scale CUSUM	8.99	6.63	3.64	2.05	1.28	0.89	0.68	0.58	0.53	0.51	0.50
2.6	*X* chart	3.52	3.19	2.50	1.84	1.35	1.03	0.82	0.69	0.61	0.56	0.53
	ABS CUSUM	3.27	2.98	2.36	1.76	1.32	1.01	0.82	0.69	0.61	0.56	0.53
	con 3-CUSUM($\mu+\sigma$)	3.54	3.26	2.63	2.00	1.51	1.16	0.92	0.76	0.66	0.59	0.55
	opt 3-CUSUM($\mu+\sigma$)	3.20	2.94	2.33	1.73	1.31	1.01	0.82	0.69	0.61	0.56	0.53
	Scale CUSUM	3.30	3.01	2.38	1.77	1.32	1.01	0.81	0.69	0.61	0.56	0.53
3.4	*X* chart	2.15	2.06	1.83	1.56	1.29	1.07	0.90	0.78	0.68	0.62	0.58
	ABS CUSUM	2.05	1.97	1.77	1.51	1.27	1.06	0.90	0.77	0.68	0.62	0.58
	con 3-CUSUM($\mu+\sigma$)	2.30	2.23	1.99	1.71	1.43	1.19	1.00	0.85	0.74	0.66	0.61
	opt 3-CUSUM($\mu+\sigma$)	2.04	1.95	1.76	1.49	1.26	1.06	0.90	0.78	0.69	0.62	0.58
	Scale CUSUM	2.06	1.98	1.78	1.52	1.27	1.06	0.90	0.77	0.68	0.62	0.58
4.2	*X* chart	1.60	1.57	1.48	1.34	1.20	1.06	0.93	0.83	0.74	0.68	0.63
	ABS CUSUM	1.56	1.53	1.44	1.32	1.18	1.05	0.93	0.83	0.74	0.68	0.63
	con 3-CUSUM($\mu+\sigma$)	1.75	1.72	1.61	1.47	1.32	1.16	1.02	0.90	0.80	0.72	0.66
	opt 3-CUSUM($\mu+\sigma$)	1.55	1.52	1.44	1.31	1.18	1.05	0.93	0.83	0.74	0.68	0.63
	Scale CUSUM	1.56	1.53	1.44	1.32	1.18	1.05	0.93	0.83	0.74	0.68	0.63
5.0	*X* chart	1.32	1.31	1.26	1.19	1.10	1.02	0.93	0.85	0.78	0.72	0.67
	ABS CUSUM	1.30	1.28	1.24	1.17	1.09	1.01	0.92	0.85	0.78	0.72	0.67
	con 3-CUSUM($\mu+\sigma$)	1.45	1.44	1.39	1.3	1.21	1.11	1.01	0.92	0.84	0.77	0.71
	opt 3-CUSUM($\mu+\sigma$)	1.30	1.28	1.24	1.17	1.10	1.00	0.93	0.84	0.78	0.72	0.67
	Scale CUSUM	1.30	1.28	1.24	1.17	1.09	1.01	0.92	0.85	0.78	0.72	0.67
5.8	*X* chart	1.15	1.14	1.12	1.08	1.02	0.97	0.91	0.85	0.79	0.74	0.70
	ABS CUSUM	1.14	1.13	1.10	1.06	1.01	0.96	0.90	0.84	0.79	0.74	0.70
	con 3-CUSUM($\mu+\sigma$)	1.27	1.25	1.22	1.18	1.12	1.05	0.99	0.92	0.85	0.79	0.74
	opt 3-CUSUM($\mu+\sigma$)	1.14	1.13	1.10	1.06	1.02	0.96	0.90	0.85	0.79	0.74	0.70
	Scale CUSUM	1.14	1.13	1.10	1.06	1.01	0.96	0.90	0.84	0.79	0.74	0.70
6.6	*X* chart	1.04	1.03	1.02	0.99	0.96	0.92	0.88	0.83	0.79	0.75	0.71
	ABS CUSUM	1.03	1.02	1.01	0.98	0.95	0.91	0.87	0.83	0.79	0.75	0.71
	con 3-CUSUM($\mu+\sigma$)	1.14	1.13	1.11	1.09	1.04	1.00	0.95	0.90	0.85	0.80	0.76
	opt 3-CUSUM($\mu+\sigma$)	1.03	1.03	1.01	0.98	0.95	0.92	0.87	0.83	0.79	0.76	0.71
	Scale CUSUM	1.03	1.02	1.01	0.98	0.95	0.91	0.87	0.83	0.79	0.75	0.71
7.4	*X* chart	0.96	0.96	0.94	0.93	0.90	0.88	0.85	0.82	0.78	0.75	0.72
	ABS CUSUM	0.95	0.95	0.94	0.92	0.90	0.87	0.85	0.81	0.78	0.75	0.72
	con 3-CUSUM($\mu+\sigma$)	1.04	1.04	1.03	1.01	0.98	0.95	0.92	0.88	0.84	0.80	0.77
	opt 3-CUSUM($\mu+\sigma$)	0.95	0.95	0.94	0.93	0.90	0.88	0.85	0.81	0.79	0.75	0.72
	Scale CUSUM	0.95	0.95	0.94	0.92	0.90	0.87	0.84	0.81	0.78	0.75	0.72
8.2	*X* chart	0.90	0.90	0.89	0.88	0.86	0.84	0.82	0.80	0.77	0.75	0.72
	ABS CUSUM	0.90	0.89	0.89	0.87	0.86	0.84	0.82	0.79	0.77	0.75	0.72
	con 3-CUSUM($\mu+\sigma$)	0.97	0.97	0.97	0.95	0.93	0.91	0.88	0.86	0.83	0.80	0.76
	opt 3-CUSUM($\mu+\sigma$)	0.90	0.90	0.89	0.88	0.86	0.84	0.82	0.80	0.77	0.75	0.72
	Scale CUSUM	0.90	0.89	0.89	0.87	0.86	0.84	0.82	0.79	0.77	0.75	0.72
9.0	*X* chart	0.85	0.85	0.85	0.84	0.83	0.81	0.79	0.78	0.76	0.74	0.72
	ABS CUSUM	0.85	0.85	0.84	0.84	0.82	0.81	0.79	0.78	0.76	0.74	0.72
	con 3-CUSUM($\mu+\sigma$)	0.92	0.92	0.91	0.90	0.89	0.87	0.85	0.83	0.81	0.78	0.76
	opt 3-CUSUM($\mu+\sigma$)	0.85	0.85	0.85	0.84	0.82	0.81	0.79	0.77	0.76	0.74	0.72
	Scale CUSUM	0.85	0.85	0.84	0.83	0.82	0.81	0.79	0.78	0.76	0.74	0.72

Comparison of Overall Performance

Obviously observing the *ATS* values at each shift point can hardly get a whole comparison picture among the control charts. A more accurate and objective comparison can be made based on the following three holistic measures:

(1) *AEQL* (Equation (4-2)).

(2) $AEQL$ / $AEQL_{\text{opt 3-CUSUM}(\mu+\sigma)}$, the ratio between the *AEQL* of a chart and that of the optimal 3-CUSUM($\mu+\sigma$) scheme.

(3) *ARATS* (Equation (4-1)), the average ratio between the *ATS* of a chart and the *ATS* of the optimal 3-CUSUM($\mu+\sigma$) scheme.

The results for the above three measures are enumerated in Table 4-6. It not only summarizes the overall performance of the five charts in three shift domains, but also lists the corresponding values when only pure mean shift or pure variance shift is considered.

(1) According to both *AEQL* and *ARATS* values in all the three shift domains, the optimal 3-CUSUM($\mu+\sigma$) scheme has the highest detection effectiveness, followed by the ABS CUSUM chart, the scale CUSUM chart, and then the *X* chart. The conventional 3-CUSUM($\mu+\sigma$) scheme ranks last. It can be concluded that the performance of the optimal 3-CUSUM($\mu+\sigma$) scheme is greatly superior to that of the conventional 3-CUSUM($\mu+\sigma$) scheme, especially when the shift domain is small. When ($\delta_{\mu\,\max} = 3$, $\delta_{\sigma,\max} = 4$), the optimal 3-CUSUM($\mu+\sigma$) scheme is more efficient than the conventional 3-CUSUM($\mu+\sigma$) scheme by about 17% from an overall viewpoint. This indicates that the 3-CUSUM($\mu+\sigma$) scheme by itself does not guarantee high detection effectiveness. The values of ζ_μ and ζ_σ (or k^X and k^{X^2}) are very critical to the overall performance of the 3-CUSUM($\mu+\sigma$) scheme. They should be determined by an optimal design so that the resultant (optimal) 3-CUSUM($\mu+\sigma$) scheme stands as the most effective chart.

(2) The overall ratios of $AEQL_{\text{ABS CUSUM}}/AEQL_{\text{opt 3-CUSUM}(\mu+\sigma)}$ for the ABS CUSUM chart in the three shift domains are equal to 1.0322, 1.0099 and 1.0017, respectively. This reveals that there is only minor difference in overall performance between these two CUSUM charts when ($\delta_{\mu,\max} \geq 3$ and $\delta_{\sigma,\max} \geq 4$) and almost no difference when ($\delta_{\mu,\max} \geq 5$ and $\delta_{\sigma,\max} \geq 6$).

(3) The $AEQL_X/AEQL_{\text{opt 3-CUSUM}(\mu+\sigma)}$ for the *X* chart decreases along with the increase

of the process shift domain. When ($\delta_{\mu,\max}$ = 3, $\delta_{\sigma,\max}$ = 4), the ratio is 1.1534, which can be regarded as a significant performance difference between these two charts. However, when the shift domain extends to ($\delta_{\mu,\max}$ = 8, $\delta_{\sigma,\max}$ = 9), the *AEQL* of the *X* chart is only 1.31% higher than that of the optimal 3-CUSUM(μ+σ) scheme.

(4) The overall ratios of $AEQL_{\text{scale CUSUM}}/AEQL_{\text{opt 3-CUSUM}(\mu+\sigma)}$ for the scale CUSUM chart in the three shift domains are slightly larger than 1.0 and decreases along with the increase of the shift domain. It shows there is minor difference in the performance between these two charts.

(5) In Table 4-6, the *AEQL* and *ARATS* values for pure mean shifts δ_μ or pure standard deviation shifts δ_σ are also presented for references. In practice, it is hard to find an assignable cause that only incurs mean shift or only results in variance shift. Compared with the optimal 3-CUSUM(μ+σ) scheme, the conventional 3-CUSUM(μ+σ) scheme is relatively better for detecting pure δ_μ but poorer for pure δ_σ, and the ABS CUSUM chart is, conversely, poorer for detecting pure δ_μ but better for pure δ_σ. It is noted that the main objective of the control charts discussed in this chapter is to detect joint shifts in δ_μ and δ_σ. Some other charts may be more effective to detect pure δ_μ or δ_σ. For example, if one is certain that there is only pure δ_μ in a process and the magnitude of δ_μ is small, he may better adopt a single CUSUM chart with a large sample size. On the other hand, if there is only large pure δ_μ, an $\overline{X}$ chart with a small sample size should be used.

Table 4-6. Results of *AEQL* and *ARATS* for Five Control Charts

$\delta_{\mu,\max}$	$\delta_{\sigma,\max}$	Chart	Overall Performance			For Pure δ_μ			For Pure δ_σ		
			AEQL	$\frac{AEQL}{AEQL_{\text{opt 3-cusum}(\mu+\sigma)}}$	*ARATS*	*AEQL*	$\frac{AEQL}{AEQL_{\text{opt 3-cusum}(\mu+\sigma)}}$	*ARATS*	*AEQL*	$\frac{AEQL}{AEQL_{\text{opt 3-cusum}(\mu+\sigma)}}$	*ARATS*
3	4	*X* chart	22.8553	1.1534	1.1925	27.7499	2.0348	2.0115	23.3857	1.1122	1.1136
		ABS CUSUM	20.4544	1.0322	1.0419	18.2006	1.3346	1.2970	20.7834	0.9885	0.9885
		con 3-CUSUM($\mu+\sigma$)	23.1686	1.1692	1.1788	13.2254	0.9698	1.0696	23.1737	1.1022	1.1088
		opt 3-CUSUM($\mu+\sigma$)	19.8159	1.0000	1.0000	13.6376	1.0000	1.0000	21.0256	1.0000	1.0000
		scale CUSUM	20.6964	1.0444	1.0562	19.1300	1.4027	1.3603	21.1591	1.0064	1.0063
5	6	*X* chart	28.6725	1.0492	1.0756	21.5613	1.5042	1.4486	27.2668	1.0572	1.0701
		ABS CUSUM	27.5969	1.0099	1.0161	16.8571	1.1760	1.1380	25.8041	1.0005	1.0013
		con 3-CUSUM($\mu+\sigma$)	31.1016	1.1381	1.1492	13.9477	0.9731	1.1044	28.9873	1.1239	1.1188
		opt 3-CUSUM($\mu+\sigma$)	27.3268	1.0000	1.0000	14.3337	1.0000	1.0000	25.7917	1.0000	1.0000
		scale CUSUM	27.6737	1.0127	1.0195	17.0017	1.1861	1.1471	25.9111	1.0046	1.0061
8	9	*X* chart	45.6106	1.0131	1.0298	22.4137	1.1891	1.1926	38.5045	1.0238	1.0403
		ABS CUSUM	45.0990	1.0017	1.0064	20.1349	1.0682	1.0601	37.6942	1.0022	1.0058
		con 3-CUSUM($\mu+\sigma$)	48.5538	1.0784	1.0849	17.5092	0.9289	1.0115	41.1256	1.0935	1.0917
		opt 3-CUSUM($\mu+\sigma$)	45.0223	1.0000	1.0000	18.8478	1.0000	1.0000	37.5856	1.0000	1.0000
		scale CUSUM	45.1286	1.0024	1.0085	20.4599	1.0854	1.0770	37.7691	1.0042	1.0097

Studies on Other issues

The charting parameters of these five charts are summarized in Table 4-7.

Table 4-7. Charting Parameters for Five Control Charts

Chart	Parameters
	($\delta_{\mu\max}$ = 3, $\delta_{\sigma,\max}$ = 4)
X chart	*UCL* = 3.00
ABS CUSUM	k = 1.45, H = 1.8426
con 3-CUSUM(μ+σ)	k^X = 0.1500, k^{X^2} = 1.2671, H_{CX} = 12.7890, H_{CX}^2 = 16.1547
opt 3-CUSUM(μ+σ)	k^X = 1.1000, k^{X^2} = 2.5781, H_{CX} = 2.4592, H_{CX}^2= 7.9809
scale CUSUM	k = 1.25, H = 0.5522, w = 0.5
	($\delta_{\mu,\max}$ = 5, $\delta_{\sigma,\max}$ = 6)
X chart	*UCL* = 3.00
ABS CUSUM	k = 1.65, H = 1.4877
con 3-CUSUM(μ+σ)	k^X = 0.1900, k^{X^2} = 1.3300, H_{CX} = 11.0230, H_{CX}^2 = 14.9322
opt 3-CUSUM(μ+σ)	k^X = 1.3500, k^{X^2} = 2.8229, H_{CX} = 1.9133, H_{CX}^2= 7.2268
scale CUSUM	k = 1.30, H = 0.4739, w = 0.5
	($\delta_{\mu,\max}$ = 8, $\delta_{\sigma\max}$ = 9)
X chart	*UCL* = 3.00
ABS CUSUM	k = 1.85, H = 1.2133
con 3-CUSUM(μ+σ)	k^X = 0.2500, k^{X^2} = 1.4597, H_{CX} = 9.1516, H_{CX}^2 = 13.1776
opt 3-CUSUM(μ+σ)	k^X = 1.6000, k^{X^2} = 3.0427, H_{CX} = 1.5114, H_{CX}^2= 6.6026
scale CUSUM	k = 1.40, H = 0.3455, w = 0.5

From this table, the following are observed:

(1) In current literature, many CUSUM charts adopt a k value equal to 0.5 (Sparks 2000). However, Table 4-3 shows the optimal value of k for both ABS CUSUM and scale CUSUM charts is always larger than one, even for the small shift domain as ($\delta_{\mu,\max}$ = 3, $\delta_{\sigma,\max}$ = 4). The curves of *AEQL* versus k of the ABS CUSUM charts in the three shift domains are illustrated in Figure 4-2. On each curve, the minimum *AEQL* is substantially smaller than the *AEQL* value with ($k \leq 1.0$). It indicates that the optimal design is able to enhance the detection effectiveness of the ABS CUSUM chart to a significant degree.

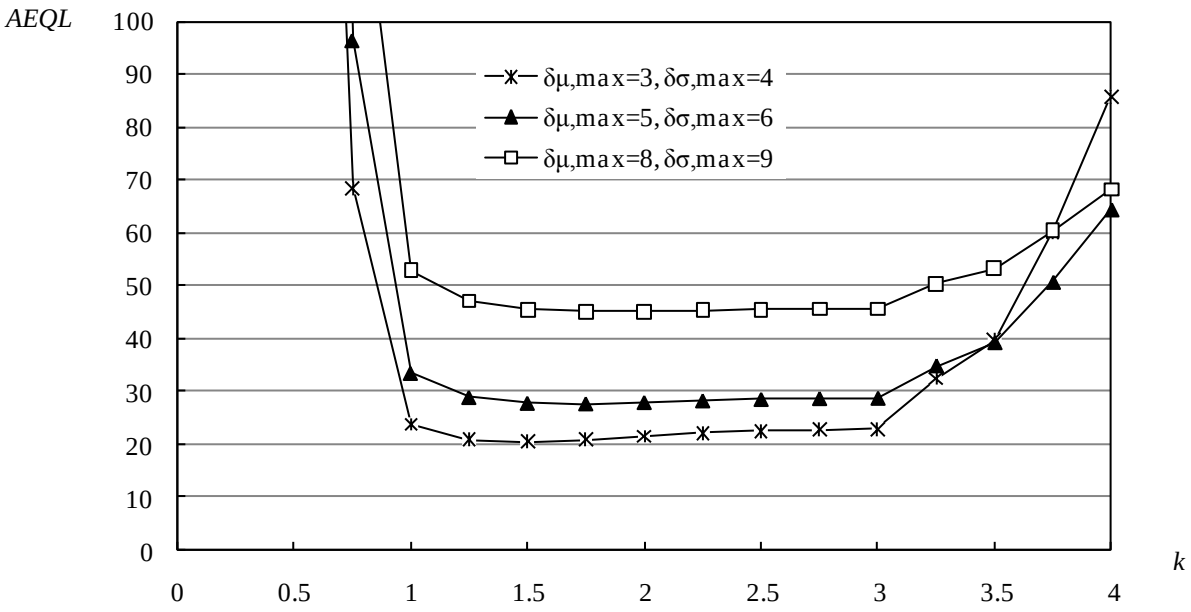

Figure 4-2. Curves of *AEQL* vs. *k* of ABS CUSUM Charts

(2) The reference parameters k^X and k^{X^2} of the optimal 3-CUSUM(μ+σ) scheme increase along with the increase of $\delta_{\mu,\max}$ and $\delta_{\sigma,\max}$. It is because that when the shift domain becomes larger, the reference parameters have to adapt themselves to detect the process shifts that tend to be larger in general. Reynolds and Stoumbos (2004*a*, *b*) also adopted larger k^X and k^{X^2} for larger shift domain.

4.4.3 Discussion on the Simplicity in Design, Implementation and Other Issues

In addition to detection effectiveness, other considerations such as the ease of understanding, implementation, design and diagnosis are also important when selecting a control chart. Here, we focus on the comparison between the most effective but complicated optimal 3-CUSUM(μ+σ) scheme and the simpler *X* chart and ABS CUSUM chart. Since computer has been widely used in today's industry, this issue will be discussed mainly under a computerized environment.

(1) The number of charting parameters to be handled during the design and operation is only one for *X* chart (*UCL*), two for an ABS CUSUM chart (*k* and *H*), but four for the optimal 3-CUSUM(μ+σ) scheme (k^X, k^{X^2}, H_{CX} and H_{CX}^2). It reveals that the *X* chart must be simpler than the ABS CUSUM chart for design and implementation, and the ABS CUSUM chart is in turn simpler than the optimal 3-CUSUM(μ+σ) scheme.

(2) By comparing the updating formulae of the *X* chart, ABS CUSUM chart (Equation (4-12)) and the optimal 3-CUSUM($\mu+\sigma$) scheme (Equation (4-16)), the first two charts are obviously simpler than the latter for implementation and understanding. The *X* chart is extremely easy to run, in which the single observation is plotted directly for each sample.

(3) The *ATS* of an *X* chart can be calculated by a simple formula (Equation (4-10) and (4-11)) and the *ATS* of an ABS CUSUM chart can be evaluated quickly by a Markov procedure (section 4.2.4). Nevertheless, it is very difficult, if not impossible, to use a three-dimensional Markov procedure to evaluate the *ATS* of a 3-CUSUM($\mu+\sigma$) scheme because of the prohibitively large matrix size and substantial computational effort required. As a result, the *ATS* of a 3-CUSUM($\mu+\sigma$) scheme can be evaluated only by simulation. Usually a very large number of simulation runs, such as 1,000,000, is required (Reynolds and Stoumbos (2006)). Even if a smaller number (e.g., 100,000) is used, the simplified optimal design (i.e., using ζ_μ as the only independent variable as in Equation (4-18)) of a typical 3-CUSUM($\mu+\sigma$) scheme still takes about seven hours of CPU time.

(4) The *X* chart is the easiest to understand for operators as the single reading *x* in each sample tells the current value of the quality characteristic *x*, rather than the value of the sample mean $\bar{x}$ or the even mysterious statistics C^{X+}, C^{X-} and C^{X^2}. This is an important issue because of an interest in involving operators in quality improvement (Box *et al*. 1997). The ease of interpretation makes the *X* chart particularly suitable for shop floor use, because it can be understood by all involved personnel including the process operator, inspector and manager (Murdoch 1979). On an *X* chart, the specification limits *LSL* and *USL* can be drawn together with the control limits (Figure 4-3), so that the operators can figure out not only the likelihood that the process is out of control but also the degree that the product meets the design specifications.

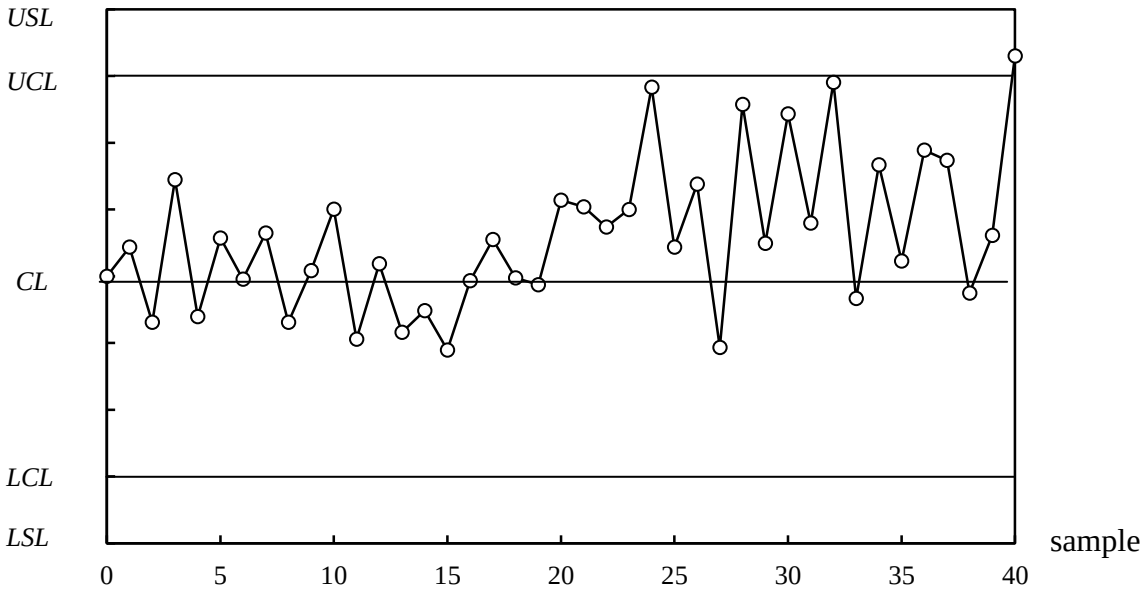

Figure 4-3. A Sample Run of *X* Chart

(5) Figure 4-4 shows the computer displays of a *X* chart, an ABS CUSUM chart and an optimal 3-CUSUM($\mu+\sigma$) scheme for monitoring a same process. The process starts in an in-control status until the tenth sample when a sustained joint shift (δ_μ = 1.0, δ_σ = 1.2) occurs. On the computer monitor, the display of the *X* chart and ABS CUSUM chart is large and clear. It is easy for the operators to figure out whether the process is in control or out of control. In contrast, the three charts of an optimal 3-CUSUM($\mu+\sigma$) scheme are quite crowded and messing for an operator to observe. They have to check all three charts in order to decide the process status.

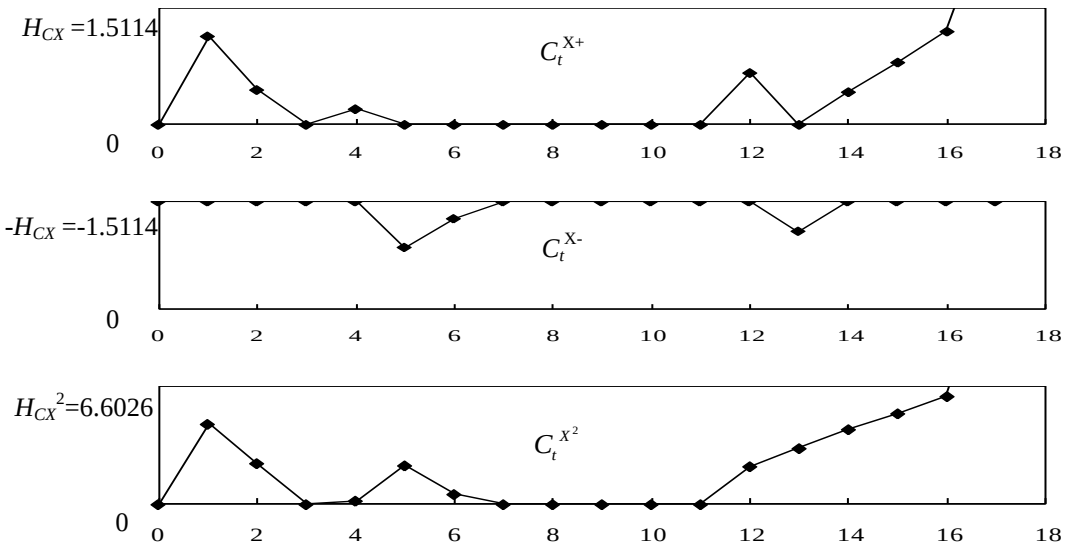

(*a*) 3-CUSUM($\mu+\sigma$) Scheme

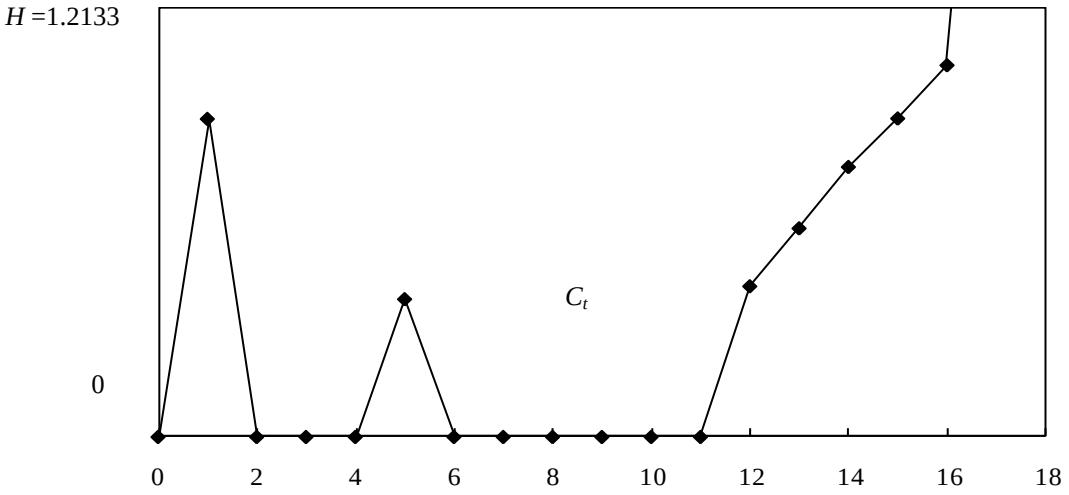

(*b*) ABS CUSUM Chart

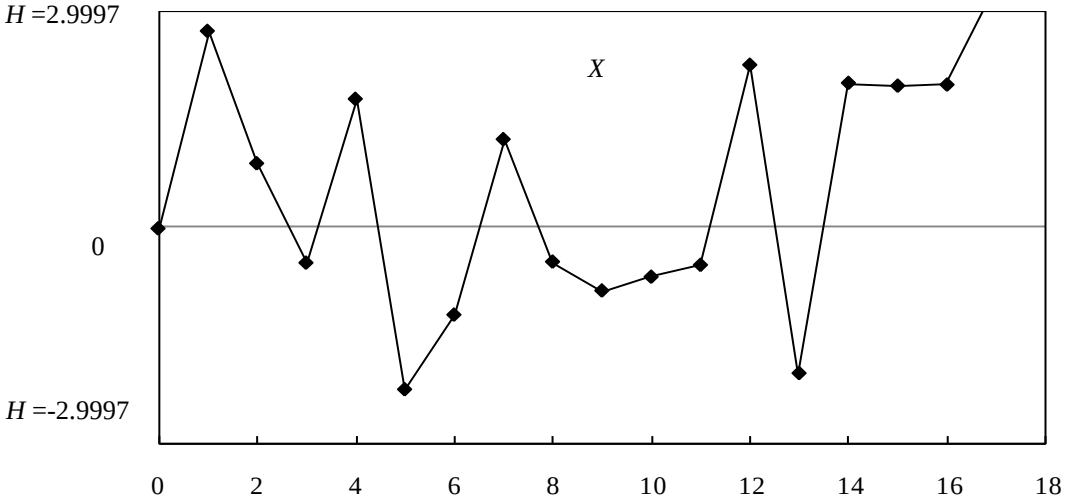

(c) *X* Chart

Figure 4-4. Computer Displays of 3-CUSUM($\mu+\sigma$), ABS CUSUM, and *X* Charts

(6) The ability of judging the changing point is different among these charts. As mentioned in section 3.3.5, when running an ABS CUSUM chart, it is straightforward to estimate the changing point. In Figure 4-4, a sustained joint shift ($\delta_\mu = 1.0$, $\delta_\sigma = 1.2$) occurs between samples 10 and 11, and the subsequent sample points are likely to increase, drifting away from zero. Eventually, sample point 17 overshoots the control limit H and indicates an out-of-control status. From the sample pattern, one may estimate that the changing point is around sample 11. However, each of the three separate CUSUM charts of a 3-CUSUM(μ+σ) scheme may suggest different change points and therefore bring about confusion for a final conclusion. For the X chart, no heuristic method indicates the change point clearly.

(7) Some people believe that the control scheme consisting of several separate charts (e.g., the 3-CUSUM(μ+σ) scheme) may provide some identification of the type of shift (mean shift, or variance shift, or both) based on the chart that signals. In fact, Reynolds and Stoumbos (2004*b*) found that no combination of separate charts can actually diagnose the type of shifts reliably in all situations. The combined scheme often produces misleading diagnostic messages (e.g. mistaking a variance shift for mean shift). From the standpoint of operators, a misleading diagnosis is even worse than no diagnosis. When using a single chart, if the information of shift type is really helpful, it can be easily determined by some post-signal procedures or estimators under a computerized environment (Reynolds and Stoumbos 2006).

(8) A single X chart or CUSUM chart can be further incorporated with runs rules and adaptive features (adaptive sample sizes and/or sampling intervals) more easily than the 3-CUSUM(μ+σ) scheme, in order to further improve the detection effectiveness.

Based on the discussion above, it is believed that the minor superiority of the optimal 3-CUSUM(μ+σ) scheme over the ABS CUSUM chart in *ATS* performance is not sufficient to outweigh the increase in the difficulty for implementation and design.

4.4.4 Summary Comments

Section 4.4 compares the performance of five control charts including the three proposed in this chapter (the X chart, ABS CUSUM chart and optimal 3-CUSUM(μ+σ)

scheme). All the charts are designed using the optimization algorithm. This design algorithm aims at designing the charts with excellent overall performance over a broad process shift domain and works out the optimal values of the charting parameters, but it does not increase the difficulty for running the control charts.

The *X* chart is inferior to the optimal 3-CUSUM(μ+σ) scheme only when the process shift domain is quite small. However, it outperforms the conventional 3-CUSUM(μ+σ) scheme. Thanks to the optimization of the reference parameter *k*, the ABS CUSUM chart is nearly as effective as the optimal 3-CUSUM(μ+σ) scheme. Most importantly, the *X* chart and ABS CUSUM chart are simpler for design and implementation compared to the optimal 3-CUSUM(μ+σ) scheme, under a computerized environment. Their computer displays are clear so that the operators can easily observe and decide the process status, and estimate the changing point. They turn the simultaneous monitoring of process mean and variance into a simple procedure. They should be the right choice for many SPC applications.

The conventional 3-CUSUM(μ+σ) scheme is obviously inferior to the optimal 3-CUSUM(μ+σ) scheme, especially when the shift domain is small. When ($\delta_{\mu,\max}$ = 3, $\delta_{\sigma,\max}$ = 4) and ($\delta_{\mu,\max}$ = 5, $\delta_{\sigma,\max}$ = 6), the *AEQL* value of the conventional 3-CUSUM(μ+σ) scheme is larger than that of the optimal 3-CUSUM(μ+σ) scheme by about 15%. This indicates that simply putting three CUSUM charts together does not guarantee high detection effectiveness. The values of ζ_μ and ζ_σ (or k^X and k^{X^2}) are very critical to the overall performance of the 3-CUSUM(μ+σ) chart. They should be determined by an optimal design so that the resultant (optimal) 3-CUSUM(μ+σ) scheme stands as the most effective chart.

The optimal 3-CUSUM(μ+σ) scheme may be considered when only small or moderate pure mean shifts will occur in a process. This optimal scheme can also serve as a benchmark for the development of new CUSUM charts, because it seems uniformly more effective than all other charts. A new chart is valuable if it has a detection effectiveness close to or higher than that of the optimal 3-CUSUM scheme and, meanwhile, demonstrates some other useful features.

The scale CUSUM is more complicated than the ABS CUSUM chart, but seems always less effective than the latter.

4.5 Example

A semiconductor company fabricates the wafer for an integrated circuit (Wu and Wang 2007). The thickness x of the wafer is a key dimension. Its nominal value and tolerance are specified as $90\pm0.01\mu m$. From the pilot runs, it is found that the distribution of x can be very well approximated by a normal one and the in-control standard deviation σ_0 is estimated as $0.0015\mu m$. The mean μ_0 can be easily adjusted to the nominal value of $90\mu m$ (i.e. the center between the specification limits). The quality engineer specifies the minimum allowable ATS_0 as 370 and a shift domain as $(0 < \delta_\mu \le 8, 1 < \delta_\sigma \le 9)$. The thickness x is converted to z conforming to a standard normal distribution.

$$z = \frac{x - 90}{0.0015}.$$

Three candidate charts, X chart, ABS CUSUM chart and optimal 3-CUSUM(μ+σ) scheme are designed based on the above specifications to detect the two-sided mean shifts and increasing variance shift. The design of the X chart and ABS CUSUM chart can be completed in less than 10 seconds of CPU time by using a computer program, while the design of the optimal 3-CUSUM(μ+σ) scheme takes about seven hours. The charting parameters and *AEQL* values of the three charts can be found in Table 4-7 and 4-8, and are listed as follows.

X chart: $UCL = 3.00$, $AEQL = 45.6106$

ABS CUSUM chart: $k = 1{,}8500$, $H = 1.2133$, $AEQL = 45.0990$

3-CUSUM(R-S) scheme: $k^X = 1.6000$, $k^{X^2} = 3.0427$, $H_{CX} = 1.5114$, $H_{CX}^2 = 6.6026$, $AEQL = 45.0223$

The *ATS* values for the three charts are showed in Table 4-6. Since the overall performance of the three charts is very close, the simplest X chart is the choice for this application.

4.6 Effect of Sampling Cost on the Design and Performance of Control Charts

This section takes the important sampling inspection cost (including the variable and fixed cost components) into consideration when determining the sample sizes $n_{\bar{X}}$, n_{CUSUM} and $n_{\text{3-CUSUM}}$ of the $\bar{X}$ chart, ABS CUSUM chart and optimal 3-CUSUM(μ+σ) scheme in the domain of statistical design. The studies show that (1) Compared to the optimal 3-CUSUM(μ+σ) scheme, the $\bar{X}$ chart and ABS CUSUM chart become more statistically effective for detecting mean and variance shifts when the fixed sampling cost cannot be neglected and/or when the shift domain is large. (2) The optimal values of the sample sizes depend on the process shift domain and the ratio between the fixed and variable sampling costs. In the general cases in which ($\delta_\mu \leq 5$, $\delta_\sigma \leq 6$), the best sample sizes are either one or two for both $n_{\bar{X}}$ and n_{CUSUM}. However, the optimal value of $n_{\text{3-CUSUM}(\mu+\sigma)}$ is always equal to one for all situations.

4.6.1 Introduction

Section 3.5 in Chapter 3 studies the effect of sampling cost on the design of control charts that only monitor process mean. In this section, the effect of sampling cost on the design of charts for monitoring both process mean and variance is investigated. The sampling cost model adopted here is identical to that in section 3.5.2. It is recalled that *A* is the resources (in terms of dollars) available for sampling inspection in a unit of time. The sampling interval *h*, sample size *n*, cost per sample *b* (fixed sampling cost) and cost per unit *c* (variable sampling cost) have the following relationship (referring to Equation (3-59)).

$$h = \frac{cn+b}{A} = \frac{c}{A}(n+B) \tag{4-21}$$

where *B* (=*b*/*c*) is the ratio between the fixed sampling cost *b* and the variable sampling cost *c*. The constant term of *c*/*A* in Equation (4-21) can be dropped as it can be considered as the time unit or a scaling for the sampling interval. Then

$$h = n + B, \tag{4-22}$$

Three charts, the $\bar{X}$ chart, ABS CUSUM chart and optimal 3-CUSUM(μ+σ) scheme, are to be studied. In common sense, it is believed that the $\bar{X}$ chart should use a sample size $n_{\bar{X}}$ = 4, 5 or 6 and the CUSUM chart often works best with a sample size n_{CUSUM} = 1 (Reynolds and Stoumbos 2004*a*, Montgomery 2009). Reynolds and

Stoumbos (2004*a*) also found that the 3-CUSUM(μ+σ) scheme using a sample size of (n = 1) is the best choice from an overall viewpoint. However, these common senses on sample sizes are obtained by only considering the variable sampling inspection cost c, but neglecting the impact of the fixed sampling cost b. Under such circumstances, the sampling interval h is proportional to the sample size n (Equation (4-22)) and the use of large sample size has little advantage. In this section, the sample sizes are optimized by taking the sampling costs c and b into consideration in order to minimize *AEQL*.

The statistic handled by the $\overline{X}$ chart is the sample mean $\bar{x}_t$ of a sample of size $n_{\overline{X}}$. The statistic C_t of the ABS CUSUM chart is also calculated based on $\bar{x}_t$ rather than the individual reading x_t.

$$\begin{aligned} &C_0 = 0 \\ &C_t = \max\left(0,\ C_{t-1} + \left|\bar{x}_t - \mu_0\right| - k\right) \end{aligned} \tag{4-23}$$

The formulae for the optimal 3-CUSUM(μ+σ) scheme also have to be modified slightly, *i.e.*, using $\bar{x}_t$ to replace x_t.

$$\begin{aligned} &C_0^{X+} = 0, \quad C_0^{X-} = 0, \quad C_0^{X^2} = 0 \\ &C_t^{X+} = \max\left(0,\ C_{t-1}^{X+}\right) + \left(\bar{x}_t - \mu_0 - k^X\right) \\ &C_t^{X-} = \min\left(0,\ C_{t-1}^{X-}\right) + \left(\bar{x}_t - \mu_0 + k^X\right) \\ &C_t^{X^2} = \max\left(0,\ C_{t-1}^{X^2}\right) + \left[\left(\bar{x}_t - \mu_0\right)^2 - k^{X^2}\right] \end{aligned} \tag{4-24}$$

4.6.2 Optimal design of the Three Charts

In order to carry out the optimal design, the minimum allowable value τ of the in-control ATS_0, the variable and fixed sampling cost c and b, the maximum shifts $\delta_{\mu,\max}$ and $\delta_{\sigma,\max}$, need to be specified. The optimal designs of the control charts which are similar to those introduced in the previous sections can be formulated as follows.

Objective function:	$AEQL$ = minimum.	
Constraint function:	$ATS_0 \geq \tau$.	(4-25)
Design variables:	independent and dependent variables, including sample size, sampling interval, control limit, and the reference parameters	

for the CUSUM-type charts.

During the optimal design, the optimal values of the independent variables will be searched in order to minimize the objective function *AEQL*. The sampling interval *h* is determined based on the sample size and sampling cost (Equation (4-22)). The control limits are adjusted so that the constraint function on ATS_0 (Equation (4-25) is satisfied.

(1) Optimal design of $\overline{X}$ chart

For an $\overline{X}$ chart, the only independent variable is the sample size $n_{\overline{X}}$, and the dependent variables are the sampling interval *h* and control limits *LCL* and *UCL*. The sampling interval *h* is determined by Equation (4-22) and the control limits are calculated using Equations (4-5) and (4-6). When the minimal *AEQL* is found at optimal $n_{\overline{X}}$, the optimal values of *h*, *LCL* and *UCL* are all determined.

(2) Optimal design of ABS CUSUM chart

For an ABS CUSUM chart, the independent variables are the sample size n_{CUSUM} and reference parameter *k*. The dependent variables are the sampling interval *h* and control limit *H*. For each pair of n_{CUSUM} and *k*, the value of *h* is determined directly by Equation (4-22), and the value of *H* is adjusted to satisfy the constraint function on ATS_0 in Equation (4-25).

(3) Optimal design of the 3-CUSUM($\mu+\sigma$) scheme

Unlike the optimal design of the optimal 3-CUSUM($\mu+\sigma$) scheme in Equation (4-18) in which $n_{3\text{-CUSUM}(\mu+\sigma)} = 1$, the sample size $n_{3\text{-CUSUM}(\mu+\sigma)}$ is treated as an independent design variables in this section. The optimal values of $n_{3\text{-CUSUM}(\mu+\sigma)}$ and ζ_μ are searched so that the *AEQL* of the optimal 3-CUSUM($\mu+\sigma$) scheme is minimized. The charting parameters *h*, ζ_σ, k^X and k^{X^2} are calculated by Equations (4-22) and (4-19) based on $n_{3\text{-CUSUM}(\mu+\sigma)}$ and ζ_μ. The control limits H_{CX} and H_{CX}^2 are determined so that the individual CUSUM charts have equal in-control ATS_0 and the overall ATS_0 of the optimal 3-CUSUM($\mu+\sigma$) scheme is equal to the specified τ.

4.6.3 Comparative Studies

In this comparative study, the charting parameters of all the charts have been optimized.

The specification τ for the in-control ATS_0 is set as 370. The comparison will be conducted in three shift domains: a small domain of ($\delta_{\mu,\max} = 3$, $\delta_{\sigma,\max} = 4$), a medium one of ($\delta_{\mu,\max} = 5$, $\delta_{\sigma,\max} = 6$), and a large one of ($\delta_{\mu,\max} = 8$, $\delta_{\sigma,\max} = 9$). The distributions of both mean shift δ_μ and standard deviation shift δ_σ are assumed to be uniform. In addition, the cost parameter B (i.e. the ratio between the fixed sampling cost b and the variable sampling cost c) takes five different values (0, 1, 3, 6, 10).

Charting Parameters

Table 4-8 shows the optimal charting parameters of the three control charts under three shift domains and five different values of the cost parameter B. For the optimal 3-CUSUM(μ+σ) scheme, the optimal value of $n_{3\text{-CUSUM}(\mu+\sigma)}$ always equals to one regardless of the value of B and the shift domain ($\delta_{\mu,\max}$, $\delta_{\sigma,\max}$). For the other two charts, the optimal values of the sample sizes $n_{\bar{X}}$ and n_{CUSUM} depend on both B and ($\delta_{\mu,\max}$, $\delta_{\sigma,\max}$). They always increase with an increase in B and/or a decrease in ($\delta_{\mu,\max}$, $\delta_{\sigma,\max}$). For example, in the small shift domain of ($\delta_{\mu,\max} = 3$, $\delta_{\sigma,\max} = 4$), $n_{\bar{X}}$ and n_{CUSUM} equal to one when $B = 0$. When $B = 3$, $n_{\bar{X}}$ and n_{CUSUM} increase to two. When B is increased to 10, $n_{\bar{X}}$ and n_{CUSUM} equal to four and three, respectively.

When the shift domain ($\delta_{\mu,\max}$, $\delta_{\sigma,\max}$) is extended, $n_{\bar{X}}$ and n_{CUSUM} become smaller for the same B value compared to that in the smaller domain ($\delta_{\mu,\max}$, $\delta_{\sigma,\max}$). For example, in the case of $B = 6$, $n_{\bar{X}} = n_{\text{CUSUM}} = 3$ in ($\delta_{\mu,\max} = 3$, $\delta_{\sigma,\max} = 4$); but $n_{\bar{X}} = n_{\text{CUSUM}} = 2$ in ($\delta_{\mu,\max} = 5$, $\delta_{\sigma,\max} = 6$) and $n_{\bar{X}} = n_{\text{CUSUM}} = 1$ in ($\delta_{\mu,\max} = 8$, $\delta_{\sigma,\max} = 9$). In the large shift domain of ($\delta_{\mu,\max} = 8$, $\delta_{\sigma,\max} = 9$), the optimal sample sizes for all charts are equal to one, except $n_{\bar{X}} = 2$ when $B = 10$.

Table 4-8. Charting Parameters and Overall Performance of Three Control Charts

B	Chart	n	h	k	UCL	H	k^X	k^{X^2}	H_{CX}	$H_{CX}{}^2$	$ARATS$	$\frac{AEQL}{AEQL_{3-\mathrm{CUSUM}(\mu+\sigma)}}$
						($\delta_{\mu,\max}$ = 3, $\delta_{\sigma,\max}$ = 4)						
	xbar	1	1.0	-	3.00	-	-	-	-	-	1.2049	1.1542
0	ABS CUSUM	1	1.0	1.45	-	1.84	-	-	-	-	1.0486	1.0332
	3-CUSUM(μ+σ)	1	1.0	-	-	-	0.95	2.42	2.89	8.43	1.0000	1.0000
	xbar	1	2.0	-	2.78	-	-	-	-	-	1.1263	1.0946
1	ABS CUSUM	1	2.0	1.45	-	1.55	-	-	-	-	1.0297	1.0195
	3-CUSUM(μ+σ)	1	2.0	-	-	-	1.10	2.58	2.12	6.38	1.0000	1.0000
	xbar	2	5.0	-	1.75	-	-	-	-	-	0.9710	1.0181
3	ABS CUSUM	2	5.0	1.02	-	0.81	-	-	-	-	0.9431	0.9938
	3-CUSUM(μ+σ)	1	4.0	-	-	-	1.40	2.87	1.27	4.67	1.0000	1.0000
	xbar	3	9.0	-	1.30	-	-	-	-	-	0.8953	0.9353
6	ABS CUSUM	3	9.0	1.03	-	0.28	-	-	-	-	0.8886	0.9293
	3-CUSUM(μ+σ)	1	7.0	-	-	-	1.50	2.96	0.90	2.77	1.0000	1.0000
	xbar	4	14.0	-	1.04	-	-	-	-	-	0.8428	0.8848
10	ABS CUSUM	3	13.0	1.20	-	0.02	-	-	-	-	0.8533	0.8898
	3-CUSUM(μ+σ)	1	11.0	-	-	-	1.15	2.63	1.18	2.48	1.0000	1.0000
						($\delta_{\mu,\max}$ = 5, $\delta_{\sigma,\max}$ = 6)						
	xbar	1	1.0	-	3.00	-	-	-	-	-	1.0759	1.0490
0	ABS CUSUM	1	1.0	1.65	-	1.49	-	-	-	-	1.0163	1.0096
	3-CUSUM(μ+σ)	1	1.0	-	-	-	1.35	2.82	1.91	7.23	1.0000	1.0000
	xbar	1	2.0	-	2.78	-	-	-	-	-	1.0462	1.0290
1	ABS CUSUM	1	2.0	1.65	-	1.23	-	-	-	-	1.0096	1.0054
	3-CUSUM(μ+σ)	1	2.0	-	-	-	1.45	2.91	1.48	5.45	1.0000	1.0000
	xbar	1	4.0	-	2.55	-	-	-	-	-	1.0274	1.0156
3	ABS CUSUM	1	4.0	1.60	-	1.03	-	-	-	-	1.0053	1.0023
	3-CUSUM(μ+σ)	1	4.0	-	-	-	1.45	2.91	1.20	3.99	1.0000	1.0000
	xbar	2	8.0	-	1.62	-	-	-	-	-	0.9635	0.9918
6	ABS CUSUM	2	8.0	1.09	-	0.57	-	-	-	-	0.9562	0.9873
	3-CUSUM(μ+σ)	1	7.0	-	-	-	1.50	2.96	0.90	2.77	1.0000	1.0000
	xbar	2	12.0	-	1.51	-	-	-	-	-	0.9334	0.9592
10	ABS CUSUM	2	12.0	1.06	-	0.49	-	-	-	-	0.9283	0.9563
	3-CUSUM(μ+σ)	1	11.0	-	-	-	1.45	2.91	0.77	1.96	1.0000	1.0000
						($\delta_{\mu,\max}$ = 8, $\delta_{\sigma,\max}$ = 9)						
	xbar	1	1.0	-	3.00	-	-	-	-	-	1.0299	1.0131
0	ABS CUSUM	1	1.0	1.85	-	1.21	-	-	-	-	1.0065	1.0020
	3-CUSUM(μ+σ)	1	1.0	-	-	-	1.60	3.04	1.51	6.60	1.0000	1.0000
	xbar	1	2.0	-	2.78	-	-	-	-	-	1.0194	1.0070
1	ABS CUSUM	1	2.0	1.80	-	1.04	-	-	-	-	1.0043	1.0004
	3-CUSUM(μ+σ)	1	2.0	-	-	-	1.50	2.96	140	5.35	1.0000	1.0000
	xbar	1	4.0	-	2.55	-	-	-	-	-	1.0113	1.0045
3	ABS CUSUM	1	4.0	1.70	-	0.90	-	-	-	-	1.0022	1.0010
	3-CUSUM(μ+σ)	1	4.0	-	-	-	1.60	3.04	1.00	3.72	1.0000	1.0000
	xbar	1	7.0	-	2.35	-	-	-	-	-	1.0075	1.0025
6	ABS CUSUM	1	7.0	1.70	-	0.68	-	-	-	-	1.0022	1.0004
	3-CUSUM(μ+σ)	1	7.0	-	-	-	1.50	2.96	0.90	2.77	1.0000	1.0000
	xbar	2	12.0	-	1.51	-	-	-	-	-	0.9803	1.0012
10	ABS CUSUM	1	11.0	1.60	-	0.60	-	-	-	-	0.9997	1.0003
	3-CUSUM(μ+σ)	1	11.0	-	-	-	1.60	3.04	0.60	1.77	1.0000	1.0000

Table 4-8 is very useful for a SPC user to select the sample sizes of the control charts for monitoring process mean and variance. It reveals that many conventional guidelines may not be appropriate. For example, the sample size $n_{\bar{X}}$ of the $\bar{X}$ chart should be set at 1 or 2 for most of the cases rather than 4 to 6. Moreover, the optimal n_{CUSUM} of the ABS CUSUM chart may not necessarily be equal to one, a larger n_{CUSUM} should be considered when B is larger.

When a larger sample size is used, the power that a chart detects a process shift in each sample becomes higher. It is a positive effect of a large n, because the increased power will reduce the *ARL*, as well as *ATS*. However, since the sampling interval h is an increasing function of the sample size n, a large n also has a negative effect that increases h, as well as *ATS*. Logically, there must be an optimal sample size that will minimize *ATS* or *AEQL*.

The sample size n increases with an increase in B, because a large fixed sampling cost b makes the sampling interval h increase in a lower rate when n increases. It makes the positive effect of a large n outweigh its negative effect, and therefore encourages the use of a larger sample size for higher detection power. On the other hand, the sample size n becomes smaller when the shift domain gets larger, because a small n makes the control chart particularly effective for detecting large process shifts.

Performance Comparison

The overall performance of the charts is compared by $AEQL/AEQL_{3\text{-CUSUM}(\mu+\sigma)}$ and *ARATS* (using optimal 3-CUSUM($\mu+\sigma$) scheme as the benchmark), as shown in Table 4-8.

From $AEQL/AEQL_{3\text{-CUSUM}(\mu+\sigma)}$, it is found that the detection effectiveness of $\bar{X}$ chart and ABS CUSUM chart increase compared to the optimal 3-CUSUM($\mu+\sigma$) scheme as B and/or ($\delta_{\mu,\max}$, $\delta_{\sigma,\max}$) increase. In many cases, these two charts even outperform the optimal 3-CUSUM($\mu+\sigma$) scheme. On the other hand, the $\bar{X}$ chart is always inferior to the ABS CUSUM chart regardless of the values of B and ($\delta_{\mu,\max}$, $\delta_{\sigma,\max}$). More findings are detailed below:

(1) Firstly, in the small shift domain ($\delta_{\mu,\max} = 3$, $\delta_{\sigma,\max} = 4$), the effect of B on a chart performance is found to be very obvious. When $B = 0$, the $\overline{X}$ chart has the worst performance. Its $AEQL_{\overline{X}}$ value is 15.4% higher than that of the optimal 3-CUSUM($\mu+\sigma$) scheme. The performance of the ABS CUSUM chart is much better than that of the $\overline{X}$ chart, but its $AEQL_{\text{CUSUM}}$ value is still 3.3% higher than that of the optimal 3-CUSUM($\mu+\sigma$) scheme. As B increases, the performance of the $\overline{X}$ chart and ABS CUSUM chart is approaching to that of the optimal 3-CUSUM($\mu+\sigma$) scheme. When B is large enough, the $\overline{X}$ and ABS CUSUM charts even outperform the optimal 3-CUSUM($\mu+\sigma$) scheme. For example, when B increases to 6, both the $\overline{X}$ chart and ABS CUSUM chart outperforms the optimal 3-CUSUM($\mu+\sigma$) scheme by more than 6%, in terms of *AEQL*.

(2) Next, in the medium shift domain of ($\delta_{\mu,\max} = 5$, $\delta_{\sigma,\max} = 6$), the *AEQL* difference among the charts is not significant. When $B = 0$, the $\overline{X}$ chart is inferior to the optimal 3-CUSUM($\mu+\sigma$) scheme by 4.9%, in terms of *AEQL*. As B approaches 10, the $AEQL_{\overline{X}}$ value of the $\overline{X}$ chart becomes smaller than that of the optimal 3-CUSUM($\mu+\sigma$) scheme by 4.1%.

(3) Finally, when the shift domain is extended to ($\delta_{\mu,\max} = 8$, $\delta_{\sigma,\max} = 9$), no matter what B value is, the optimal 3-CUSUM($\mu+\sigma$) scheme always has the best overall performance. But the difference in *AEQL* between any charts becomes negligible.

Table 4-8 also shows that similar conclusion can be reached if the three charts are compared based on *ARATS*.

The *AEQL* comparison of the control charts is illustrated in Figure 4-5. Generally, the cost parameter B plays an important role on the design and performance of a chart, especially when the shift domain is small. It is usually believed that the optimal 3-CUSUM($\mu+\sigma$) scheme considerably or significantly outperforms the ABS CUSUM chart and the latter excels the $\overline{X}$ chart. Figure 4-5 reveals that this hypothesis is true only when B is close to zero (i.e. no fixed sampling cost b) and the shift domain is also small. When the shift domain is moderate or large, there is little difference among the overall performance of the charts from a practical viewpoint. On the other

hand, when the shift domain is small, the $\overline{X}$ chart is inferior to the optimal 3-CUSUM(μ+σ) scheme for small *B*, but outperforms the latter for large *B*. By taking all the factors into consideration, the detection effectiveness of the optimal 3-CUSUM(μ+σ) scheme may not be higher than that of the other two charts. But the ABS CUSUM chart always more or less outperforms the $\overline{X}$ chart.

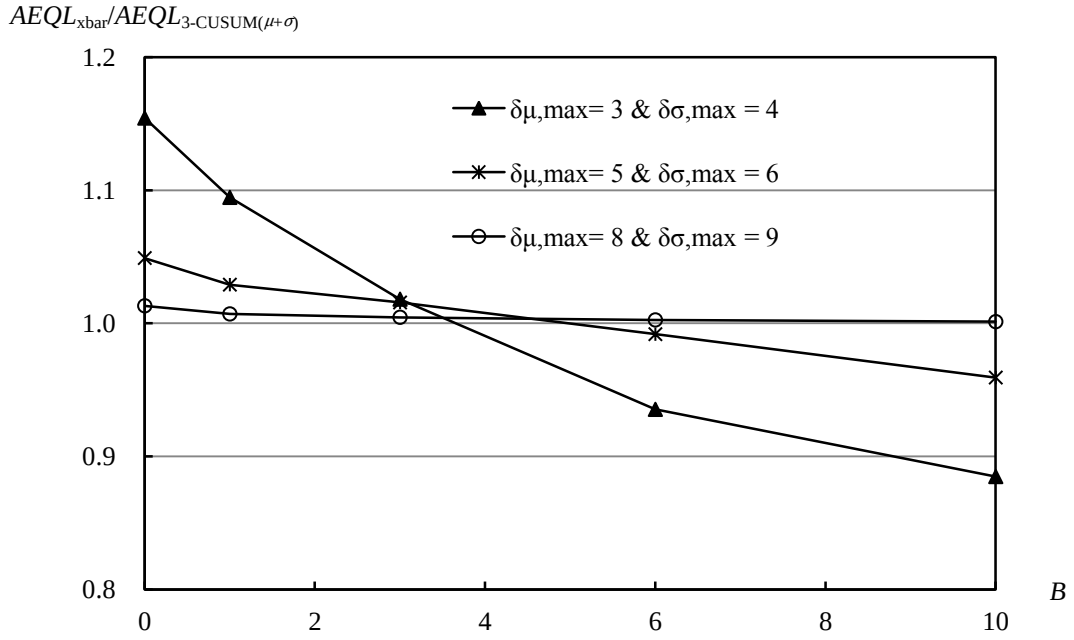

Figure 4-5(*a*). $AEQL_{\text{xbar}}$/ $AEQL_{\text{3-CUSUM}(\mu+\sigma)}$ at Different *B* Levels

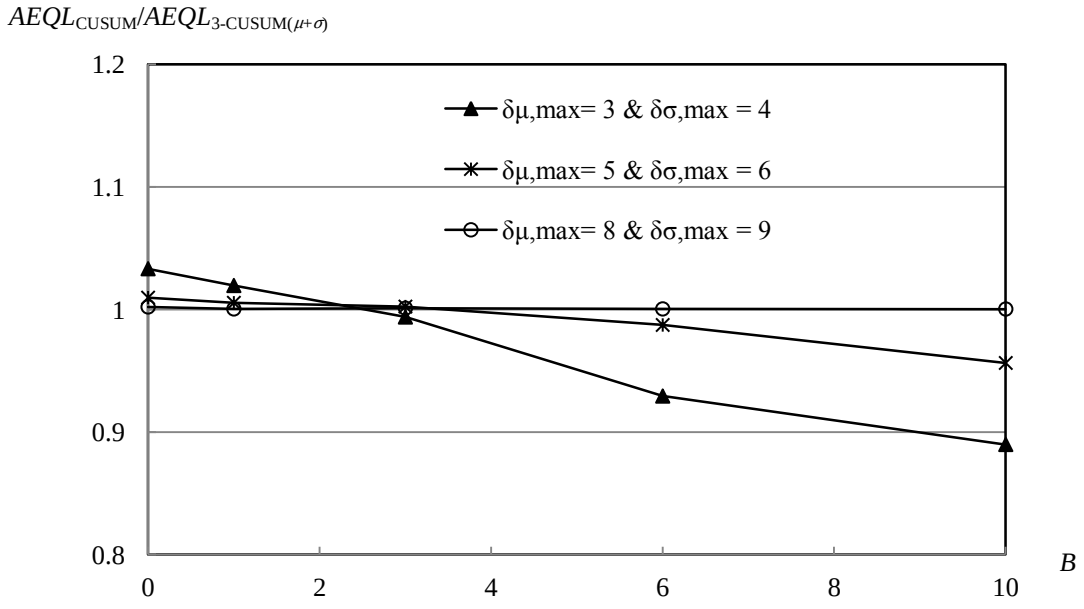

Figure 4-5(*b*). $AEQL_{\text{CUSUM}}$/ $AEQL_{\text{3-CUSUM}(\mu+\sigma)}$ at Different *B* Levels

To further investigate why the performance of these charts is similar, we choose a general case in which (τ = 370, B = 3, $\delta_{\mu,\max}$ = 5, $\delta_{\sigma,\max}$ = 6) to study the *ATS* values under different shifts.

Table 4-9 displays the *ATS* values of the three charts in this case. It can be seen that when there are only small pure mean shifts or small pure standard deviation shifts, the *ATS* of the $\overline{X}$ chart is considerably larger than that of the other two charts. This agrees with the traditional viewpoint that the $\overline{X}$ chart is insensitive to small process shifts. However, beyond this limited region of small shifts, there is no perceptible difference among the *ATS* values of the three charts in each cell. Consequently, the performance measures, *AEQL* and *ARATS*, calculated over the whole shift domain show little difference in overall performance.

Table 4-9. *ATS* Values of Three Control Charts

(τ = 370, $\delta_{\mu,\max}$ = 5, $\delta_{\sigma,\max}$ = 6, B = 3)

δ_σ	Chart	δ_μ										
		0.0	0.5	1.0	1.5	2.0	2.5	3.0	3.5	4.0	4.5	5.0
1.0	xbar	370	185	63.7	25.2	11.7	6.32	3.93	2.82	2.32	2.10	2.03
	ABS CUSUM	370	174	54.2	20.3	9.66	5.59	3.74	2.81	2.33	2.12	2.03
	3-CUSUM(μ+σ)	370	162	48.5	18.3	9.03	5.41	3.70	2.80	2.33	2.12	2.03
1.5	xbar	42.8	35.4	23.0	14.3	9.16	6.21	4.47	3.43	2.80	2.43	2.22
	ABS CUSUM	39.3	32.5	21.1	13.2	8.54	5.89	4.33	3.38	2.80	2.44	2.23
	3-CUSUM(μ+σ)	39.4	32.2	20.7	12.8	8.33	5.75	4.26	3.36	2.80	2.44	2.23
2.0	xbar	17.8	16.5	13.5	10.4	7.92	6.06	4.76	3.85	3.22	2.79	2.49
	ABS CUSUM	16.6	15.5	12.8	9.95	7.62	5.89	4.67	3.81	3.21	2.79	2.50
	3-CUSUM(μ+σ)	16.6	15.5	12.8	9.95	7.62	5.89	4.67	3.81	3.21	2.79	2.50
2.5	xbar	11.0	10.6	9.57	8.25	6.94	5.78	4.84	4.10	3.53	3.10	2.77
	ABS CUSUM	10.5	10.1	9.20	7.98	6.75	5.67	4.77	4.06	3.51	3.09	2.78
	3-CUSUM(μ+σ)	10.5	10.2	9.21	7.99	6.72	5.65	4.73	4.05	3.50	3.08	2.79
3.0	xbar	8.11	7.95	7.50	6.85	6.13	5.41	4.76	4.19	3.71	3.32	3.01
	ABS CUSUM	7.86	7.71	7.29	6.69	6.01	5.33	4.70	4.16	3.70	3.32	3.01
	3-CUSUM(μ+σ)	7.88	7.72	7.30	6.73	6.02	5.32	4.70	4.16	3.70	3.31	3.00
3.5	xbar	6.57	6.49	6.26	5.91	5.48	5.03	4.58	4.16	3.78	3.45	3.17
	ABS CUSUM	6.43	6.35	6.13	5.80	5.40	4.97	4.54	4.14	3.77	3.45	3.17
	3-CUSUM(μ+σ)	6.45	6.33	6.16	5.81	5.36	4.94	4.53	4.13	3.77	3.43	3.17
4.0	xbar	5.63	5.59	5.45	5.24	4.98	4.68	4.37	4.07	3.78	3.51	3.27
	ABS CUSUM	5.54	5.50	5.37	5.17	4.92	4.64	4.34	4.05	3.76	3.50	3.26
	3-CUSUM(μ+σ)	5.56	5.52	5.36	5.17	4.92	4.66	4.33	4.05	3.76	3.48	3.25
4.5	xbar	5.00	4.97	4.89	4.76	4.58	4.38	4.17	3.94	3.72	3.51	3.31
	ABS CUSUM	4.95	4.92	4.84	4.71	4.55	4.35	4.14	3.93	3.71	3.50	3.30
	3-CUSUM(μ+σ)	4.94	4.94	4.83	4.71	4.53	4.35	4.15	3.93	3.70	3.51	3.29
5.0	xbar	4.55	4.54	4.48	4.39	4.27	4.13	3.97	3.81	3.64	3.47	3.31
	ABS CUSUM	4.52	4.50	4.45	4.36	4.24	4.11	3.96	3.80	3.63	3.47	3.31
	3-CUSUM(μ+σ)	4.55	4.52	4.44	4.34	4.25	4.10	3.97	3.77	3.63	3.47	3.30
5.5	xbar	4.22	4.21	4.17	4.10	4.02	3.92	3.80	3.68	3.55	3.42	3.28
	ABS CUSUM	4.19	4.18	4.14	4.08	4.00	3.90	3.79	3.67	3.54	3.41	3.28
	3-CUSUM(μ+σ)	4.18	4.19	4.16	4.06	4.00	3.91	3.78	3.68	3.53	3.41	3.28
6.0	xbar	3.96	3.95	3.92	3.88	3.82	3.74	3.65	3.56	3.46	3.35	3.24
	ABS CUSUM	3.94	3.94	3.91	3.86	3.80	3.73	3.64	3.55	3.45	3.35	3.24
	3-CUSUM(μ+σ)	3.96	3.91	3.92	3.86	3.79	3.74	3.66	3.54	3.45	3.34	3.25

4.6.4 Example

A manufacturing company produces stainless steel drills that will be used on precision drilling machine. The diameter x of the drill with a specification of $(8.0 \pm 0.1mm)$ is a key dimension and has to receive strict control. The Qualy Control (QC) team wishes to select a simple but effective control chart to monitor the mean and variance of x. From pilot runs, it is found that x can be very well approximated by a normal distribution and the in-control standard deviation σ_0 is estimated as $0.012mm$. The mean μ_0 can be easily adjusted to the nominal value of $8.0mm$. The QC team specifies the minimum allowable ATS_0 as 370 and a shift domain of $(0 < \delta_\mu \leq 5,\ 1 < \delta_\sigma \leq 6)$. It further finds that the time for preparing a sampling inspection (fixed sampling cost b) is 60 seconds and the time for inspecting one drill (variable sampling cost c) is 20 seconds. Thus, the value of B is equal to three. In this example, the sampling cost is assumed to be proportional to the operational time required. In order to standardize the design and operation, the diameter x is converted to z conforming to a standard normal distribution.

$$z = \frac{x - 8.0}{0.012}.$$

Three control charts will be studied: the $\bar{X}$ chart, ABS CUSUM chart and optimal 3-CUSUM(μ+σ) scheme. For this example with (τ = 370, $\delta_{\mu,\max}$ = 5, $\delta_{\sigma,\max}$ = 6, B = 3), the three charts are designed and the charting parameters and *AEQL* values are listed as below:

$\bar{X}$ chart: n = 1, h = 4.0, UCL = 2.55, $AEQL$ = 95.07.

ABS CUSUM chart: n = 1, h = 4.0, k = 1.60, H = 1.03, $AEQL$ = 93.82.

optimal 3-CUSUM(μ+σ) scheme: n = 1, h = 4.0, k^X = 1.45, k^{X^2} = 2.91, H_{CX} = 1.20, H_{CX}^2= 3.99, $AEQL$ = 93.60.

The *ATS* values are displayed in Table 4-9. By comparing the *AEQL* values of the charts, it can be seen that the optimal 3-CUSUM(μ+σ) scheme has the best overall performance. However, the ABS CUSUM chart and $\bar{X}$ chart are inferior to the optimal 3-CUSUM(μ+σ) scheme by only 0.24% and 1.57%, respectively, in terms of *AEQL*.

Based on this study, the QC team decides to use the $\overline{X}$ chart, because this chart is obviously simpler to use and not much slower for detecting process shifts than other charts. The floor operators are most familiar with the $\overline{X}$ chart. Moreover, since the optimal sample size $n_{\overline{X}}$ is one, the $\overline{X}$ chart becomes the simplest *X* chart. The operators can plot the observed reading of *x* on the *X* chart directly without even calculating the sample mean $\bar{x}$.

4.6.5 Application Using Real Field Data

This section will show how these three control charts perform in a real situation. A manufacturer uses auto screw driver to assemble two parts. The torque should be set in a specified range to avoid destroying the part if it is too high and also to avoid losing connection if it is too low. In addition, the torque exerted on the parts must be as stable as possible, because large variability may cause irregular functions. According to documentation, the lower and upper specifications of the torque are 6 in-ibs and 9 in-ibs, respectively. The target torque is 7.5 in-ibs and standard deviation is 0.5 in-ibs. During operation, it is found that the time for preparing torque testing is almost the same as that for testing itself (B = 1). In order to make the control chart behave like a three-sigma Shewhart chart when the process is in control, ATS_0 of the control charts is set as 370, B = 1 and ($\delta_{\mu,\max}$ = 3, $\delta_{\sigma,\max}$ = 4). From Table 4-8, the parameters of the control charts can be picked up as follows.

$\overline{X}$ chart:	n = 1, h = 2.0, UCL = 2.78, $ARATS$ = 1.1263, $AEQL$ ratio = 1.0946
ABS CUSUM chart:	n = 1, h = 2.0, k = 1.45, H = 1.55, $ARATS$ = 1.0297, $AEQL$ ratio = 1.0195
optimal 3-CUSUM(μ+σ) scheme:	n = 1, h = 2.0, k^X = 1.10, k^{X^2} = 2.58, H_{CX} = 2.12, H_{CX}^2= 6.38, $ARATS$ = 1.0000, $AEQL$ ratio = 1.0000

As indicated, one torque reading of screwdriver is taken for every two hours. Table 4-10 shows the torque readings recorded in about two days.

Table 4-10. Torque Reading *vs*. Time Series

Sequence	Torque	Sequence	Torque	Sequence	Torque	Sequence	Torque
1	7.317	2	7.326	3	7.477	4	7.654
5	7.600	6	7.627	7	7.406	8	7.361
9	7.494	10	7.565	11	7.450	12	7.273
13	7.530	14	7.468	15	8.335	16	7.538
17	7.459	18	7.503	19	7.521	20	7.432
21	7.317	22	7.453	23	7.397	24	7.776
25	6.717	26	6.031	27	7.806	28	7.850
29	7.806	30	6.735	31	6.956	32	7.151
33	7.823	34	6.027	35	7.593	36	7.452
37	7.531	38	7.310	39	7.425	40	7.514
41	7.107	41	6.956	43	6.089	44	5.460

The next step is to standardize these data and calculate the plotted data for ABS CUSUM chart and the optimal 3-CUSUM($\mu+\sigma$) scheme according to Equations (4-23) and (4-24).

Figure 4-6 shows the actual run length of control charts using above real data.

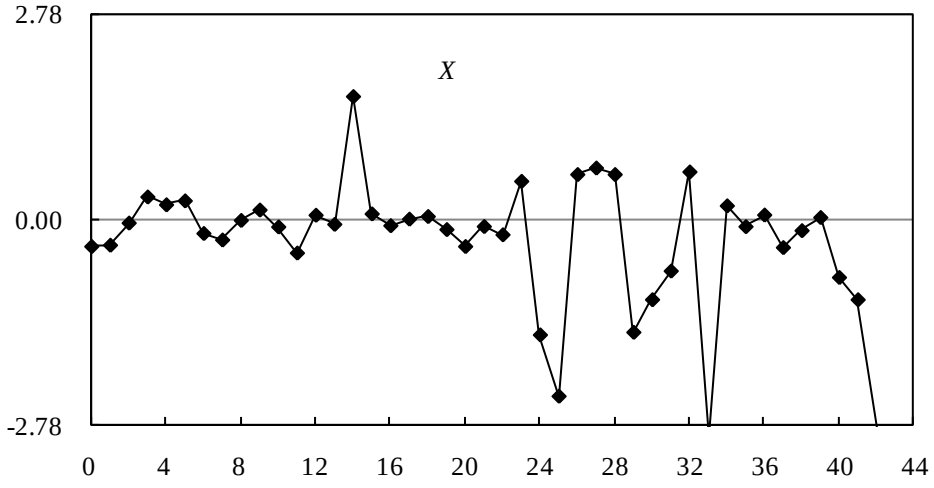

(*a*) *X* Chart

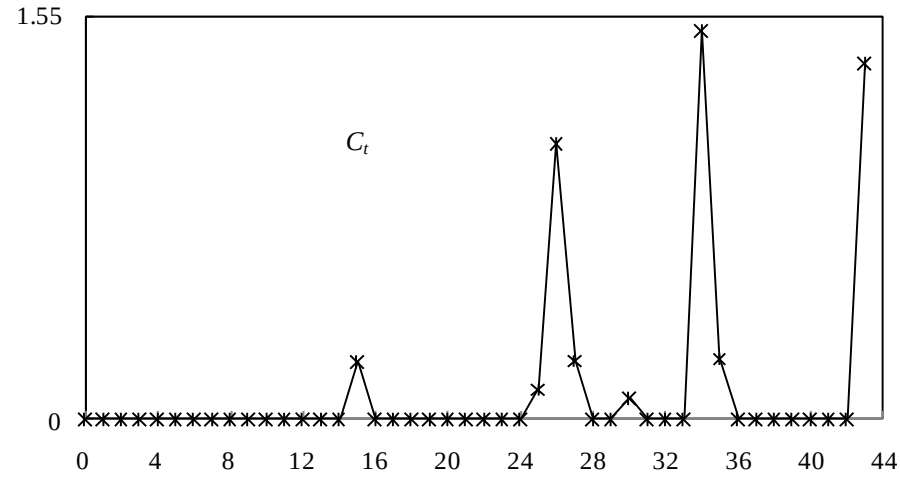

(*b*) ABS CUSUM Chart

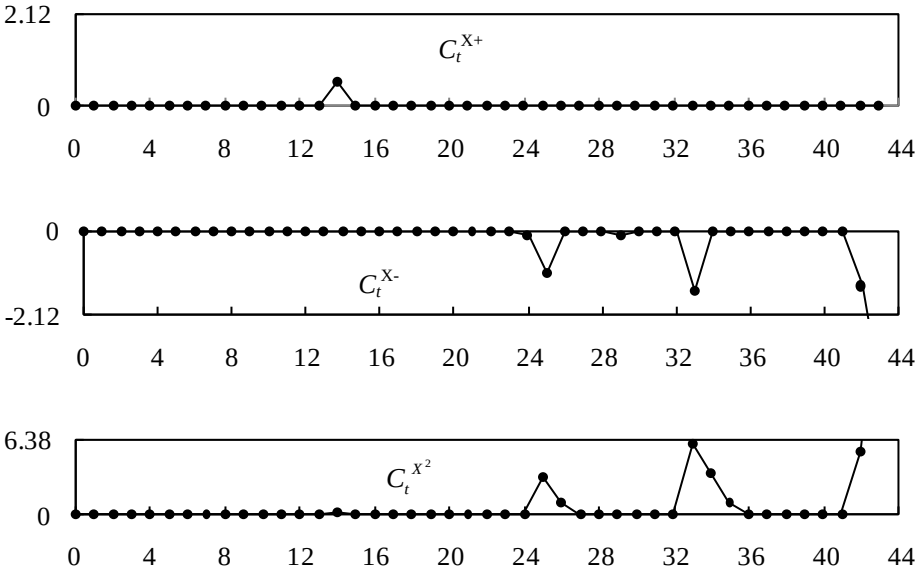

(*c*) optimal 3-CUSUM(μ+σ) Scheme

Figure 4-6 Illustration of Three Control Charts Using Real Data

It is observed that the *X* chart signals the out-of-control process status at point 33. The variability of these data becomes larger from point 24. The ABS CUSUM chart has not issued an out-of-control signal in this showcase. However, the 34th point is very close to the control limit. The optimal 3-CUSUM(μ+σ) scheme signals at point 44, indicating a decreasing mean shift together with a variance shift.

This illustration also shows that the *X* chart is more convenient to operate and understand. It is not inferior much to the other charts in detection effectiveness, and

sometime it may be even superior to others, just as shown in Figure 4-6. However, it should be noted that the *ARATS* and *AEQL* measures are more reliable indicators of the chart performance from an overall viewpoint.

4.6.6 Summary Comments

This section studies the effect of sampling cost on the overall performance of the $\overline{X}$ chart, ABS CUSUM chart, and optimal 3-CUSUM(μ+σ) scheme for monitoring process mean and variance. Both the variable component *c* and fixed component *b* have been taken into consideration. Since the fixed sampling cost is an indispensable component of the total sampling inspection cost for most of the SPC applications, this study is important and useful. The proposed approach is viable and feasible as the ratio *B* between *b* and *c* can be determined easily and accurately. The results bring about several interesting findings.

Firstly, it is found that the fixed sampling cost *b* essentially influences the performance of the control charts. Since the fixed sampling cost often exists, neglecting it discriminately may result in improper designs. When there is no fixed sampling cost or $b = 0$, the optimal 3-CUSUM(μ+σ) scheme always has the smallest *AEQL*. However, as *b* increases, the superiority of the optimal 3-CUSUM(μ+σ) scheme is deteriorated. When *b* is sufficiently large, the $\overline{X}$ chart and ABS CUSUM chart may even outperform the optimal 3-CUSUM(μ+σ) scheme. The performance of the control charts is also affected by the shift domain. When shift domain is large, there is almost no difference in performance among the charts.

The $\overline{X}$ chart is very simple for understanding, implementation and design and shows no-inferiority in detection effectiveness to other charts from holistic viewpoint. It makes the simultaneous monitoring of process mean and variance become a very simple procedure. This chart may be suitable for many SPC applications in which both the mean and variance of a variable need be monitored. The optimal 3-CUSUM(μ+σ) scheme may be considered only when process shift is small and fixed sampling cost is low.

It is also found that the optimal values of the sample sizes $n_{\overline{X}}$ and n_{CUSUM} are not four

and one, respectively, even if the fixed sampling cost *b* is zero. The optimal sample size for an application can be identified from Table 4-9 or determined by an optimal design.

The findings obtained in this study and in section 3.5 may be somewhat different from those presented in some previous studies for economic charts. While this study aims at the best statistical performance with a consideration of the sampling cost, the economic designs seek the lowest average SPC cost and have to handle a large number of cost factors some of which (e.g., cost of a false alarm) are very difficult to determine. Almost all economic models consider only one, or at most a few, process shifts and do not evaluate the chart performance over the entire mean shift domain. In fact, different economic designs use various features and assumptions and may result in opposite conclusions. For example, while some concluded that the CUSUM chart is significantly more economical than the Shewhart chart (Keats and Simpson, 1994), others found that the economic advantage of the CUSUM chart is usually not substantial (Nenes and Tagaras 2008). It seems that the conclusions from an economic design are usually valid only for a relatively specific model. Contrarily, the optimization model proposed in this study can be used in all statistical designs for the $\bar{X}$, ABS CUSUM and optimal 3-CUSUM(μ+σ) charts, and the results can be applied to general SPC applications with or without the fixed sampling cost *b*. Moreover, both the variable and fixed sampling costs dealt with by this optimization model can be estimated easily and accurately.

4.7 Effect of Process Shift Distributions on Chart Design and Performance

This study examines the influence of process shift distributions on the optimal designs and overall performance assessment of the *X*, ABS CUSUM and optimal 3-CUSUM($\mu+\sigma$) charts. The results have revealed that the overall performance of the ABS CUSUM and optimal 3-CUSUM($\mu+\sigma$) charts is practically identical no matter the charts are designed with the uniform assumption or based on the real probability distributions of process shifts, and no matter what the real distributions are. The *X* chart is also nearly equally effective when process shift domain is large. As a general guideline, when designing an optimal chart, the designers can simply assume the uniform distributions for process shifts and may not have to make effort to estimate these distributions. In this section, the fixed sampling cost *b* is assumed to be zero.

4.7.1 Introduction

In section 4.6.3, it is found that, under the uniform distribution assumption for process shifts (*uniform assumption* for short), the optimal 3-CUSUM($\mu+\sigma$) scheme and ABS CUSUM chart have almost the same *AEQL* value. Or in other words, the overall detection effectiveness of these two charts is nearly equal. Furthermore, even the simplest *X* chart produces an *AEQL* value close to that of these two CUSUM schemes, unless the shift domain is quite small. This finding is called the *performance equality property*. A SPC user may consider to adopt the simple ABS CUSUM chart (or even the simplest *X* chart) as its detection effectiveness is almost the same as that of the complicated 3-CUSUM($\mu+\sigma$) scheme.

However, there are two mistrusts or obstacles to the replacement of the optimal 3-CUSUM($\mu+\sigma$) scheme by the simpler ABS CUSUM or *X* charts. Firstly, it is unclear whether the performance equality property is still true if the real probability distributions of δ_μ and δ_σ are non-uniform (the usual cases). Secondly, if the real probability distributions of δ_μ and δ_σ can be determined or estimated, whether a chart designed based on the real distributions will significantly outperform the counterpart designed based on the uniform assumption.

This section studies the influence of the probability distributions of δ_μ and δ_σ on the optimal designs of three control charts (*X* chart, ABS CUSUM chart and optimal

3-CUSUM(μ+σ) scheme) and on the relative performance of these charts. It has been found that, no matter the charts are designed based on the uniform assumption or the real probability distributions and no matter what the real distributions are, the performance equality property almost always holds. Or in other words, the overall *ATS* performance of the charts is always very close. Moreover, it has been observed that, a control chart designed based on the real distributions is only slightly more effective than the counterpart chart designed based on the uniform assumption. These findings are useful to the SPC practitioners. They no longer need to worry about or spend effort to estimate the real probability distributions of δ_μ and δ_σ. Instead they can conduct the optimal design of the control chart by simply using the uniform distribution. Moreover, they are reassured that the ABS CUSUM chart (even the *X* chart for large shift domains) is nearly as effective as the optimal 3-CUSUM(μ+σ) scheme from an overall viewpoint for any probability distributions of δ_μ and δ_σ. They can select the ABS CUSUM chart or *X* chart for their SPC applications and enjoy the simplicity of these charts in understanding, design and implementation, without worrying any discernable loss in detection effectiveness.

4.7.2 Optimal design of Control Charts

As in the previous sections, the following optimization model will be used to design the three charts: *X* chart, ABS CUSUM chart and optimal 3-CUSUM(μ+σ) chart.

Objective function:	*AEQL* = minimum.	
Constraint function:	$ATS_0 = \tau$.	(4-26)
Design variables:	charting parameters, *i.e.*, *UCL*, *H*, *k*, H_{CX}, k^X, k^{X^2}	

It is noted that in the previous sections, when calculating the performance measure *AEQL* (Equation(4-2)) and *ARATS* (Equation(4-1)), it is always assumed that process shifts (δ_μ, δ_σ) follow uniform distribution. In this section, δ_μ and δ_σ may follow non-uniform distributions, but they are independent of each other, therefore the joint density function is equal to $f_\mu(\delta_\mu)f_\sigma(\delta_\sigma)$. Consequently, *ARATS* and *AEQL* can be expressed as follows:

$$ARATS = \int_0^{\delta_{\mu,\max}} \int_1^{\delta_{\sigma,\max}} \frac{ATS(\delta_\mu,\delta_\sigma)}{ATS_{\text{benchmark}}(\delta_\mu,\delta_\sigma)} f_\mu(\delta_\mu) f_\sigma(\delta_\sigma) d\delta_\mu d\delta_\sigma , \quad (4\text{-}27)$$

$$AEQL = \int_{0}^{\delta_{\mu,\max}} \int_{1}^{\delta_{\sigma,\max}} (\delta_\mu^2 + \delta_\sigma^2 - 1) ATS(\delta_\mu, \delta_\sigma) f_\mu(\delta_\mu) f_\sigma(\delta_\sigma) d\delta_\mu d\delta_\sigma \,, \tag{4-28}$$

If uniform distribution is assumed,

$$f_\mu(\delta_\mu) = \frac{1}{\delta_{\mu,\max}}, \qquad f_\sigma(\delta_\sigma) = \frac{1}{\delta_{\sigma,\max} - 1}. \tag{4-29}$$

To design the control charts, the specifications are determined below:

(1) The minimum allowable value τ of the in-control ATS_0 is set as 370.

(2) The maximum shifts $\delta_{\mu,\max}$ and $\delta_{\sigma,\max}$ are the same as those used in sections 4.4.2 and 4.6.3: a small shift domain of ($\delta_{\mu,\max} = 3$, $\delta_{\sigma,\max} = 4$), a middle one of ($\delta_{\mu,\max} = 5$, $\delta_{\sigma,\max} = 6$), and a large one of ($\delta_{\mu,\max} = 8$, $\delta_{\sigma,\max} = 9$).

(3) Probability distributions of δ_μ and δ_σ

In real SPC applications, the probability distributions of δ_μ and δ_σ are likely to be non-uniform. In this section, the following beta distributions will be used to represent different types of non-uniform marginal probability distributions of δ_μ and δ_σ.

$$\begin{aligned} f_{\delta_\mu}(\delta_\mu) &= \frac{\Gamma(a_\mu + b_\mu)}{\Gamma(a_\mu)\Gamma(b_\mu)} \cdot \frac{\delta_\mu^{a_\mu - 1} \cdot (\delta_{\mu,\max} - \delta_\mu)^{b_\mu - 1}}{(\delta_{\mu,\max})^{a_\mu + b_\mu - 1}}, \\ f_{\delta_\sigma}(\delta_\sigma) &= \frac{\Gamma(a_\sigma + b_\sigma)}{\Gamma(a_\sigma)\Gamma(b_\sigma)} \cdot \frac{(\delta_\sigma - 1)^{a_\sigma - 1} \cdot (\delta_{\sigma,\max} - \delta_\sigma)^{b_\sigma - 1}}{(\delta_{\sigma,\max} - 1)^{a_\sigma + b_\sigma - 1}}. \end{aligned} \tag{4-30}$$

The curves of these two marginal probability functions for ($\delta_{\mu,\max} = 5$, $\delta_{\sigma,\max} = 6$) are illustrated in Figure 4-7:

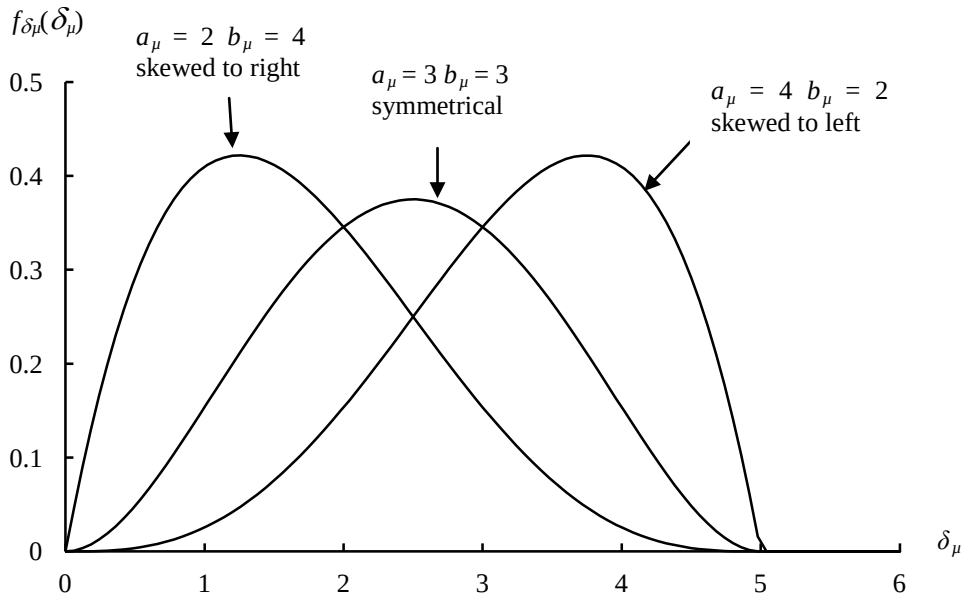

(*a*) $f_{\delta\mu}(\delta_\mu)$

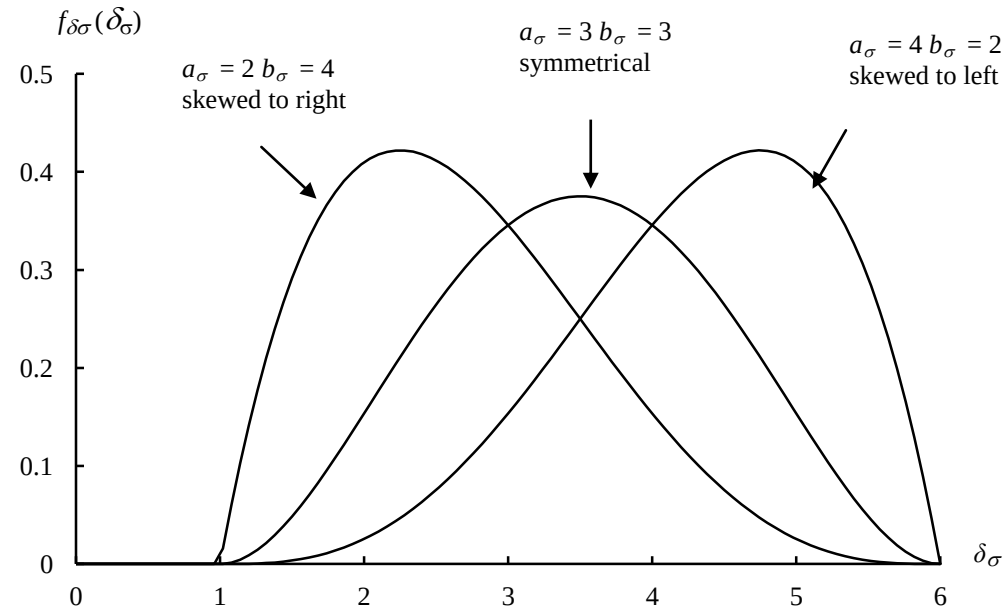

(*b*) $f_{\delta\sigma}(\delta_\sigma)$

Figure 4-7. Marginal Probability Functions $f_{\delta\mu}(\delta_\mu)$ and $f_{\delta\sigma}(\delta_\sigma)$

The skewness of a beta distribution is determined by the parameters a and b (a_μ and b_μ for δ_μ, and a_σ and b_σ for δ_σ). If ($a < b$), δ_μ (or δ_σ) has a probability distribution skewed to right. This represents the situations where most of the shifts cluster to the lower end within the shift domain. If ($a > b$), δ_μ (or δ_σ) has a probability distribution skewed to left. This arises when most of the shifts cluster to the upper end, or when all

small shifts have been truncated to avoid over-correction that may introduce extra variability into the process (Woodall 1985). Finally, if ($a = b$), δ_μ (or δ_σ) has a symmetrical probability distribution. In this section, nine different cases, or different combinations of the values of a_μ, b_μ, a_σ, and b_σ, for the marginal probability distributions of δ_μ and δ_σ will be studied. Table 4-11 lists these nine cases together with the uniform distribution case.

Table 4-11. Marginal Probability Distributions $f_{\delta\mu}(\delta_\mu)$ and $f_{\delta\sigma}(\delta_\sigma)$

No.	$f_{\delta\mu}(\delta_\mu)$			$f_{\delta\sigma}(\delta_\sigma)$		
	a_μ	b_μ		a_σ	b_σ	
1	2	4	Skew to right	2	4	Skew to right
2	2	4	Skew to right	3	3	Symmetrical
3	2	4	Skew to right	4	2	Skew to left
4	3	3	Symmetrical	2	4	Skew to right
5	3	3	Symmetrical	3	3	Symmetrical
6	3	3	Symmetrical	4	2	Skew to left
7	4	2	Skew to left	2	4	Skew to right
8	4	2	Skew to left	3	3	Symmetrical
9	4	2	Skew to left	4	2	Skew to left
10	uniform			uniform		

4.7.3 Comparison when Charts are Designed Based on Uniform Assumption

As aforementioned in section 3.1.3, it is very difficult to estimate the probability distributions of δ_μ and δ_σ in practice. Most likely, the optimal designs of the control charts have to be carried out by using the uniform assumption. Namely, the objective function *AEQL* in Equation (4-26) will be determined by Equations (4-28) and (4-29). This section will study the performance of control charts that are designed based on the uniform assumption, but applied to different non-uniform distribution of δ_μ and δ_σ.

If the process shifts δ_μ and δ_σ actually follow the uniform distribution, the performance equality property holds as found in the performance comparison in section 4.4 and section 4.6. That is, the overall performance of the ABS CUSUM chart (or even the *X* chart when process shift is large) is almost identical to that of the optimal 3-CUSUM(μ+σ) scheme when measured by both *ARATS* and *AEQL*. The problem is that, if the real probability distributions of (δ_μ, δ_σ) are non-uniform, whether the control charts designed under the uniform assumption still uphold performance equality property?

We first consider a general case in which $\delta_{\mu,\max} = 5$ and $\delta_{\sigma,\max} = 6$. The *X* chart, ABS CUSUM chart and optimal 3-CUSUM(μ+σ) scheme are designed (the latter two

charts are resulted from the optimal designs based on uniform assumption) and the charting parameters are enumerated below:

X chart:	LCL = -2.9997, UCL = 2.9997.
ABS CUSUM:	k = 1.7000, H = 1.4141.
Optimal 3-CUSUM(μ+σ):	k^X = 1.5500, k^{X^2} = 3.0005, H_{CX} = 1.5845, H_{CX}^2 = 6.7210.

If the true distributions of process shifts are uniform, the *ATS* values of the three charts are listed in Table 4-5. Now, suppose the true distribution of process shift are non-uniform, *i.e.*, parameters for Equation (4-30) are a_μ = 2, b_μ = 4, a_σ = 4, b_σ= 2 (δ_μ is skew to right and δ_σ is skew to left), the *ATS* values of the three control charts over the process shift domain are showed in Table 4-12. From this Table, it can be observed that the optimal 3-CUSUM(μ+σ) scheme produces considerably smaller *ATS* values than the ABS CUSUM chart and *X* chart in a small region where both δ_μ and δ_σ are minor (in the top-left corner). However, beyond this small region, there are only insignificant differences in *ATS* values among the three charts in each cell. Specifically, $ATS_{\text{ABS CUSUM}}$ is very close to $ATS_{\text{3-CUSUM}(\mu+\sigma)}$ in most of the cells.

Another table of *ATS* values when the true process shift follows another non-uniform distributions, *i.e.*, ($\delta_{\mu,\max}$ = 8, $\delta_{\sigma,\max}$ = 9, a_μ = 4, b_μ = 2, a_σ = 2, b_σ= 4), is also worked out similarly (Table 4-13). It is found that, at each out-of-control cell, the differences among the *ATS* values produced by the three charts are again quite smaller. From these tables, it can be concluded that for most of the cases, the differences in *ATS* values of charts (especially the differences between the $ATS_{\text{ABS CUSUM}}$ and $ATS_{\text{3-CUSUM}(\mu+\sigma)}$) are insignificant.

Table 4-12. *ATS* Values of Three Control Charts

($\delta_{\mu,\max} = 5$, $\delta_{\sigma,\max} = 6$, $a_\mu = 2$, $b_\mu = 4$, $a_\sigma = 4$, $b_\sigma = 2$)

δ_σ	Chart	δ_μ										
		0.0	0.5	1.0	1.5	2.0	2.5	3.0	3.5	4.0	4.5	5.0
1.0	*X*	370	155	43.4	14.5	5.80	2.74	1.50	0.95	0.69	0.57	0.52
	ABS CUSUM	370	138	31.1	9.01	3.69	1.98	1.26	0.89	0.69	0.58	0.53
	3-CUSUM($\mu+\sigma$)	373	122	25.7	7.67	3.30	1.87	1.23	0.88	0.69	0.58	0.53
1.5	*X*	21.5	16.9	10.0	5.75	3.45	2.21	1.50	1.09	0.84	0.69	0.60
	ABS CUSUM	18.1	14.2	8.39	4.81	2.93	1.93	1.37	1.03	0.82	0.69	0.61
	3-CUSUM($\mu+\sigma$)	18.0	13.8	7.97	4.54	2.80	1.85	1.34	1.02	0.82	0.69	0.60
2.0	*X*	6.98	6.36	5.01	3.69	2.68	1.97	1.49	1.17	0.95	0.79	0.69
	ABS CUSUM	6.09	5.58	4.45	3.32	2.45	1.84	1.42	1.13	0.93	0.79	0.69
	3-CUSUM($\mu+\sigma$)	6.05	5.51	4.37	3.25	2.39	1.81	1.40	1.11	0.92	0.79	0.69
2.5	*X*	3.84	3.68	3.25	2.72	2.22	1.80	1.47	1.21	1.02	0.88	0.77
	ABS CUSUM	3.49	3.35	2.99	2.54	2.10	1.72	1.42	1.18	1.01	0.87	0.77
	3-CUSUM($\mu+\sigma$)	3.49	3.32	2.98	2.51	2.06	1.70	1.40	1.17	1.00	0.86	0.77
3.0	*X*	2.65	2.59	2.41	2.16	1.90	1.64	1.41	1.22	1.06	0.93	0.83
	ABS CUSUM	2.48	2.42	2.27	2.05	1.82	1.59	1.38	1.20	1.05	0.93	0.83
	3-CUSUM($\mu+\sigma$)	2.47	2.41	2.27	2.03	1.81	1.58	1.37	1.20	1.05	0.92	0.83
3.5	*X*	2.05	2.02	1.94	1.81	1.65	1.49	1.34	1.20	1.07	0.97	0.87
	ABS CUSUM	1.96	1.93	1.85	1.74	1.60	1.46	1.31	1.18	1.06	0.96	0.87
	3-CUSUM($\mu+\sigma$)	1.95	1.92	1.85	1.74	1.59	1.46	1.31	1.18	1.07	0.96	0.87
4.0	*X*	1.71	1.69	1.64	1.57	1.47	1.37	1.26	1.16	1.07	0.98	0.90
	ABS CUSUM	1.65	1.63	1.59	1.52	1.44	1.34	1.24	1.15	1.06	0.97	0.90
	3-CUSUM($\mu+\sigma$)	1.65	1.63	1.58	1.52	1.44	1.35	1.24	1.14	1.05	0.97	0.90
4.5	*X*	1.48	1.47	1.44	1.39	1.33	1.26	1.19	1.12	1.04	0.97	0.91
	ABS CUSUM	1.44	1.43	1.41	1.36	1.31	1.24	1.18	1.11	1.04	0.97	0.91
	3-CUSUM($\mu+\sigma$)	1.44	1.43	1.40	1.36	1.31	1.24	1.17	1.11	1.03	0.97	0.91
5.0	*X*	1.32	1.32	1.30	1.27	1.23	1.18	1.13	1.07	1.02	0.96	0.91
	ABS CUSUM	1.30	1.29	1.27	1.25	1.21	1.16	1.11	1.06	1.01	0.96	0.91
	3-CUSUM($\mu+\sigma$)	1.30	1.29	1.28	1.25	1.21	1.16	1.11	1.06	1.01	0.95	0.91
5.5	*X*	1.21	1.20	1.19	1.17	1.14	1.11	1.07	1.03	0.98	0.94	0.90
	ABS CUSUM	1.19	1.19	1.18	1.16	1.13	1.10	1.06	1.02	0.98	0.94	0.90
	3-CUSUM($\mu+\sigma$)	1.19	1.19	1.18	1.16	1.12	1.10	1.06	1.02	0.98	0.94	0.90
6.0	*X*	1.12	1.12	1.11	1.09	1.07	1.05	1.02	0.99	0.95	0.92	0.89
	ABS CUSUM	1.11	1.11	1.10	1.08	1.06	1.04	1.01	0.98	0.95	0.92	0.88
	3-CUSUM($\mu+\sigma$)	1.11	1.11	1.10	1.08	1.06	1.04	1.01	0.98	0.95	0.92	0.89

Table 4-13. *ATS* Values of Three Control Charts

($\delta_{\mu,\max} = 8$, $\delta_{\sigma,\max} = 9$, $a_\mu = 4$, $b_\mu = 2$, $a_\sigma = 2$, $b_\sigma = 4$)

δ_σ	Chart	δ_μ										
		0.0	0.8	1.6	2.4	3.2	4.0	4.8	5.6	6.4	7.2	8.0
1.0	X	370	71.0	11.9	3.14	1.23	0.69	0.54	0.50	0.50	0.50	0.50
	ABS CUSUM	369	61.1	8.48	2.36	1.09	0.68	0.54	0.51	0.50	0.50	0.50
	3-CUSUM($\mu+\sigma$)	372	52.9	7.07	2.15	1.07	0.68	0.54	0.51	0.50	0.50	0.50
1.8	X	9.96	7.30	3.97	2.20	1.34	0.91	0.69	0.58	0.53	0.51	0.50
	ABS CUSUM	8.91	6.57	3.61	2.04	1.27	0.89	0.68	0.58	0.53	0.51	0.50
	3-CUSUM($\mu+\sigma$)	8.56	6.34	3.46	1.98	1.26	0.88	0.69	0.58	0.53	0.51	0.50
2.6	X	3.52	3.19	2.50	1.84	1.35	1.03	0.82	0.69	0.61	0.56	0.53
	ABS CUSUM	3.28	2.99	2.37	1.77	1.32	1.01	0.81	0.69	0.61	0.56	0.53
	3-CUSUM($\mu+\sigma$)	3.22	2.93	2.34	1.75	1.31	1.01	0.81	0.69	0.61	0.56	0.53
3.4	X	2.15	2.06	1.83	1.56	1.29	1.07	0.90	0.78	0.68	0.62	0.58
	ABS CUSUM	2.06	1.98	1.77	1.52	1.27	1.06	0.90	0.77	0.68	0.62	0.58
	3-CUSUM($\mu+\sigma$)	2.04	1.96	1.76	1.51	1.27	1.05	0.90	0.78	0.69	0.62	0.58
4.2	X	1.60	1.57	1.48	1.34	1.20	1.06	0.93	0.83	0.74	0.68	0.63
	ABS CUSUM	1.56	1.53	1.44	1.32	1.18	1.05	0.93	0.83	0.74	0.68	0.63
	3-CUSUM($\mu+\sigma$)	1.56	1.53	1.44	1.31	1.18	1.04	0.93	0.83	0.74	0.68	0.63
5.0	X	1.32	1.31	1.26	1.19	1.10	1.02	0.93	0.85	0.78	0.72	0.67
	ABS CUSUM	1.30	1.28	1.24	1.17	1.09	1.01	0.92	0.85	0.78	0.72	0.67
	3-CUSUM($\mu+\sigma$)	1.29	1.29	1.24	1.17	1.09	1.01	0.93	0.84	0.77	0.72	0.67
5.8	X	1.15	1.14	1.12	1.08	1.02	0.97	0.91	0.85	0.79	0.74	0.70
	ABS CUSUM	1.14	1.13	1.10	1.06	1.01	0.96	0.90	0.84	0.79	0.74	0.70
	3-CUSUM($\mu+\sigma$)	1.14	1.13	1.11	1.07	1.01	0.96	0.90	0.85	0.79	0.74	0.70
6.6	X	1.04	1.03	1.02	0.99	0.96	0.92	0.88	0.83	0.79	0.75	0.71
	ABS CUSUM	1.03	1.02	1.01	0.98	0.95	0.91	0.87	0.83	0.79	0.75	0.71
	3-CUSUM($\mu+\sigma$)	1.03	1.03	1.01	0.98	0.95	0.92	0.87	0.83	0.79	0.75	0.71
7.4	X	0.96	0.96	0.94	0.93	0.90	0.88	0.85	0.82	0.78	0.75	0.72
	ABS CUSUM	0.95	0.95	0.94	0.92	0.90	0.87	0.84	0.81	0.78	0.75	0.72
	3-CUSUM($\mu+\sigma$)	0.95	0.95	0.94	0.93	0.90	0.88	0.84	0.81	0.78	0.75	0.72
8.2	X	0.90	0.90	0.89	0.88	0.86	0.84	0.82	0.80	0.77	0.75	0.72
	ABS CUSUM	0.9	0.89	0.89	0.87	0.86	0.84	0.82	0.79	0.77	0.75	0.72
	3-CUSUM($\mu+\sigma$)	0.89	0.90	0.89	0.87	0.86	0.84	0.82	0.79	0.77	0.75	0.72
9.0	X	0.85	0.85	0.85	0.84	0.83	0.81	0.79	0.78	0.76	0.74	0.72
	ABS CUSUM	0.85	0.85	0.84	0.83	0.82	0.81	0.79	0.78	0.76	0.74	0.72
	3-CUSUM($\mu+\sigma$)	0.86	0.85	0.84	0.83	0.83	0.81	0.79	0.77	0.76	0.74	0.72

Table 4-14 displays the *AEQL* values of the three charts within three different shift domains. In this table, under each combination of $\delta_{\mu,\max}$ and $\delta_{\sigma,\max}$, there are ten cells. The top-left cell corresponds to uniformly distributed δ_μ and δ_σ, and other nine cells for the nine beta distributions with different a_μ, b_μ, a_σ, and b_σ (see Table 4-11). Each cell contains the *AEQL* values of the three charts for a particular combination of $\delta_{\mu,\max}$, $\delta_{\sigma,\max}$, a_μ, b_μ, a_σ, and b_σ.

Firstly, it can be seen that the *AEQL* values of the three charts (especially for the ABS CUSUM and optimal 3-CUSUM(μ+σ) charts) are close when the real distributions of δ_μ and δ_σ are uniform. This is the equal performance property under the uniform assumption that is already found in section 4.6.3.

Secondly, if δ_μ and δ_σ have beta distributions, the *AEQL* values produced by all the charts become smaller, in general, when the probability distributions $f_{\delta_\mu}(\delta_\mu)$ and/or $f_{\delta_\sigma}(\delta_\sigma)$ are skewed to right; but the *AEQL* values become larger when $f_{\delta_\mu}(\delta_\mu)$ and/or $f_{\delta_\sigma}(\delta_\sigma)$ are skewed to left. However, the difference in *AEQL* values among the three charts in each cell (for a given set of $\delta_{\mu,\max}$, $\delta_{\sigma,\max}$, $f_{\delta_\mu}(\delta_\mu)$ and $f_{\delta_\sigma}(\delta_\sigma)$) are still insignificant. It is recalled that in this section, the control charts are designed based on the uniform assumption (i.e., the objective function *AEQL* in Equation (4-26) is calculated by using the uniformly distributed $f_{\delta_\mu}(\delta_\mu)$ and $f_{\delta_\sigma}(\delta_\sigma)$ in Equation (4-29)), but the *AEQL* values displayed in Table 4-15 are evaluated based on the real probability distributions (e.g., $f_{\delta_\mu}(\delta_\mu)$ and $f_{\delta_\sigma}(\delta_\sigma)$ are calculated by Equation (4-30) assuming beta distributions). It is because that the control charts (even designed by uniform assumption) must be applied to the real processes with different $f_{\delta_\mu}(\delta_\mu)$ and $f_{\delta_\sigma}(\delta_\sigma)$.

Table 4-14. *AEQL* Values of Three Control Charts

			$f_{\delta\mu}(\delta_\mu)$			
			uniform	$a_\mu = 2$ $b_\mu = 4$	$a_\mu = 3$ $b_\mu = 3$	$a_\mu = 4$ $b_\mu = 2$
			($\delta_{\mu,\max} = 3$, $\delta_{\sigma,\max} = 4$)			
	uniform	X	22.37177			
		ABS CUSUM	20.20126			
		3-CUSUM($\mu+\sigma$)	19.70282			
	$a_\sigma=2$ $b_\sigma=4$	X		21.78046	20.64141	19.60460
		ABS CUSUM		18.42919	17.80019	17.42199
		3-CUSUM($\mu+\sigma$)		17.75753	17.04237	16.72239
	$a_\sigma=3$ $b_\sigma=3$	X		21.20652	21.03675	20.93982
		ABS CUSUM		19.17240	19.35707	19.65988
		3-CUSUM($\mu+\sigma$)		19.03985	19.10062	19.30175
	$a_\sigma=4$ $b_\sigma=2$	X		22.20409	22.54754	22.97988
		ABS CUSUM		20.90852	21.47531	22.16431
		3-CUSUM($\mu+\sigma$)		20.92008	21.38315	22.02787
			($\delta_{\mu,\max} = 5$, $\delta_{\sigma,\max} = 6$)			
	uniform	X	27.97964			
		ABS CUSUM	27.04431			
		3-CUSUM($\mu+\sigma$)	26.86624			
	$a_\sigma=2$ $b_\sigma=4$	X		22.31592	22.28102	22.64970
		ABS CUSUM		20.77276	21.17803	21.99776
$f_{\delta\sigma}(\delta_\sigma)$		3-CUSUM($\mu+\sigma$)		20.49239	20.93922	21.82982
	$a_\sigma=3$ $b_\sigma=3$	X		25.57803	26.68448	28.08589
		ABS CUSUM		24.60604	25.94886	27.59944
		3-CUSUM($\mu+\sigma$)		24.50205	25.85759	27.50683
	$a_\sigma=4$ $b_\sigma=2$	X		30.08653	31.78089	33.84062
		ABS CUSUM		29.41026	31.23868	33.45107
		3-CUSUM($\mu+\sigma$)		29.38570	31.21597	33.38323
			($\delta_{\mu,\max} = 8$, $\delta_{\sigma,\max} = 9$)			
	uniform	X	44.22233			
		ABS CUSUM	43.79724			
		3-CUSUM($\mu+\sigma$)	43.72603			
	$a_\sigma=2$ $b_\sigma=4$	X		28.85897	31.49116	35.29282
		ABS CUSUM		28.16452	31.07509	35.09923
		3-CUSUM($\mu+\sigma$)		28.02136	30.98958	35.07613
	$a_\sigma=3$ $b_\sigma=3$	X		37.85408	41.79236	46.71207
		ABS CUSUM		37.36327	41.44769	46.50838
		3-CUSUM($\mu+\sigma$)		37.29607	41.46203	46.53285
	$a_\sigma=4$ $b_\sigma=2$	X		48.35478	53.05411	58.88116
		ABS CUSUM		47.97691	52.75839	58.67763
		3-CUSUM($\mu+\sigma$)		47.95179	52.74498	58.72228

Table 4-15 displays the ratios of $AEQL_X/AEQL_{3\text{-CUSUM}(\mu+\sigma)}$ and $AEQL_{\text{ABS CUSUM}}/AEQL_{3\text{-CUSUM}(\mu+\sigma)}$ in each cell as in Table 4-13. The ratios of $AEQL_{\text{ABS CUSUM}}/AEQL_{3\text{-CUSUM}(\mu+\sigma)}$ reveal that $AEQL_{\text{ABS CUSUM}}$ is larger than $AEQL_{3\text{-CUSUM}(\mu+\sigma)}$ in some cases but smaller than the latter in other cases. Anyway, $AEQL_{\text{ABS CUSUM}}$ and $AEQL_{3\text{-CUSUM}(\mu+\sigma)}$ are always close to each other, especially when $\delta_{\mu,\max} \geq 5$ and $\delta_{\sigma,\max} \geq 6$. This fact strongly suggests that the performance equality property is valid even if the real probability distributions of δ_μ and δ_σ is non-uniform, and there is almost no difference in overall performance between the ABS CUSUM and the optimal 3-CUSUM($\mu+\sigma$) charts. On the other hand, the ratios of $AEQL_X/AEQL_{3\text{-CUSUM}(\mu+\sigma)}$ indicates that, in a small shift domain (e.g., $\delta_{\mu,\max} = 3$, $\delta_{\sigma,\max} = 4$), $AEQL_X$ may exceed $AEQL_{3\text{-CUSUM}(\mu+\sigma)}$ by more than 10%, especially when the probability distributions $f_{\delta_\mu}(\delta_\mu)$ and/or $f_{\delta_\sigma}(\delta_\sigma)$ are skewed to right. However, when the shift domain expands to ($\delta_{\mu,\max} = 5$, $\delta_{\sigma,\max} = 6$) and then ($\delta_{\mu,\max} = 8$, $\delta_{\sigma,\max} = 9$), this difference diminishes to about 5% and 1%, respectively. This means that, as long as the shift domain is moderately large, the performance equality property is also approximately true for the *X* chart even when the actual probability distributions of δ_μ and δ_σ are different from a uniform one.

Table 4-15. Ratios of $AEQL_x/AEQL_{3\text{-CUSUM}(\mu+\sigma)}$ and $AEQL_{\text{ABS CUSUM}}/AEQL_{3\text{-CUSUM}(\mu+\sigma)}$

			$f_{\delta\mu}(\delta_\mu)$			
			uniform	$a_\mu = 2\ b_\mu = 4$	$a_\mu = 3\ b_\mu = 3$	$a_\mu = 4\ b_\mu = 2$
			($\delta_{\mu\max} = 3$, $\delta_{\sigma,\max} = 4$)			
	uniform	X	1.13546			
		ABS CUSUM	1.02530			
	$a_\sigma=2\ b_\sigma=4$	X		1.22655	1.21118	1.17236
		ABS CUSUM		1.03782	1.04447	1.04184
	$a_\sigma=3\ b_\sigma=3$	X		1.11380	1.10136	1.08487
		ABS CUSUM		1.00696	1.01343	1.01855
	$a_\sigma=4\ b_\sigma=2$	X		1.06138	1.05445	1.04322
		ABS CUSUM		0.99945	1.00431	1.00619
			($\delta_{\mu,\max} = 5$, $\delta_{\sigma,\max} = 6$)			
	uniform	X	1.04144			
		ABS CUSUM	1.00663			
	$a_\sigma=2\ b_\sigma=4$	X		1.08899	1.06408	1.03756
$f_{\delta\sigma}(\delta_\sigma)$		ABS CUSUM		1.01368	1.01140	1.00769
	$a_\sigma=3\ b_\sigma=3$	X		1.04391	1.03198	1.02105
		ABS CUSUM		1.00424	1.00353	1.00337
	$a_\sigma=4\ b_\sigma=2$	X		1.02385	1.01810	1.01370
		ABS CUSUM		1.00084	1.00073	1.00203
			($\delta_{\mu,\max} = 8$, $\delta_{\sigma\max} = 9$)			
	uniform	X	1.01135			
		ABS CUSUM	1.00163			
	$a_\sigma=2\ b_\sigma=4$	X		1.02989	1.01619	1.00618
		ABS CUSUM		1.00511	1.00276	1.00066
	$a_\sigma=3\ b_\sigma=3$	X		1.01496	1.00797	1.00385
		ABS CUSUM		1.00180	0.99965	0.99947
	$a_\sigma=4\ b_\sigma=2$	X		1.00840	1.00586	1.00271
		ABS CUSUM		1.00052	1.00025	0.99924

Table 4-16 shows the *ARATS* values (Equation (4-27)) of the charts in different cells, using the optimal 3-CUSUM($\mu+\sigma$) schemes as the benchmark. Interestingly enough, the *ARATS* values in Table 4-16 often match closely with the corresponding *AEQL* ratios in Table 4-15. This means that similar conclusions regarding the performance equality property can be reached based on both indices *AEQL* and *ARATS*. Since the information carried by *AEQL* and *ARATS* is almost the same, only the *AEQL* values of the control charts will be discussed in the remaining of this section.

Table 4-16. Values of *ARATS* of *X* and ABS CUSUM Charts
(Using optimal 3-CUSUM($\mu+\sigma$) scheme as benchmark)

			$f_{\delta\mu}(\delta_\mu)$			
			uniform	$a_\mu = 2\ b_\mu = 4$	$a_\mu = 3\ b_\mu = 3$	$a_\mu = 4\ b_\mu = 2$
			($\delta_{\mu,\max} = 3$, $\delta_{\sigma,\max} = 4$)			
	uniform	*X*	1.16316			
		ABS CUSUM	1.03284			
	a_σ=2 b_σ=4	*X*		1.23737	1.23109	1.19250
		ABS CUSUM		1.04034	1.05134	1.04772
	a_σ=3 b_σ=3	*X*		1.12129	1.11478	1.09382
		ABS CUSUM		1.01056	1.01725	1.01933
	a_σ=4 b_σ=2	*X*		1.06775	1.05837	1.04860
		ABS CUSUM		0.99878	1.00472	1.00609
			($\delta_{\mu,\max} = 5$, $\delta_{\sigma\,\max} = 6$)			
	uniform	*X*	1.05600			
		ABS CUSUM	1.00885			
	a_σ=2 b_σ=4	*X*		1.09770	1.07352	1.04468
$f_{\delta\sigma}(\delta_\sigma)$		ABS CUSUM		1.01567	1.01283	1.00873
	a_σ=3 b_σ=3	*X*		1.04981	1.03905	1.02537
		ABS CUSUM		1.00379	1.00428	1.00507
	a_σ=4 b_σ=2	*X*		1.02808	1.02149	1.01503
		ABS CUSUM		1.00170	1.00175	1.00165
			($\delta_{\mu,\max} = 8$, $\delta_{\sigma,\max} = 9$)			
	uniform	*X*	1.02150			
		ABS CUSUM	1.00376			
	a_σ=2 b_σ=4	*X*		1.03884	1.02134	1.00817
		ABS CUSUM		1.00814	1.00380	1.00038
	a_σ=3 b_σ=3	*X*		1.01942	1.01244	1.00569
		ABS CUSUM		1.00314	1.00158	0.99961
	a_σ=4 b_σ=2	*X*		1.00942	1.00632	1.00202
		ABS CUSUM		0.99948	0.99972	0.99879

To sum up, this section reveals that the control charts designed based on uniform assumption can uphold the performance equality property regardless of the real probability distributions of the process shifts δ_μ and δ_σ. The main reason is that the *ATS* values produced by these charts are nearly the same for different δ_μ and δ_σ (see Table 4-4 to 4-6, 4-12 and 4-13). For example, referring to Equation (4-28),

$$\begin{aligned} & AEQL_{\text{ABS CUSUM}} - AEQL_{\text{3-CUSUM}(\mu+\sigma)} \\ &= \int_0^{\delta_{\mu,\max}} \int_1^{\delta_{\sigma,\max}} (\delta_\mu^2 + \delta_\sigma^2 - 1)\left[ATS_{\text{ABS CUSUM}}(\delta_\mu, \delta_\sigma) - ATS_{\text{3-CUSUM}(\mu+\sigma)}(\delta_\mu, \delta_\sigma) \right] f(\delta_\mu, \delta_\sigma) d\delta_\mu d\delta_\sigma \\ &\approx \int_0^{\delta_{\mu,\max}} \int_1^{\delta_{\sigma,\max}} (\delta_\mu^2 + \delta_\sigma^2 - 1) \cdot (0) \cdot f(\delta_\mu, \delta_\sigma) d\delta_\mu d\delta_\sigma = 0. \end{aligned} \tag{4-31}$$

This means that $AEQL_{\text{ABS CUSUM}}$ is always approximately equal to $AEQL_{\text{3-CUSUM}(\mu+\sigma)}$ regardless of the probability density function $f(\delta_\mu, \delta_\sigma)$. Or in other words, the performance equality property is always true under any probability distributions of δ_μ and δ_σ.

4.7.4 Comparison when Charts are Designed Based on Real Probability Distribution of δ_μ and δ_σ

In this section, it is assumed that the actual or real distributions $f_{\delta_\mu}(\delta_\mu)$ and $f_{\delta_\sigma}(\delta_\sigma)$ of process shifts δ_μ and δ_σ are known or can be estimated by some approaches. If the control charts are designed based on the real probability distributions, whether their overall performance will be much better than the counterpart charts that are designed based on the uniform assumption? And whether the performance equality property is still true between the ABS CUSUM and optimal 3-CUSUM($\mu+\sigma$) charts? It is noted that the design of an *X* chart only indicate the determination of the control charts based on the specified τ, and is therefore indifferent to the probability distributions of δ_μ and δ_σ.

We first consider a general case in which $\delta_{\mu,\max} = 5$, $\delta_{\sigma,\max} = 6$, and δ_μ and δ_σ follow the beta distributions characterized by $a_\mu = 2$, $b_\mu = 4$, $a_\sigma = 4$, $b_\sigma = 2$ (i.e., the probability distribution of δ_μ is skewed to right and that of δ_σ is skewed to left). Firstly, both ABS CUSUM and optimal 3-CUSUM($\mu+\sigma$) charts are designed using the

uniform assumption (i.e., using Equation (4-29) to calculate the objective function (Equation (4-26)) during the optimal design). A subscript [*U*] is used to identify the charts that are designed with uniform assumption and their charting parameters.

ABS CUSUM$_{[U]}$: $k_{[U]} = 1.7000$, $H_{[U]} = 1.4141$.

Optimal 3-CUSUM(μ+σ) $_{[U]}$: $k^{X}_{[U]} = 1.5500$, $k^{X^2}_{[U]} = 3.0005$,

$H_{CX[U]} = 1.5845$, $H_{CX}{}^{2}{}_{[U]} = 6.7210$.

The corresponding *AEQL* values of the two charts are very close as below:

$AEQL_{\text{ABS CUSUM}[U]\_[R]} = 29.4103$

$AEQL_{\text{3-CUSUM}(\mu+\sigma)[U]\_[R]} = 29.3857$

The subscript [*U*]_[*R*] attached to the above *AEQL* means that the chart is designed with the uniform assumption but the *AEQL* is evaluated under the real distributions (for this case, the beta distributions with $a_\mu = 2$, $b_\mu = 4$, $a_\sigma = 4$, $b_\sigma = 2$).

Next, both the ABS CUSUM and optimal 3-CUSUM(μ+σ) charts are re-designed using the real probability distributions of δ_μ and δ_σ (i.e., using Equation (4-30) with $a_\mu = 2$, $b_\mu = 4$, $a_\sigma = 4$ and $b_\sigma = 2$ to calculate the objective function (Equation(4-26)). The charting parameters are listed below:

ABS CUSUM$_{[R]}$: $k_{[R]} = 1.7500$, $H_{[R]} = 1.3441$.

Optimal 3-CUSUM(μ+σ) $_{[R]}$: $k^{X}_{[R]} = 1.7500$, $k^{X^2}_{[R]} = 3.1644$,

$H_{CX[R]} = 1.3225$, $H_{CX}{}^{2}{}_{[R]} = 6.3932$.

The subscript [*R*] means that the chart is designed based on the real probability distributions. The corresponding *AEQL* values (with a subscript [*R*]_[*R*] meaning that both the design of the chart and the evaluation of *AEQL* are based on the real distributions) are shown below:

$AEQL_{\text{ABS CUSUM}[R]\_[R]} = 29.3983$

$AEQL_{\text{3-CUSUM}(\mu+\sigma)[R]\_[R]} = 29.3179$

It can be observed that $AEQL_{\text{ABS CUSUM}[R]\_[R]}$ is smaller than $AEQL_{\text{ABS CUSUM}[U]\_[R]}$ by only 0.041% and $AEQL_{\text{3-CUSUM}(\mu+\sigma)[R]\_[R]}$ is smaller than $AEQL_{\text{3-CUSUM}(\mu+\sigma)[U]\_[R]}$ by only 0.231%. This means that the ABS CUSUM chart design based on the real probability distributions can achieve little improvement compared with the ABS CUSUM chart

designed with uniform assumption when both charts are applied to a same process. Similar conclusion can be made for the optimal 3-CUSUM(μ+σ) chart.

Figure 4-8 displays the curve of $AEQL_{[U]\_[U]}$ versus $k_{[U]}$ and the curve of $AEQL_{[R]\_[R]}$ versus $k_{[R]}$ for the ABS CUSUM chart in this case. For each given k ($k_{[U]}$ or $k_{[R]}$) value, the control limit H will be adjusted to ensure $ATS_0 = \tau$. If the ABS CUSUM chart is designed with the uniform assumption, the optimal solution of ($k_{[U]}$ = 1.70, point *C*) can be found from the bottom curve of $AEQL_{[U]\_[U]}$ versus $k_{[U]}$. On the other hand, if the chart is designed based on the real probability distributions, the optimal solution of ($k_{[R]}$ = 1.75, point *B*) can be identified from the top curve of $AEQL_{[R]\_[R]}$ versus $k_{[R]}$. Then, the ordinate of point *A* indicates the *AEQL* value if the ABS CUSUM chart is designed with the uniform assumption and applied to the real process, and the ordinate of point *B* indicates the *AEQL* value if the chart is designed based on the real probability distributions. It is observed that the top curve of $AEQL_{[R]\_[R]}$ versus $k_{[R]}$ is quite flat in a wide range around the optimal point *B*. Consequently, the difference between the two *AEQL* values (the ordinates of the two points *A* and *B*) is very small. This explains why the ABS CUSUM chart designed with uniform assumption produces almost same *AEQL* value as its counterpart chart designed based on the real probability distributions.

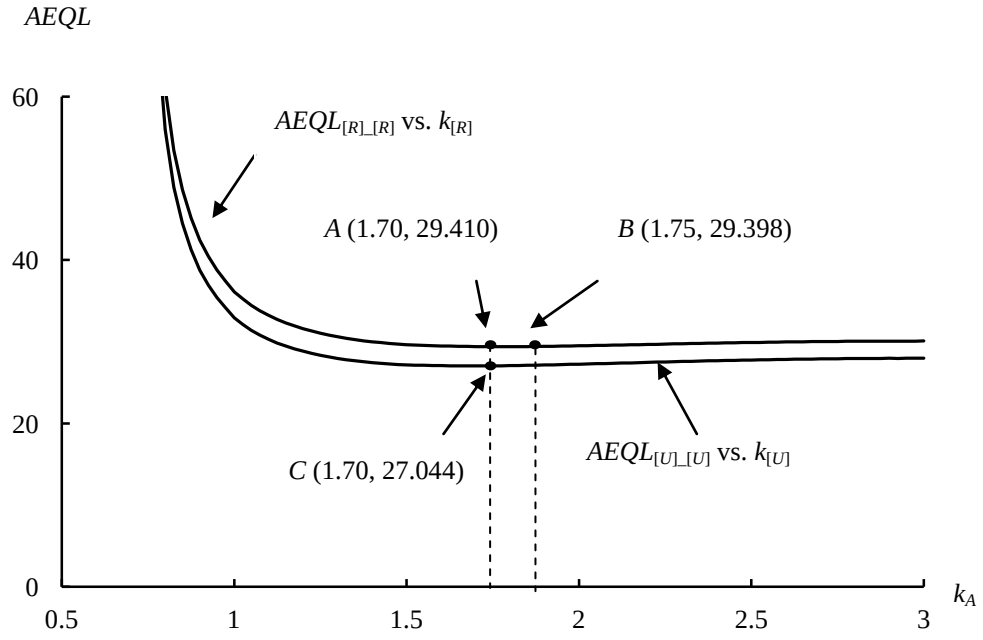

Figure 4-8. *AEQL* vs. *k* for ABS CUSUM Chart

Figure 4-8 also highlights the importance of the optimal design of the control charts. If k is set around or smaller than one (as commonly recommended), the resultant *AEQL* will be increased drastically. Table 4-17 displays the ratio of $AEQL_{[R]\_[R]}/AEQL_{[U]\_[R]}$ of the ABS CUSUM chart (i.e., the ratio of the *AEQL* values of two ABS CUSUM charts, one of which is designed by using the real probability distributions and another based on uniform assumption) for all the cases studied in the last section. It can be seen that, this ratio is always no larger than but very close to one. This reveals that the optimal design based on real probability distributions can improve the overall performance of the ABS CUSUM chart, but only to an insignificant degree.

Table 4-17. Ratios of $AEQL_{[R]\_[R]}$ / $AEQL_{[U]\_[R]}$ of ABS CUSUM Chart

		$f_{\delta\mu}(\delta_\mu)$		
		$a_\mu = 2\ b_\mu = 4$	$a_\mu = 3\ b_\mu = 3$	$a_\mu = 4\ b_\mu = 2$
$f_{\delta\sigma}(\delta_\sigma)$		($\delta_{\mu,\max} = 3$, $\delta_{\sigma,\max} = 4$)		
	$a_\sigma=2\ b_\sigma=4$	0.99291	0.99908	0.99941
	$a_\sigma=3\ b_\sigma=3$	1.00000	0.99850	0.99527
	$a_\sigma=4\ b_\sigma=2$	0.99613	0.99409	0.99103
		($\delta_{\mu,\max} = 5$, $\delta_{\sigma,\max} = 6$)		
	$a_\sigma=2\ b_\sigma=4$	0.99492	0.99943	0.99951
	$a_\sigma=3\ b_\sigma=3$	0.99986	0.99981	0.99876
	$a_\sigma=4\ b_\sigma=2$	0.99959	0.99898	0.99811
		($\delta_{\mu,\max} = 8$, $\delta_{\sigma,\max} = 9$)		
	$a_\sigma=2\ b_\sigma=4$	0.99816	0.99995	0.99988
	$a_\sigma=3\ b_\sigma=3$	0.99991	1.00000	0.99978
	$a_\sigma=4\ b_\sigma=2$	1.00000	0.99995	0.99969

Table 4-18 displays the same ratio of $AEQL_{[R]\_[R]}$ / $AEQL_{[U]\_[R]}$ of the optimal 3-CUSUM(μ+σ) scheme. Similar conclusions can be drawn for this chart based on the data on Table 4-17. This is noted that, in a few cases, this *AEQL* ratio is slightly larger than one. This may be caused by the variability of the simulation results, as the *ATS* of the optimal 3-CUSUM(μ+σ) scheme is evaluated by simulation (with an iteration number of 100,000).

In section 4.6.3, it has been found that the overall performance of the ABS CUSUM and optimal 3-CUSUM(μ+σ) charts are nearly the same if the charts are designed based on the uniform assumption. In this section, it is observed that, the charts designed based on the uniform assumption perform almost equally well as the charts designed by using the real probability distributions of δ_μ and δ_σ. As a result, the performance of the ABS CUSUM and optimal 3-CUSUM(μ+σ) charts must still be nearly equal if both charts are designed using the real probability distributions. Or in other words, the performance equality property is again held when the charts are designed based on the real probability distributions.

Table 4-18. Ratios of $AEQL_{[R]\_[R]}$ / $AEQL_{[U]\_[R]}$ of optimal 3-CUSUM(μ+σ) Scheme

		$f_{\delta\mu}(\delta_\mu)$		
		$a_\mu = 2\ b_\mu = 4$	$a_\mu = 3\ b_\mu = 3$	$a_\mu = 4\ b_\mu = 2$
$f_{\delta\sigma}(\delta_\sigma)$		($\delta_{\mu,\max} = 3$, $\delta_{\sigma,\max} = 4$)		
	a_σ=2 b_σ=4	0.98967	0.99509	0.99996
	a_σ=3 b_σ=3	0.99999	1.00309	0.99795
	a_σ=4 b_σ=2	0.99564	0.99310	0.99206
		($\delta_{\mu,\max} = 5$, $\delta_{\sigma,\max} = 6$)		
	a_σ=2 b_σ=4	0.99251	0.99775	1.00045
	a_σ=3 b_σ=3	1.00013	0.99945	0.99727
	a_σ=4 b_σ=2	0.99683	0.99812	0.99717
		($\delta_{\mu,\max} = 8$, $\delta_{\sigma,\max} = 9$)		
	a_σ=2 b_σ=4	0.99950	1.00096	1.00116
	a_σ=3 b_σ=3	1.00000	1.00139	0.99972
	a_σ=4 b_σ=2	0.99888	0.99789	1.00062

4.7.5 Summary Comments

The studies in this section suggest that the designers of the *X*, ABS CUSUM, and optimal 3-CUSUM(μ+σ) charts need not worry about the probability distributions of δ_μ and δ_σ or make effort to estimate them for the designs and performance evaluation of the charts, because designing the charts based on the real probability distributions can hardly make any difference or improve the detection effectiveness. The most practical and efficient approach is to optimize the control charts using the uniform assumption. These optimal control charts are shown to work equally well as the charts designed by

using the real probability distributions. Moreover, thanks to the performance equality property, the SPC practitioners can always select the simple ABS CUSUM chart to monitor both mean and variance of a variable. They may even consider the simplest *X* chart when the shift domain is reasonably large. Compared with the optimal 3-CUSUM(μ+σ) scheme, the ABS CUSUM chart and *X* chart, especially the latter, have salient benefits of ease in understanding, design and implementation.

Based on the results and discussions, the followings are recommended:

(1) Select the ABS CUSUM chart for most of the SPC applications in which both mean and variance of a variable need be monitored.

(2) The charting parameters of the ABS CUSUM chart must be determined by an optimal design using the uniform assumption. The estimation of the real probability distributions $f_{\delta_\mu}(\delta_\mu)$ and $f_{\delta_\sigma}(\delta_\sigma)$ is unnecessary.

(3) During the implementation, even though $f_{\delta_\mu}(\delta_\mu)$ and $f_{\delta_\sigma}(\delta_\sigma)$ are unknown and varying, the ABS CUSUM chart is deemed to work equally well as an optimal 3-CUSUM(μ+σ) scheme.

(4) If the process shift domain is large, the simplest *X* chart can be adopted.

4.8 Summary of Chapter 4

This chapter begins with the introduction of three charts: *X* chart, ABS CUSUM chart and optimal 3-CUSUM($\mu+\sigma$) scheme. The *X* chart is able to detect process shifts in both mean and variance, and its detection effectiveness is often close to that of more complicated chart, especially when process shift domain is large. The ABS CUSUM chart is also sensitive to two-sided mean shifts and increasing variance shifts by inspecting the absolute value of sample mean shift. The optimal 3-CUSUM($\mu+\sigma$) scheme is developed based on the model proposed by Reynolds and Stoumbos (2004*a*). It has the highest detection effectiveness but is very difficult to design and implement.

Same as for the optimal design in chapter 3, *AEQL* is used as the objective function in this chapter. Using the optimization model, the optimal sample size of $\overline{X}$ chart is discussed and a single *X* chart is found to outperform the $\overline{X}$ chart with (n = 4) to a significant degree. The optimal design is also proved to have improved the overall effectiveness of the 3-CUSUM($\mu+\sigma$) scheme to a significant degree.

Then the performance of five control charts (the *X* chart, ABS CUSUM chart, the optimal and conventional 3-CUSUM($\mu+\sigma$) schemes, and the scale CUSUM chart) are systematically compared. Though the optimal 3-CUSUM($\mu+\sigma$) scheme has the highest overall effectiveness, its superiority weakens as the shift domain expands. The *X* chart and ABS CUSUM chart seem more attractive because of their comparable performance and the simplicity in understanding, design and implementation.

The performance of $\overline{X}$ chart (or *X* chart), ABS CUSUM chart and optimal 3-CUSUM($\mu+\sigma$) scheme are further studied for two issues. Firstly, the effect of sampling cost on the design of control charts for monitoring process mean and variance is examined. It is found that the $\overline{X}$ and ABS CUSUM charts become very effective and even outperform the optimal 3-CUSUM($\mu+\sigma$) scheme when the fixed sampling cost cannot be neglected and/or when the shift domain is large. The optimal values of $n_{\overline{X}}$ and n_{CUSUM} depend on the process shift domain and the ratio between the fixed and variable sampling costs.

Secondly, the effect of the probability distributions of process shifts on the designs

and performance of the three charts is investigated. It is shown that the control charts designed optimally based on the assumed uniform distributions of δ_μ and δ_σ are almost as effective as the charts designed based on the real distributions. Moreover, even if δ_μ and δ_σ follow non-uniform distributions, the performance equality property still holds. That is, the three control charts are almost equally effective in detecting process shifts in mean and variance if they are designed by an optimization algorithm. These results confirm that the optimal design is always an effective way to improve the chart performance regardless of the probability distributions of δ_μ and δ_σ.

Chapter 5
Conclusions

5.1 Conclusions

This thesis proposes several new CUSUM charts for detecting process shifts in mean and/or variance and compares their overall performance systematically. The overall performance measure, *AEQL*, is taken as the objective function for optimal design of the control charts. Except for this, other performance metrics are also investigated in almost every comparison study. These include the Average Time to Signal (*ATS*), the Average Ratio of *ATS* (*ARATS*). Moreover, in addition to the detection effectiveness, other types of metrics, such as simplicity in design and operation, easiness for data plotting, display and understanding, even the working environment, are considered when control charts are compared. These proposed charts in this thesis stand as the most effective charts under different conditions. Furthermore, in order to broaden the application of these charts, the effect of sampling cost and distribution of process shift on the design and performance of the charts has also been investigated.

Chapter 3 proposes two new charts for detecting mean shifts. The optimal *X*&CUSUM chart is developed based on a combined scheme of an *X* chart and a CUSUM chart. The adaptive CUSUM (ACUSUM II) chart dynamically adapts the reference parameter *k* and the exponential parameter *w* in accordance with the current estimated mean shift. The purpose of both charts is to detect both large and small shifts in mean. The performance of these two charts are compared with that of the conventional CUSUM chart, optimal CUSUM chart, ACUSUM I chart and 3-CUSUM(μ) chart in different mean shift domains. It is found that the ACUSUM II chart stands as the most effective single chart for detecting mean shifts. The optimal *X*&CUSUM chart is also more effective than the Lucas' *X*&CUSUM chart and many other charts. The overall effectiveness of the ACUSUM II and optimal *X*&CUSUM charts is close to the most effective optimal 3-CUSUM(μ) chart, but they are superior to the optimal 3-CUSUM(μ) chart in the simplicity for design and implementation.

At the end of chapter 3, the effect of sampling cost on the design and performance of the

$\bar{X}$ chart, CUSUM chart and $\bar{X}$ & CUSUM chart is studied. It is found that the fixed sampling cost significantly influences the performance of the control charts, and that the optimal values of the sample sizes $n_{\bar{X}}$ and n_{CUSUM} are not four and one, respectively. The optimal sample size of a chart for an application should be determined by the optimal design.

Table 5-1 lists a summarized guidance regarding the applicability and limitation of these charts. Among them, the optimal *X*&CUSUM chart, ACUSUM II chart and optimal 3-CUSUM(μ) chart are developed in this thesis.

Table 5-1 Advantages and Limitation of Control Charts for Monitoring Process Mean Shift

Chart Name	Advantages	Limitation
Conventional CUSUM	Simplest, single chart, sensitive to minor shift	Unable to detect medium and large shifts quickly
Optimal *X*&CUSUM	Effective, suitable for small and large shift, easy to design and understand	Use two sub-charts
ACUSUM II	Highly effective, flexible to change parameter according to on-line data, one chart	Complicated to design, difficult to understand
Optimal 3-CUSUM(μ)	Most effective for detecting large and small mean shift	Complicated, time-consuming to design, use three sub-charts

Chapter 4 proposes another three charts, the *X* chart, ABS CUSUM chart and optimal 3-CUSUM($\mu+\sigma$) scheme, to detect shifts in process mean and variance. The comparison study is conducted among these three charts and other two charts (the conventional 3-CUSUM($\mu+\sigma$) scheme and scale CUSUM chart). The results indicate that the optimal design greatly enhance the performance of various types of control charts. The optimal 3-CUSUM($\mu+\sigma$) scheme is the most effective chart, while the conventional 3-CUSUM($\mu+\sigma$) scheme has the worst performance from an overall viewpoint. The ABS CUSUM chart and *X* chart are nearly as effective as the optimal 3-CUSUM($\mu+\sigma$) scheme, especially when the process shift domain is large. However, the *X* chart and ABS CUSUM chart excel other charts in the simplicity in design, understanding and implementation.

Chapter 4 also extends the study of the effect of sampling cost on chart design and performance to the cases where both mean and standard deviation shift are involved. It has been found that the fixed sampling cost again essentially influences the performance of the control charts. As the fixed sampling cost increases, the $\overline{X}$ chart and ABS CUSUM chart become more effective compared with the optimal 3-CUSUM($\mu+\sigma$) scheme. This study also indicates that the optimal sample size for a control chart is usually quite different from the value commonly recommended. It should be determined by an optimal design.

The effect of the probability distribution of process shift on the design and performance of the control charts is also studied in chapter 4. Nine different distributions of process shifts are studied on three charts (the X chart, ABS CUSUM chart and optimal 3-CUSUM($\mu+\sigma$) schemes). The study reveals that the overall performance of the ABS CUSUM and optimal 3-CUSUM($\mu+\sigma$) charts is practically identical no matter the charts are designed based on the uniform assumption or the real probability distributions of process shifts, and no matter what the real distributions are. The X chart is also nearly equally effective when process shift domain is large.

Table 5-2 lists a summarized guidance regarding the applicability and limitation of these charts. It is noted that all the charts are developed in this thesis.

Table 5-2 Advantages and Limitations of Control Charts for Monitoring Process Mean and Variance

Chart Name	Advantages	Limitation
X	Simplest, single chart, and effective in general	Ineffective t for detecting small shifts
ABS CUSUM	Highly effective, suitable for shifts of different sizes, easy to design and understand, provide change point information	Relatively ineffective for detecting large shift
opt 3-CUSUM($\mu+\sigma$)	Most effective, suitable for large and small shifts	Complicated, difficult to design, large number of chart parameters

5.2 Contributions

This thesis has made the following original contributions to the literature and practice of quality engineering. Among these contributions, the first four are most important.

(1) Develop the optimal $\overline{X}$ & CUSUM chart and ACUSUM II for detecting process mean shift δ_μ. Both charts are very effective. The ABS CUSUM chart outperforms all single CUSUM charts. Meanwhile, both charts are easy to design and implement.

(2) Develop the *X* chart, ABS CUSUM chart and optimal 3-CUSUM($\mu+\sigma$) scheme for detecting process mean shift δ_μ and standard deviation shift δ_σ. The optimal 3-CUSUM($\mu+\sigma$) scheme is the most effective chart, and the ABS CUSUM chart is nearly equally effective. In addition, *X* chart is also very effective when shift domain is large. Furthermore, the *X* and the ABS CUSUM, especially the *X* chart, are very easy to design and run. They turn the simultaneous monitoring of mean and variance to a very simple procedure.

(3) Study the effect of sampling cost on the design and performance of the charts. It is found that the fixed sampling cost has significant impact. Some simple charts (such as the *X* or $\overline{X}$ chart) become very effective compared with the complicated charts when fixed sampling cost is high. Moreover, it is found that the optimal sample sizes of many charts are quite different from the values conventionally recommended. The optimal sample size for a chart in a particular application should be determined by an optimal design.

(4) Study the effect of the probability distribution of δ_μ and δ_σ on the design and performance of the charts. It is found that control charts designed based on uniform distribution assumption often perform equally well as those designed based on the real distribution of δ_μ and δ_σ. Moreover, the *X* chart, ABS CUSUM chart and optimal 3-CUSUM($\mu+\sigma$) scheme are almost equally effective no matter the real distributions of δ_μ and δ_σ are uniform or non-uniform. As a result, control chart can be designed based on a uniform distribution, and the chart can be selected mainly based on the simplicity in design and operation.

(5) Study the optimal design of many charts. An index *AEQL* (average extra quadratic loss) is proposed to evaluate the overall performance of the control charts and to work as the objective functions for the optimal design. The optimal design is proven to be able to improve the overall performance of various types of control

charts effectively and significantly. Meanwhile it will not increase the difficulty in chart operation.

(6) Carry out systematic performance comparison among many different types of control charts. In addition to detection effectiveness, the simplicity of the charts in design and implementation is also discussed and compared in details. The results of these studies, together with plenty data presented in many tables, will greatly facilitate the SPC users to identify a most suitable chart for their applications.

5.3 Future Research

There are some promising areas for future research.

(1) Firstly, many studies in this thesis are based on some common conventions and assumptions, such as the known in-control mean μ_0 and standard deviation σ_0. It is interesting to carry out further studies on how the performances of the control charts will be affected when μ_0 and σ_0 are estimated. It would also be interesting to investigate the chart performance when δ_μ and δ_σ are correlated rather than independent.

(2) Secondly, all the process shifts are assumed to be sustained in this project. They will be removed only when being detected by the control charts. However, there are many other types of process shifts. Future work can be explored to develop CUSUM charts to detect transient shifts and drifts.

(3) Thirdly, this project focuses on the study of CUSUM charts. Similar studies (e.g. the impact of fixed sampling cost and the distributions of δ_μ and δ_σ) may be conducted for other types of charts, such as the EWMA charts and SPRT (sequential probability ratio test) charts.

(4) Fourthly, the control charts proposed in this thesis focuses on examining a single variable. In many practical applications, it is necessary to monitor several variables at the same time because there is correlation among them. The multivariate control chart is the one that is effective to solve such problems. Though a lot of works have been done in this field (Khoo 2004, Costa and Machado 2011, Yang and Rahim 2005), little attention has been received for developing charts that are highly effective for detecting small and moderate shifts in mean and variance for multivariate process (Zhang et al. 2010). Thus this should be desirable to develop a single multivariate CUSUM chart to detect process shifts in mean and variance. Furthermore, economic design of multivariate CUSUM chart using Taguchi's quality loss function would also be a challenging future work.

(5) It has been proved that the control charts utilizing both variable sample sizes and variable sampling intervals (VSSI feature) are able to achieve the highest detection effectiveness. It is interest to study, as a future work, whether the VSSI feature will significantly improve the performance of the new charts proposed in this thesis.

References

Annadi, H. P.; Keats, J. B.; Runger, G. C. and Montgomery, D. C. (1995). "An Adaptive Sample Size CUSUM Control Chart." International Journal of Production Research, v33, pp. 1605–1616.

Box, G. P.; Coleman, D. E. and Baxley, R. V. (1997) "A comparison of statistical process control and engineering process control." Journal of Quality Technology, v29, pp. 128-130.

Brook, D. and Evans, D. A. (1972). "An Approach to the Probability Distribution of CUSUM Run Length." Biometrika, v59, pp. 539-549.

Castagliola, P.; Celano, G.; Fichera, S. and Nunnari, V. (2008). "A Variable Sample Size S^2-EWMA Control Chart for Monitoring the Process Variance." International Journal of Reliability, Quality and Safety Engineering, v15, pp. 181-201.

Chen, A. and Chen, Y. K. (2007). "Design of EWMA and CUSUM Control Charts Subject to Random Shift Sizes and Quality Impacts." IIE Transactions, v39, pp. 1127 – 1141.

Chen, G. and Cheng, S. W. (1998). "Max-chart: Combining X-bar Chart and S Chart." Statistica Sinica, v8, pp. 263–271.

Chen, G.; Cheng, S. W. and Xie, H. S. (2001). "Monitoring Process Mean and Variability with One EWMA Chart." Journal of Quality Technology, v33, pp. 223-233.

Cheng, S. W. and Thaga, K. (2006). "Single Variables Control Charts: An Overview." Quality and Reliability Engineering International, v22, pp. 811-820.

Chou, C. Y.; Chen, C. H. and Liu, H. R. (2000). "Economic-Statistical Design of X Charts for Non-Normal Data by Considering Quality Loss." Journal of Applied Statistics, v27, pp.939-951.

Costa, A. F. B. and Magalhães, M. S. de. (2007). "An Adaptive Chart for Monitoring the Process Mean and Variance." Quality and Reliability Engineering International, v23, pp. 821-831.

Costa, A. F. B. and Machado, M. A. G. (2011). "Monitoring the Mean Vector and the Covariance Matrix of Multivariate Processes with Sample Means and Sample Ranges." Produção, v21, pp. 197-208.

Costa, A. F. B.; Magalh ães, M. S. de. and Epprecht, E. K. (2009). "Monitoring the Process Mean and Variance Using a Synthetic Control Chart with Two-Stage Testing." International Journal of Production Research, v47, pp. 5067–5086.

Costa, A. F. B. and Rahim, M. A. (2006*a*). "A Single EWMA Chart for Monitoring Process Means and Process Variance." Quality Technology and Quantitative Management, v3, pp. 295-305.

Costa, A. F. B. and Rahim, M. A. (2006*b*). "A Synthetic Control Chart for Monitoring the Process Mean and Variance." Journal of Quality in Maintenance Engineering, v12, pp. 81-88.

Crosier, R. B. (1986). "A New Two-sided Cumulative Sum Quality Control Scheme." Technometrics, v28, pp. 187-194.

Daudin, J. J. (1992). "Double Sampling *X* charts." Journal of Quality Technology, v24, pp. 78–87.

Del Castillo, E.; Mackin, P. and Montgomer,y D. C. (1996). "Multiple-Criteria Optimal Design of *X* Control Charts." IIE Transactions, v28, pp. 467-474.

Domangue, R. and Patch, S. C. (1991). "Some Omnibus Exponentially Weighted Moving Average Statistical Process Monitoring Schemes." Technometrics, v33, pp. 299-313.

Duncan, A. J. (1956). "The Economic Design of $\bar{X}$ Charts Used to Maintain Current Control of A Process." Journal of American Statistical Association, v51, pp. 228-242.

Dragalin, V. (1997). "The Design and Analysis of 2-CUSUM Procedure." Communications in Statistics – Simulation and Computation, v26, pp. 67–81.

Elsayed, E. A. and Chen, A. (1994). "An Economic Design of Control Chart using Quadratic Loss Function." International Journal of Production Research, v32, pp. 873-887.

Ewan, W. D. and Kemp, K. W. (1960). "Sampling Inspection of Continuous Processes with No Autocorrelation between Successive Results." Biometrika, v47, pp. 363-380.

Flaig, J. J. (1991). "Adaptive Control Charts." Statistical Process Control in Manufacturing. Editor: Keats, J. B. and Marcel, Dekker. New York.

Garvin, D. A. (1987). "Competing in the Eight Dimensions of Quality." Harvard Business Review, v87, pp. 101-109.

Grabov, P. and Ingman, D. (1996). "Adaptive Control Limits for Bivariate Process Monitoring." Journal of Quality Technology, v28, pp. 320-330.

Hawkins, D. M. (1981). "A CUSUM for A Scale Parameter." Journal of Quality Technology, v69, pp. 48-57.

Hawkins, D. M. (1993). "Cumulative Sum Control Charting: An Underutilized SPC Tool." Quality Engineering, v5, pp. 463-477.

Hawkins, D. M. and Olwell, D. H. (1998). Cumulative sum charts and charting for quality improvement. Springer – Verlag, New York, NY.

Ho, L. L. and Trindade, A. L. G. (2009). "Economic Design of An *X* chart for Short-Run Production." International Journal of Production Economics, v120, pp. 613-624.

Jarrett, J. E. and Pan, X. (2007). "The quality control chart for monitoring multivariate autocorrelated processes." Computational Statistics & Data Analysis, v51, pp. 3862-3870.

Jensen, W. A.; Bryce, G. R. and Reynolds, M. R. (2008). "Design Issues for Adaptive Control Charts." Quality and Reliability Engineering International, v24, pp. 429-445.

Jensen, W. A.; Jones, L. A.; Champ, C. W. and Woodall, W. H. (2006). "Effects of Parameter Estimation on Control Chart Properties: A Literature Review." Journal of Quality Technology, v38, pp. 349-364.

Jiao, J. X. and Helo, P. T. (2008). "Optimization Design of A CUSUM Control Chart Based on Taguchi's Loss Function." The International Journal of Advanced Manufacturing Technology, v14, pp. 1234-1243.

Keats, J. B.; Del Castillo, E.; Collani, E. and Saniga, E. (1997). "Economic Modeling for Statistical Process Control." Journal of Quality Technology, v29, pp. 144-147.

Keats, J. B. and Simpson, J. R. (1994). "Comparison of the *X* and the CUSUM Control Charts in An Economic Model." Economic Quality Control, v9, pp. 203-220.

Khoo, M. B. C. A. (2004). "A New Bivariate Control Chart for Monitoring the Multivariate Process Mean and Variance Simultaneously." Quality Engineering, v17, pp. 109-118.

Khoo, M. B. C. (2005). "Determining The Time of A Permanent Shift in The Process Mean of CUSUM Control Charts." Quality Engineering, v17, pp. 87-93.

Klyatis, L. M. and Klyatis, E. L. (2006). Accelerated Quality and Reliability Solutions. Elsevier Science.

Lashkari, R. S. and Rahim, M. A. (1982). "An Economic Design of Cumulative Sum Charts to Control Non-Normal Process Means." Computers and Industrial Engineering, v6, pp. 1-18.

Liu, J. Y.; Xie, M. and Goh, T. N. (2006). "CUSUM Chart with Transformed Exponential Data." Communications in Statistics - Theory and Methods, v35, pp. 1829-1843.

Liu, J. Y.; Xie, M.; Goh, T. N. and Chan, L. Y. (2007). "A Study of EWMA Chart with Transformed Exponential Data." International Journal of Production Research, v45, pp. 743–763.

Lorenzen, T. J. and Vance, L. C. (1986). "The Economic Design of Control Charts: A Unified Approach." Technometrics, v28, pp. 3-10.

Lorden, G. and Eisenberger, I. (1973). "Detection of Failure Rate Increases." Technometrics, v15, pp.167–175.

Lucas, J. M. (1982). "Combined Shewhart-CUSUM Quality Control Schemes." Journal of Quality Technology, v14, pp. 51-59.

Lucas, J. M. and Crosier, R. B. (1982). "Robust CUSUM: A Robustness Study for CUSUM Quality Control Schemes." Communications in Statistics, Part A—Theory and Methods, v11, pp. 2669–2687.

Luceño, A. and Puig-Pey, J. (2002). "An Accurate Algorithm to Compute the Run Length Probability Distribution, and Its convolutions, for A CUSUM Chart to Control Normal Mean." Computational Statistics & Data Analysis, v38, pp. 249-261.

Magalhães, M. S. D.; Costa, A. F. B. and Neto, F. D. M. (2009). "A Hierarchy of Adaptive $\overline{X}$ Control Charts." International Journal of Production Economics, v 119, pp. 271-283.

Messaoud, A.; Weihs, C. and Hering, F. (2008). "Detection of Chatter Vibration in A Drilling Process Using Multivariate Control Charts." Computational Statistics & Data Analysis, v52, pp. 3208-3219.

McCormick, K. (2002). Quality (Pharmaceutical Engineering Series). Butterworth Heinemann, Woburn, MA.

McWilliams, T. P. (1994). "Economic, Statistical, and Chart Designs." Journal of

Quality Technology, v26, pp. 227-233.

Montgomery, D. C. (2009). Introduction to Statistical Quality Control. John Wiley & Sons, New York.

Murdoch, J. (1979). Control Charts. The Macmillan Press Ltd. London.

Nenes, G. and Tagaras, G. (2008). "An Economic Comparison of CUSUM and Shewhart Charts." IIE Transactions, v40, pp. 133–146.

Nishina, K. (1992). "A Comparison of Control Charts from the Viewpoint of Change-Point Estimation." Quality and Reliability Engineering International, v8, pp. 537-541.

Nocedal, J. and Wright, S. J. (1999). Numerical Optimization. Springer-Verlag, New York.

Quesenberry, C. P. (1993). "The Effect of Sample Charts." Journal of Quality Technology, v25, pp. 237–247.

Page, E. S. (1954). "Continuous Inspection Schemes." Biometrika, v41, pp. 100-115.

Prabhu, S. S.; Runger, G. C. and Keats, J. B. (1993). "An Adaptive Sample Size Xbar Chart." International Journal of Production Research, v31, pp. 2895–2909.

Prabhu, S. S.; Montgomery, D. C. and Runger, G. C. (1994). "A Combined Adaptive Sample Size Adaptive Sampling Interval Scheme for the *X* Control Chart." Journal of Quality Technology, v26, pp. 164-176.

Rahim, M. A. and Lashkari, R. S. (1982). "An Economic Design of Cumulative Sum Charts to Control Non-Normal Process Means." Computers and Industrial Engineering, v6, pp. 1-18.

Reynolds, M. R., Jr.; Amin, R. W. and Arnold, J. C. (1990). "CUSUM Charts with Variable Sampling Intervals." Technometrics, v32, pp. 371-384.

Reynolds, M. R., Jr., Amin, R. W., Arnold, J. C. and Nachlas, J. A. (1988). "*X* Charts with Variable Sampling Intervals." Technometrics, v30, pp. 181–192.

Reynolds, M. R., Jr. and Glosh, B. K. (1981). "Designing Control Charts for Means and Variances." ASQC Quality Congress Transactions, American Society for Quality Control, San Francisco, CA, pp. 400-407.

Reynolds, M. R., Jr. and Stoumbos, Z. G. (2004*a*). "Should Observations be Grouped for Effective Process Monitoring." Journal of Quality Technology, v36, pp. 343-366.

Reynolds, M. R., Jr. and Stoumbos, Z. G. (2004*b*). "Control Charts and the Efficient

Allocation of Sampling Resources." Technometrics, v46, pp. 200-214.

Reynolds, M. R., Jr. and Stoumbos, Z. G. (2005). "Should Exponentially Weighted Moving Average and Cumulative Sum Charts be Used with Shewhart Limits?." Technometrics, v47, pp. 409-424.

Reynolds, M. R., Jr. and Stoumbos, Z. G. (2006). "Comparisons of Some Exponentially Weighted Moving Average Control Charts for Monitoring the Process Mean and Variance." Technometrics, v48, pp. 550-567.

Riaz, M. and Does, R. J. M. M. (2008). **"**A process variability control chart." Computational Statistics. Published online.

Runger, G. C. and Pignatiello, J. J., Jr. (1991). "Adaptive Sampling for Process Control." Journal of Quality Technology, v23, pp. 135–155.

Saniga, E. M. (1989). "Economic Statistical Control-Chart Designs with An Application to $\overline{X}$ and *R* Charts." Technometrics, v31, pp. 313-320.

Saniga, E. M.; Davis, D. J. and McWilliams, T. P. (1995). "Economic, Statistical, and Economic-Statistical Design of Attribute Charts." Journal of Quality Technology, v27, pp. 56-73.

Serel, D. A. and Moskowitz, H. (2008). "Joint Economic Design of EWMA Control Charts for Mean and Variance." European Journal of Operational Research, v184, pp. 157-168.

Sheu, S. H. and Lu, S. L. (2008). "Monitoring Autocorrelated Process Mean and Variance Using a GWMA Chart Based on Residuals." Asia - Pacific Journal of Operational Research, v25, pp.781-792.

Shu, L. and Jiang, W. (2006). "A Markov Chain Model for the Adaptive CUSUM Control Chart." Journal of Quality Technology, v38, pp. 135-147.

Shu, L.; Jiang, W. and Wu, S. (2007). "A One-Sided EWMA Control Chart for Monitoring Process Means." Communications in Statistics - Simulation and Computation, v36, pp. 901-920.

Shu, L.; Jiang, W. and Wu, Z. (2008). "Adaptive CUSUM Procedures with Markovian Mean Estimation." Computational Statistics & Data Analysis, v52, pp. 4395-4409.

Siddall, J. N. (1982). Optimal Engineering Design: Principles and Applications. M. Dekker, New York.

Siddall, J. N. (1983). Probabilistic Engineering Design – Principles and Applications.

Marcel Dekker, New York.

Siegmund, D. (1985). Sequential Analysis: Tests and Confidence Intervals. Springer-Verlaq, New York.

Siegmund, D. and Venkatraman, E. S. (1995). "Using the Generalized Likelihood Ratio Statistic for Sequential Detection of A Change-Point." Annual Statistics, v23, pp. 255–271.

Sparks, R. S. (2000). "CUSUM Charts for Signalling Varying Location Shifts." Journal of Quality Technology, v32, pp. 157-171.

Stoumbos, Z. G.; Reynolds, M. R., Jr.; Ryan, T. P. and Woodall, W. H. (2000). "The State of Statistical Process Control as We Proceed into the 21st Century." Journal of the American Statistical Association, v95, pp. 992-998.

Sullivan, J. H. and Woodall, W. H. (1996). "A Control Chart for Preliminary Analysis of Individual Observations." Journal of Quality Technology, v28, pp. 265-278.

Tagaras, G. (1998). "A Survey of Recent Developments in the Design of Adaptive Control Charts." Journal of Quality Technology, v30, pp. 212-231.

Taguchi, G. and Wu, Y. (1980). Introduction to Off-Line Quality Control. Central Japan Quality Control Association, Nagoya, Japan.

Torng, C. C., Lee, P. H. and Liao, N. Y. (2009). "An Economic-Statistical Design of Double Sampling $\overline{X}$ Control Chart." International Journal of Production Economics, v120, pp. 495-500.

Uys, N. and Lombard, F. (2007). "A Note on Two-Sided Cusums for A Normal Mean." Technometrics, v49, pp. 195-198.

Van, Dobben de Bruyn C. C. (1968). Cumulative Sum test: Theory and practice. London, Charles Griffin.

White, E. M. and Schroeder, R. (1987). "A Simultaneous Control Chart." Journal of Quality Technology, v19, pp. 1–10.

Woodall, W. H. (1983). "The Distribution of the Run Length of One-Sided CUSUM Procedures for Continuous Random Variables." Technometrics, v25, pp. 295-301.

Woodall, W. H. (1984). "On the Markov Chain Approach to the Two-Sided CUSUM Procedure." Technometrics, v26, pp. 41-46.

Woodall, W. H. (1985). "The Statistical Design of Quality Charts." Statistician, v34, pp. 155-160.

Woodall, W. H. (1986). "Weaknesses of the Economic Design of Control Charts."

Technometrics, v28, pp. 408-410.

Woodall, W. H. (1990). "CUSUM Charts with Variable Sampling Intervals: Discussion." Technometrics, v32, pp. 389-391.

Woodall, W. H. (2000). "Controversies and Contradictions in Statistical Process Control." Journal of Quality Technology, v32, pp. 341-350.

Woodall, W. H. and Adams, B. M. (1993). "The Statistical Design of CUSUM Charts." Quality Engineering, v5, pp. 559-570.

Woodall, W. H.; Lorenzen, T. J. and Vance, L. C. (1986). "Weaknesses of the Economic Design of Control Charts." Technometrics, v28, pp. 408-410.

Woodall, W. H. and Montgomery, D. C. (1999). "Research Issues and Ideas in Statistical Process Control." Journal of Quality Technology, v31, pp. 376-386.

Wu, Z. and Luo, H. (2004). "Optimal design of the adaptive sample size and sampling interval np control chart." Quality and Reliability Engineering International, v20, pp. 553–570.

Wu, Z.; Shamsuzzaman, M. and Pan, E. S. (2004). "Optimization Design of the Control Charts Based on Taguchi's Loss Function and Random Process Shifts." International Journal of Production Research, v42, pp. 379-390.

Wu, Z. and Tian, Y. (2005). "Weighted-Loss-Function CUSUM Chart for Monitoring Mean and Variance of a Production Process." International Journal of Production Research, v43, pp. 3027-3044.

Wu, Z. and Wang, Q. N. (2007). "A Single CUSUM Chart Using a Single Observation to Monitor a Variable." International Journal of Production Research, v45, pp. 719-741.

Yang, S. F. and Rahim, M. A. (2005). "Economic Statistical Process Control for Multivariate Quality Characteristics Under Weibull Shock Model." International Journal of Production Economics, v98, pp. 215-226.

Yi, G.; Coleman, S. and Ren, Q. (2006). "CUSUM Method in Predicting Regime Shifts and Its Performance in Different Stock Markets Allowing for Transaction Fees." Journal of Applied Statistics, v33, pp. 647-661.

Yu, F. J., Rahim, M. A. and Chin, H. (2007). "Economic Design of VSI $\overline{X}$ Control Charts." International Journal of Production Research, v45, pp. 5639–5648.

Yu, F. J. and Wu, H. H. (2004). "An Economic Design for Variable Sampling Interval MA Control Charts." The International Journal of Advanced Manufacturing

Technology (SCI), v24, pp. 41-47.

Zhang, C. W.; Xie, M. and Goh, T. N. (2008). "Economic Design of Cumulative Count of Conforming Charts under Inspection by Samples." International Journal of Production Economics, v111, pp. 93-104.

Zhang, J. J.; Li, Z. H. and Wang, Z. J. (2010). "A Multivariate Control Chart for Simultaneously Monitoring Process Mean and Variability." Computational Statistics and Data Analysis, v54, pp. 2244-2252.

Zhang, J. J.; Zou, C. L. and Wang, Z. J. (2011). "A New Chart for Detecting the Process Mean and Variability." Communications in Statistics-Simulation and Computation, v40, pp. 728-743.

Zhang, S. and Wu, Z. (2006). "Monitoring the Process Mean and Variance by the *WLC* Scheme with Variable Sampling Intervals." IIE Transactions, v38, pp. 377-387.

Zhang, S. and Wu, Z. (2007). "A CUSUM Scheme with Variable Sample Sizes for Monitoring Process Shifts." International Journal of Manufacturing Technology, v33, pp. 977-987.

Zhao, Y.; Tsun, F. and Wang, Z. (2005). "Dual CUSUM Control Schemes for Detecting A Range of Mean Shifts." IIE Transactions, v37, pp. 1047-1057.

Zeifman, M. I. and Ingman, D. (2005). "Modelling of Unexpected Shift in SPC." Journal of Applied Statistics, v32, pp. 375-386.

Zimmer, L. S.; Montgomery, D. C. and Runger, G. C. (1998). "Evaluation of A Three-State Adaptive Sample Size *X* Control Chart." International Journal of Production Research, v36, pp.733–743.